EFFECT OF LAND USE ON FLOOD DISASTER: A CASE STUDY OF HINDON RIVER

A DISSERTATION

Submitted in partial fulfillment of the

Requirement for the award of the degree

Of

MASTER OF TECHNOLOGY

In

IRRIGATION WATER MANAGEMENT

(CIVIL)

By

NABIN KUMAR SINGH

DEPARTMENT OF WATER RESOURCES DEVELOPMENT AND

MANAGEMENT INDIAN INSTITUTE OF TECHNOLOGY ROORKEE

ROORKEE - 247 667

May, 2018

CANDIDATE'S DECLARATION

I hereby declare that the work carried out in this dissertation titled **"Effect of Land use on flood disaster: A case study of Hindon River, India"** is presented on behalf of partial fulfillment of the requirement for the award of the degree of **Master of Technology** with specialization in **Irrigation Water Management**, submitted to the Department of **Water Resource Development and Management**, Indian Institute of Technology Roorkee, India, under the guidance of **Professor S.K. Mishra**, WRD&M, IIT Roorkee, & **Dr. Harinarayan Tiwari.**

I have not submitted the matter embodied in this report for the award of any other degree or diploma.

Date: May, 2018
Place: IIT Roorkee

Nabin Kumar Singh
Enrollment No: 16548012

CERTIFICATION

This is to certify that the above statement made by the candidate is correct to the best of my knowledge and belief.

.....

Dr. Harinarayan Tiwari
Freelance Researcher
PhD, WRD&M
Indian Institute of Technology-
Roorkee Roorkee - 247667 (UK)

.....

Prof. S. K. Mishra
Professor & Head
Department of WRD&M,
Indian Institute of Technology -Roorkee
Roorkee - 247667 (UK)

ACKNOWLEDGEMENT

It is my great pleasure in expressing my heartfelt gratitude to my supervisor **Prof. S. K. Mishra**, HoD, Department of Water Resources Development and Management, Indian Institute of Technology Roorkee,for his valuable guidance and infilling support for completion of the dissertation **"EFFECT OF LAND USE ON FLOOD DISASTER : A CASE STUDY IN HINDON RIVER"**. I am highly obliged to him for his keen interest, guidance and encouragement towards this work. Working under his guidance is a privilege and an excellent learning experience.

I am also grateful to **Dr. Harinarayan Tiwari**, Freelance Researcher, PhD, Department of Water Resources Development and Management, IIT Roorkee for his valuable instruction & guidance in friendly way and made me complete my dissertation work successfully.

I would like to extend my sincere gratitude to **Dr. Ashish Pandey,** Associate Professor, WRD&M, Indian Institute of Technology, Roorkee for introducing remote sensing to us and help us learn and explore ideas relate to GIS and Remote sensing which is helped us in our dissertation work.

I would also like to express my sincere gratitude to **Prof. Deepak Khare** and **Prof. M.L Kansal**, Professor of Water Resource Department and Management, IIT Roorkee for his kind guidance and cooperation. I would like to thank **Mr. Lakhwinder Singh Dhiman,** Research scholar, WRD&M, who helped me working with software like Arc GIS & ERDAS Imagine.

I am eternally grateful to my family, for their love, moral support, prayers they gave me in every phase of my life. Finally, I am very much grateful to almighty God who gave me strength and power to finish my assigned report on time, without his grace and blessing it was impossible to me.

Last but not least I would like to all friends, teaching and non-teaching staffs who supported me directly or indirectly and helped me to complete my report successfully.

NABIN KUMAR SINGH

Enrolment No: 16548012

M.TECH. (IWM)

ABSTRACT

Floods are among the most devastating natural hazards in the world, leading to more economic and social damages than any other natural phenomena. Flood is dependent on both hydrologic as well as hydraulic parameters. River flow is governed by hydrologic parameters like discharge and hydraulic parameters like velocity, boundary shear stress and water surface profile. Due to increase in population and consequent decrease in per capita resources, the population of rural area often migrates towards city. The population of city areas is increasing while the settlement area remains constant, and it disturbs the existing land use pattern. A number of people start residing on flood plains leading to flood plain encroachment or changing the land use according to their desires/needs. Since the change in land use pattern for urban settlement or vegetation or industrialization affects the hydraulic behavior of river, it is imperative to understand the sensitivity of land use changes on hydraulic parameters. The land use changes affect the surface roughness which, in turn, affects velocity and consequently the depth of flow for a given discharge. The present study has dealt with the sensitivity analysis of roughness coefficient in terms of Manning's n on inundation and finally on flooding.

The lower region of Hindon River has been taken as present study area. Hindon is a tributary of River Yamuna. It originates from lower Himalayas in Saharanpur district of Uttar Pradesh State and flows to a length of about 400 km and passes through six districts namely Muzaffarnagar, Meerut, Baghpat, Ghaziabad and Gautambudh Nagar until its confluences with River Yamuna. This study presents change in hydraulic parameters like water surface profile due to change in land use, i.e. the change in land use will cause change in Manning's roughness coefficient, n. Land use map is prepared from landsat-8 imagery by using ERDAS Imagine software. Surveyed data is then incorporated in ASTER DEM and modified in Arc GIS. The Manning's roughness coefficient used for present study is obtained by taking into account the pattern of land use. There are four sets of Manning's n (= 0.035, 0.0543, 0.0613 and 0.076) value used in the study obtained by combining different land uses. The objective of this study is to compare the results thus obtained with different time steps and different cell sizes. Flood inundation map is prepared with unique discharge to quantify the change in inundation by change in land use. The results of this study are found to be consistent with the usual expectations.

TABLE OF CONTENT

LIST OF FIGURES

LIST OF TABLES

ABBREVIATIONS

ASTER	Advanced Space borne Thermal Emission and Reflection
AHP	Analytical Hierarchical Process
CWC	Central Water Commission
DEM	Digital Elevation Model
DHI	Danish Hydraulic Institute
DRIP	Dam Rehabilitation and Improvement Project
EAP	Emergency Action Plan
ESRI	Environmental System Research Institute
ERDAS	Earth Resource Development Assessment System
FAO	Food and Agriculture Organization
FDA	Flood Damage Reduction Analysis
Geo RAS	Geospatial River Analysis System
GIS	Geographic Information System
GloFAS	Global Flood Awareness System
GPM	Global Precipitation Measurement
GPS	Global Position System
GPS RTK	Global Positioning System Real-Time Kinematic
GUI	Graphical User Interface
HEC	Hydrologic Engineering Center
HMS	Hydrologic Modeling System
IDW	Inverse Distance Weightage
LiDAR	Light Detection and Ranging
LULC	Land Use Land Cover
NCR	National Capital Region
NLCD	National Land Cover Dataset
NLCP	National Lake Conservation Plan
NRSC	Natural Resources Conservation Service
NRSC	National Remote Sensing Center
PAR	Population at Risk
RAS	River Analysis System
SFIM	Sub-Pixel Flood Inundation Mapping

SRTM	Shuttle Radar Topography Mission
TIN	Triangular Irregular Network
UNESCO	United Nations Educational, Scientific and Cultural Organization
USACE	United States Army Corps of Engineers
UTM	Universal Transverse Mercator
WSE	Water Surface Elevation

1. INTRODUCTION

Due to population growth, alteration and development activities in the catchment area has been increased. As a result, runoff generation process is changed, especially through decreasing the infiltration capacity of the soil and the change of soil cover. This has led to increase in runoff flow resulting in increasing flood hazards. Particularly for large scale floods, the process of formation of flood is affected by factors like geomorphology of the catchment area and then preceding rainfall condition (Flood and Tools, 2016). Hydrological responses to rainfall depend on local characteristics of soil, such as water storage capacity and infiltration rates. The type and density of vegetation cover and land-use characteristics are also important for hydrologic response to rainfall. Environmental degradation together with uncontrolled urban development in high-risk zones, such as historical inundation plains and at the base of mountain ranges, leads to an increased vulnerability of those communities on the floodplains to catastrophic events.

Floods are among the most devastating natural hazards in the world, widely distributed leading to significant economic and social damages than any other natural phenomena. The flooding has been affecting the entire country during the monsoon period between July and September. The country experienced major floods frequently in some part. The increase of human population and standards of living demand more harvest and production from the earth resources, especially the land resources. In most societies it is not easy to increase the per unit production rate and as a result, to meet the needs, the arable lands are increased at the expense of the natural land cover. The land cover is the part of the ecosystems. The destruction of this state causes many problems such as soil erosion and increase of the surface run off. One example of this process is happening in the Hindon Basin. Here, local farmers are always transforming the forest areas into the agricultural lands and agricultural lands are used for settlement purposes. Floods are important natural disasters which cause physical and moral damages and have a hydrographic origin. It is also important that artificial human effects on hydrographic structures cause flood. Recent technologies help scientists to make successful researches about floods. In this regard, GIS and HEC RAS are both are most widely used tools for flood related research. In addition to these two technologies hydrological software are also used in actively (Akar et al., 2009).

Soil, land use/ cover, and topography are the three primary watershed characteristics that govern rainfall-runoff-erosion response in watersheds. Alteration of soil and topography is limited to small scales. Therefore, variation of watershed hydrologic response over time depends primarily on changes in the type and distribution of land cover, and thus, the study on the effect of land use change would allow planners to plan for improving catchment by introducing catchment treatment plan (Tanguas et al., 2008).

1.1. Need of Study

Land use is basically governed by environmental factors such as soil characteristics, climate, topography, vegetation, and industrialization. At the same time, it also reflects the importance of land as a key and finite resource for most human for various purposes including settlements, agriculture, forestry, industry, energy production, recreation, water storage etc. Often unwise or unplanned land use causes various forms of environmental degradation, for sustainable utilization of the land ecosystems. Therefore, it is necessary to know the natural characteristics, its quality, productivity, extent and location, suitability, and their limitations. With the population growth, the needs of population are also growing for purpose of settlement, agriculture or recreational works. Consequently, flood plains are used for settlements, agriculture or other recreational work. The change in flood plain (i.e. encroachment or change in land use), the roughness coefficient factor is also changed which may result in extensive flood.

A study carried out by the Department of Geography of the Delhi School of Economics in 2013, claims that in coming years, the core of Noida city may expand into the major floodplain of the River Yamuna and the Hindon River (Chandra, 2013). This will create increasing flood risk, arising largely from growth of economic activity on vulnerable lands or perhaps from growing flood frequencies. This study also showed that there were losses of farmland, forest as well as agricultural land; and shrub since 1995 with more than 36 % of the forest and 22% of the shrub areas being transformed into settlements. Moreover, from the land use map of Hindon basin, it can be clearly seen that there is flood plain encroachment and how flood plain is being used for settlement purpose in Greater Noida (Singh and Singh, 2011). In such a scenario, the objective of study is to observe how the changes in land use aggravated the flood risk.

1.2. Objectives of the study

Flooding, a major natural disaster, affects many parts of the world including developed countries. Every year there is loss of billions of dollars in property damage, infrastructure, and damage of agricultural product as well as significant number of human lives due to flood disaster. Flood hazards and losses though cannot be totally controlled but can be prevented or minimized by providing reliable information to the public about the flood risk through flood inundation maps. The objective of this study is given as follows:

- To study the sensitivity of Manning's roughness for varying land uses on flood inundation.
- To study the sensitivity of cell size on computation of flood level.
- To study the sensitivity of time step on computation of flood level
- To derive a flood inundation map for the worst possible situation.

In this study, HEC RAS 2D Model has been employed.

1.3. Research Gap

The research/study on effect of land use on flood inundation makes planner as well as general public aware about how flood level may go high by using flood plain unwisely for settlement or for any other purposes. Moreover, considering seriousness of land use change, planner can develop a policy to conserve or use the existing land in wise and planned way such that the risk of flood disaster is reduced. In general land use change in flood plain is the conversion of flood plain to agricultural lands or for urban settlements which result in roughness factor & hence causing higher flooding depth for same discharge.

Several studies on Hindon River have been carried for water quality improvement or to access water quality or to improve water quality. But hardly study report is available on flood disaster cause and remedy especially for Hindon River.

Present study basically deals with sensitivity analysis of roughness coefficient by varying land use change on flood inundation map. The stability of HEC RAS model largely depend on time step and cell size. Hardly some studies on effect of cell size and time step has been done so far. As far as Hindon River is considered, none of the study report is available which justifies regarding such studies done before to present study area. Hence the proposed study also deals with effect of cell size and time step on flood level.

2. LITERATURE REVIEW

2.1. Background

Literature review is conducted to understand the latest advancement in the relative field. Research papers published by authors are reviewed to understand the concept and to decide which method is to be adopted to conduct the present study. The following text presents in brief the literature review related to flood inundation mapping.

Hicks & Peacock (2005) conducted flood forecast study using two-step procedure, firstly flood routing was conducted using the hydrological model and resulting peak floods were converted to water level forecasts using hydraulic models. In present study, HECRAS steady flow model was used. By this it was very convenient to extend floodplain delineation in flood forecasting applications. The advantage of this model is that the accuracy for flood forecasting can be improved and simplified into one step process which saves time of flood forecasting. This study shows that flood routing and flood level forecasting can be easily done using HECRAS Model. Thus, application of this model can save significant time that use lapse in calibration of model as well as eliminates one extra step that would require running a second model to determine corresponding flood level forecast.

Yang et al., (2006) developed an approach to delineate floodplain of river on part of south nation river system in Ontario, Canada. Flood plain mapping was done by using Arc GIS and HEC- RAS. Numerical model simulations were performed to generate water surface profile for six different storm events. Triangular irregular network (TIN) terrain model was developed by using geo-referenced maps integrated with DEM and floodplain zones for 6 design storm events were reproduced by overlaying the integrated terrain model with the corresponding water surface. Validation of the model was carried out using 100-year flood zone of Bear Brook sub-watershed. The study shows that HEC-RAS model used for river network provides upgraded simulations with better computational routine. HEC RAS also supports import and export of GIS data and allows to view the river reach and cross-section data in its interface. This study mainly focusses on integration the HEC RAS hydraulic model with GIS map for inundation floodplain zoning.

Kalyanpu et al., (2009) conducted study for sorting out errors occurred in using LU/LC map to estimate Manning's roughness coefficient (i.e. n) in hydrological model on watershed scale. The study was conducted on watershed of area 23 $km^2$and estimated

Manning's n using the National Land Cover Dataset (NLCD). They compared two Manning's roughness coefficient, n map produced by two different methods and found significant difference in estimation of Manning's n value so obtained. And from the study it was found that there is 50% difference in Manning's n in 90% of study area. This study showed that the increasing trend deviation in peak of hydrograph would increase in the Manning's n deviation and concluded that the use of Manning's n values from NLCD datasets is acceptable for medium to large watershed.

Panahi et al., (2010) investigated the impact of the land use/cover changes on the stream discharge in the Madarsu Basin and tried to find floods which had equal rain but different discharges. Since their objective was to understand the impact of the land use/cover change. Thus, they selected floods with equal rainfall so that it will automatically eliminate the effect of the rainfall variations. For this reason, they analyzed the daily rainfall and discharge rates of station during the 1960-2007 period. As the images of above mentioned flood event were not available. Therefore, they selected the images of the closest times to these dates i.e. 1964 and 2003. The characteristics of floods in 1960 & 2007 and their hydrographs are drawn by using same rainfall of 28.3 mms in both floods.

It was observed that the peak discharge of the 2003 flood and 1964 floodwere3.69 m^3/sand 0.37 m^3/s respectively. The flood of 2003 produced much higher runoff than that in 1964. As rainfall was equal in both floods and both are isolated in a dry period, it is reasonable to assume that the only controlling factor should be the variations of the land surface. As a result, they examined the surface characteristics of the Basin among which the land use/cover and soil properties are very important.

Yerramilli (2012) developed systematic approach to identify flood hazard and thus assessment of vulnerability of region towards inundation by using GIS & HEC RAS. HEC-RAS hydraulic model & GIS tool was used to simulate flood event and vulnerability risk assessment and spatially depicting the degree of exposure or vulnerability of the region towards a hazard event in terms of inundation extent, water levels and depth. HEC-RAS model simulation results gave same result as that of the observed inundation depth record at that location.

Alexakis et al., (2013) delineated watershed through DEM and then, the watershed was divided to 13 individual sub-basins. Land use maps derived from the ASTER images of 2000 and 2010 were incorporated to the same hydrological model consecutively. All the

other data (such as soil, precipitation and temperature) were related to the catchment regime during the 2003 flood event. Concerning soil data these were extracted from the integrated search of CORINE and FAO (Food and Agriculture Organization of the United States) soil map datasets. The meteorological data (precipitation data) was acquired by the research from "Kionia" and "Mantra tou Kampiou" rain gauges. It was seen that the flood of 2003 with the simulated flow results with varying land use data for 2000 and 2010 proved that in the case of 2010 model the run off rates were constantly higher that might be due to the expanded urban area cover that increases the phenomenon of surface run off.

Saghafian et al., (2015) used HMS model to predict land use effects on floods of Golestan watershed for various design rainfall conditions. First, maximum daily rainfall depths measured at stations inside and adjacent to Golestan watershed were statistically analyzed and daily storm depths corresponding to different return periods were estimated. The spatial distribution of design rainfalls was determined based on the inverse distance squared method. Rainfall hyetographs were made to follow the average temporal pattern of a recording rain gauge in the area. Comparison of the Golestan watershed land use maps of 1967 and 1996 shows that forest and rangelands have been converted into cultivated areas. The area of cultivated lands has risen by 13%, which mostly occurred on hill slopes. During the same period, the total forest area has decreased from 1,437.2 to 1,243.9 km^2, i.e. a reduction of about 200 sq. km. In this study, the relative effect of land use change was quantified through simulating the flood hydrographs of Golestan watershed using a hydrologic model. The simulation results indicate that land cover deterioration has increased the flood peak and volume.

Khaleghi1 et al., (2015) carried out flood plain modeling by feeding maximum flood discharge with different return periods as well as required cross sections with other detailed such as the coefficient of roughness of the main channel of Lighvan Chai River. The simulation results were shown in the flood levels on cross sections. Flood levels area showed that by increasing the discharge of longer return periods as a result, flood made more surface flooding. Moreover, elaboration of flood zoning was affected by topographical features of the Lighvan Chai River valleys as well as human intervention in river channel and river banks such as construction, agricultural, and channel narrowing. Anywhere the valley width and the channel have increased, the width of the flood area has increased and water has expanded in wider area. Conversely, anywhere the valleys and channel width have been narrowing, the

width of flood area has reduced in the same proportion and also the depth of flood levels has increased.

Land use change of Lighvan basin was analyzed in two time periods (2000 and 2010). Land use changes from 2000-2010 shows decreasing of dense pasture, barren land (-54.3) and Irrigated farming (-0.5); increasing of residential area (88.9), weak pasture (45.5) and rain fed farming (38.6). Land use along the study-reach flood plain was predominately by trees, vegetation, residential area and agricultural farming. By using land use maps and flood zoning map in different return period showed that flooded area in rain-fed farming, garden and residential area has increased but the flooded area in barren land and irrigated farming has decreased.

Demiret et al., (2016) prepared flood hazard maps for the Mert River Basin, Samsun, Turkey, by using GIS and Hydrologic Engineering Centre River Analysis System (HEC-RAS). In this river basin, both human life and amount of property damages were experienced in 2012 flood. The preparation of flood risk maps employed in the study includes the following steps:

a) Digitization of topographical data and preparation of digital elevation model using Arc GIS,
b) Emulation of flood lows of different return periods using a hydraulic model (i.e. HEC-RAS), and preparation of flood risk maps by integrating the results of (1) and (2).

3D hazard maps were obtained for the Q_{10}, Q_{25}, Q_{50}, and Q_{100} floods. The flood maps demonstrated that some areas are highly affected from flood for low return period (Q_{10}) event. Approximately 30% of the area and 650 housing were affected in the downstream of the Mert River by Q_{10} flood, whose maximum flood depth reached 6.2m. Due to improper urban planning noticeable floods occurred for the 100-year return period on the d/s of the Mert River with three bridges under flood. Flood hazard map of the 2012 was prepared by using GIS and HEC-RAS model. when result Q10 and 2012 floods were compared there were similarity in simulated result. It was concluded that floods in that region could be prevented by adding embankment as well as regulation structure in the bottom of the river or else the most of this flooded area would be forested.

Khattak et al., (2015) used HEC-RAS model for flood plain mapping. The major objective of study was assessing the suitability of HEC-RAS model in simulating water surface profiles and determining the area of inundation under different return-period floods for Kabul River situated in Pakistan. It involved routing of the flood by making use of

natural channel geometry in the sub-reaches Analysis carried out using Kolmogorov–Smirnov test indicated that LP3 is the best fit distribution for both Warsak dam and Nowshera bridge gauging station on River Kabul. LP3 distribution was used to estimate the values of 10-, 50-, 100-, 200-, 500-, and 1000-year flood. Using the HEC-RAS model, and Arc GIS, an analysis of areas likely to be inundated under different return-period floods was marked.

Analysis of results clearly indicated that the 100-year return-period flood at Warsak could inundate 400% area more than the normal flow. To ensure safety of people and property from flooding, the floodplains should be preserved or restored its natural state without developing it. The extent of inundation shown by the satellite image of the 2010 flood was similar to 2010 flood resulting from HEC-RAS model. This result demonstrated the capability of the model to simulate open water floods and produce water levels at the desired locations with reasonable accuracy.

The results of this case study indicate that the simulation of flood levels for a given floods can easily be performed using the HEC-RAS. Moreover, simulation of flood using this model does not require expensive acquisition of channel geometry data between cities. Employing this approach would enable concerned agencies of government in Pakistan to plan for significant reduction of flood damages in the Kabul River basin.

Sahoo et al., (2015) developed flood inundation map and flood hazard map using features such as flood depth and inundated area; land use; and population density and road networks. They concluded that the rate of increase in flood depth with rainfall intensity was more than the rate of spatial spreading in flooded areas. Moreover, the central portion of the city was ranked as more vulnerable to flood hazard whereas peripheral portion of the city was more flood prone land use was considered. Finally, this study highlighted the importance of inundation area & flood depth as the primary and most sensitive parameter for describing flood hazard ranking in comparison to parameters like population density, land use, and road networks.

Rahmati et al., (2016) prepared flood hazard zoning map and inundation map for 50 year and 100-year flood were prepared using Arc GIS and HEC RAS model for some part of the Bashar River downstream of Yasooj city, Iran. Four parameters distance to the flow channels, elevation, land use, and land slope, were considered as the main criteria for flood hazard mapping in the framework of GIS whereas HEC-RAS hydraulic model was used to simulate inundated areas. The cross-sectional geometry of the channel, peak discharges & Manning's

roughness coefficients n, were used as the model input. The flood hazard zoning map and inundation map thus prepared were overlaid and compared. It was concluded that the AHP using HEC RAS and GIS technique can be reliable for prediction of flood extent and also can be suggested for assessment of the flood hazard potential in no or less data regions.

Bhandari et al., (2017) conducted two-dimensional unsteady flow modeling using HEC-RAS 5.0.3 in Brazos watershed. Flood routing was done for 20km flood event of 2016 with flow hydrograph, Manning's n value and other geometric data. The model was calibrated using measured water surface elevation. The model was evaluated for a month. They concluded that maximum depth, maximum velocity and maximum water surface elevation and maximum inundation occurred at the peak flow. They also concluded that HEC-RAS model gives good result with small time step and small cell size but it requires more time for model simulation with small cell size and small time step.

Mai & De Smedt (2017) used combined hydrological and hydraulic model for flood prediction in Huong river basin, Vietnam. In this study, spatial distributed hydrological model Wet Spa was coupled with the hydraulic HEC-RAS model for simulation. The model was calibrated and validated with the observed flow and water surface elevation data of 2002 to 2005 and 2006 to 2007 respectively. They found that the water surface elevation and flood occurrence time were well predicted by using soil data, land use, and topography. Further, they concluded that the model was also suitable for predicting flood inundation and flood risk. The coupled model can also use as a tool for flood control management to reduce the loss of lives, property, and infrastructure.

2.2. HEC-RAS 5.0.3 Model

In the previous version of HEC-RAS, it was possible to perform the only one-dimensional analysis. Then, Hydraulic Engineering Centre added the ability to perform two-dimensional (2D) hydrodynamic routing within the unsteady flow analysis portion of HEC-RAS Version 5.0.3. Introduction of HEC RAS 5.0.1 or higher version, one can now it is possible to perform one-dimensional unsteady flow modeling, two-dimensional unsteady flow modeling based on Saint Venant equation or Diffusion wave equation as well as combined 1D and 2D unsteady-flow routing. 2D modeling can be performed by adding 2D flow area elements into the model in the same manner as adding a storage area. A 2D flow area in geometric editor added to extent of flow study required by drawing a polygon. The flow mesh is developed by linking the two-dimensional flow areas to one-dimensional model elements and/ or directly connecting

boundary conditions to the two-dimensional flow areas.

2.2.1. HEC-RAS Two-Dimensional Flow Modeling Advantages/Capabilities:

- Capable of performing one dimensional, two dimensional as well as and combined 1D and 2D modeling.
- Saint Venant or Diffusion wave equations in two dimensions
- Implicit Finite volume solution algorithm.
- 1D and 2D coupled solution algorithm.
- Unstructured or structured computational meshes.
- Detailed hydraulic table properties for 2D computational cells and cell faces.
- Detailed flood mapping and flood animations.
- Multi-processor-based solution algorithm.
- 64-Bit and 32-Bit computational engines.
- No linking interface like HEC Geo RAS is required
- Floodplain and floodway encroachment modeling
- Multiple profile computations.
- Levee overtopping.

2.2.2. HEC-RAS Two-Dimensional Flow Modeling Current Limitations:

- More flexibility for adding internal hydraulic structures inside of 2D flow areas.
- Sometimes it gives projection error even if we use same repetitive process.
- Currently cannot perform sediment transport erosion/deposition in 2D flow areas.
- Currently cannot perform water quality modeling in 2D flow areas.
- Cannot connect Pump stations to 2D flow area cells.

2.2.3. One-Dimensional Model:

The one-dimensional (1D) models used for flow modeling considers flow as in one direction only i.e., in X-axis (stream flow direction). The one-dimensional models use St. Venant Equation for calculating the flood wave. Earlier versions of HEC-RAS developed by Hydrologic Engineering Centre of USACE characterize the terrain through cross-section perpendicular to the flow direction. One dimensional model determine how the peak flood wave attenuates as it moves downstream, travel time, velocity, maximum water level along the reach and change in shape of the hydrograph. These parameters are governed by cross-sectional area, bed slope, geometry of river, overbank and backwater area, Manning's roughness coefficient, existing water in river reaches and computation solution scheme. Depending on the accuracy required, Field survey or Topographic maps are required to select

the routing parameters and details required to carry out the study such as Manning's roughness coefficient, ineffective area and overbank area, bridges and other structures in downstream reaches and channel storage.

2.2.2 Two-Dimensional Model:

Models like MIKE 21, FLO-2D, LISFLOOD-FP and latest version of HEC-RAS 5.0.3, the cross-section details used by one-dimensional models to depict the river bed data are replaced by grids and mesh wither in the form of a square (regular interval) or polygon (irregular interval) associated with elevation. In the 2D hydrodynamic model, water propagates by the cell to cell evaluation basis. Parameters varying with a change of cell can be assigned differently to each cell. Advancement in the field of Remote Sensing, GIS and DEM greatly improved the development of two- dimensional hydrodynamic model. 2D hydrodynamic models are grid or mesh based depth averaged model which gives information regarding inundation area, Water surface elevation, Water depth, Shear stress, Velocity of flow. Arrival time, Duration of the flood, Percentage time inundated, etc.

2.3. FLOW-2D

FLOW-2D model is developed based on MUDFLOW model in 1989. This predicts the flood hazard, sediment-laden flow, and debris flow over the alluvial river and this uses a grid system to determine floodplain based on elevation, roughness coefficient and it is good in predicting flow path and area. In this sediment-laden and without sediment modeling of flow can be done. In this model, discharge is estimated grid wise based on the depth of flow over each sector. The depth of flow is obtained by summing up all sector depth from all the four sides of the grid. The accuracy of the model is dependent on the density of grid system and the data availability.

2.4. LISFLOOD-FP

LISFLOOD-FP is a two-dimensional hydrodynamic model which has been designed for simulation of floodplain inundation over complex topography. This model is computationally efficient manner. It has the capability of simulating grids up to million of cells for dynamic flood events. It can take benefit of new sources of terrain information from remote sensing techniques such as airborne laser altimetry and satellite interferometric radar etc.

The model can predict water depth in each grid cell at each time step, and hence it can simulate the dynamic propagation of flood waves over fluvial, coastal and estuarine floodplains. It is a non-commercial, research code that has been developed as part of an effort to improve our

basic understanding of flood hydraulics, flood inundation forecast, and flood risk assessment.

2.5. Flood Inundation Map

Flood Inundation Map (FIM) is a map that delineates the area that would probably be inundated by the particular flood event. The flooding may be caused either by controlled or uncontrolled flow or as a result of a dam failure. FIM is required to understand the effects of flooding on any important structures such as buildings, roadways, airport, railways, streets and/or any particular region of interest. FIM provides important information, like depth and spatial extent of flooded zones, required by the municipal authorities to inform the citizens about the major flood prone areas and adopt appropriate flood management strategies. Specifically, Inundation maps can be used for following purposes:

- Preparedness (What if worst condition)
- Timely Response tied to real-time gage& forecast information
- Mitigation and Planning - flood risk analyses
- Recovery - damage assessment
- Environmental and Ecological Assessments like wetlands identification, hazardous spill cleanup etc.

3. STUDY AREA

Hindon River, a tributary of River Yamuna originates in the lower Himalayan region in Saharanpur district. It flows between Ganges and River Yamuna for 400 kilometers and also passes through the important cities of Uttar Pradesh State namely Muzaffarnagar, Meerut, Bhagpat, Ghaziabad. The river finally merged with Yamuna river in Gautambudh Nagar district just outside Delhi. It contributes as a major source of surface and ground water resources of the area.

3.1. Location

The Hindon river basin is formed as a part of Middle-Ganga alluvial aquifer of North India having flat topography. This basin is located under the geographic latitudes 290 10' - 290 30' N and longitudes 7800'-780 15' E as shown in location map below. The study area is the lowest portion of the watershed, it covers 4 km on the upstream side of Yamuna Express highway bridge (Greater Noida region) and 2.9 km downstream of the same as shown in Figure 1. The study area falls in Gautam Budha Nagar district.

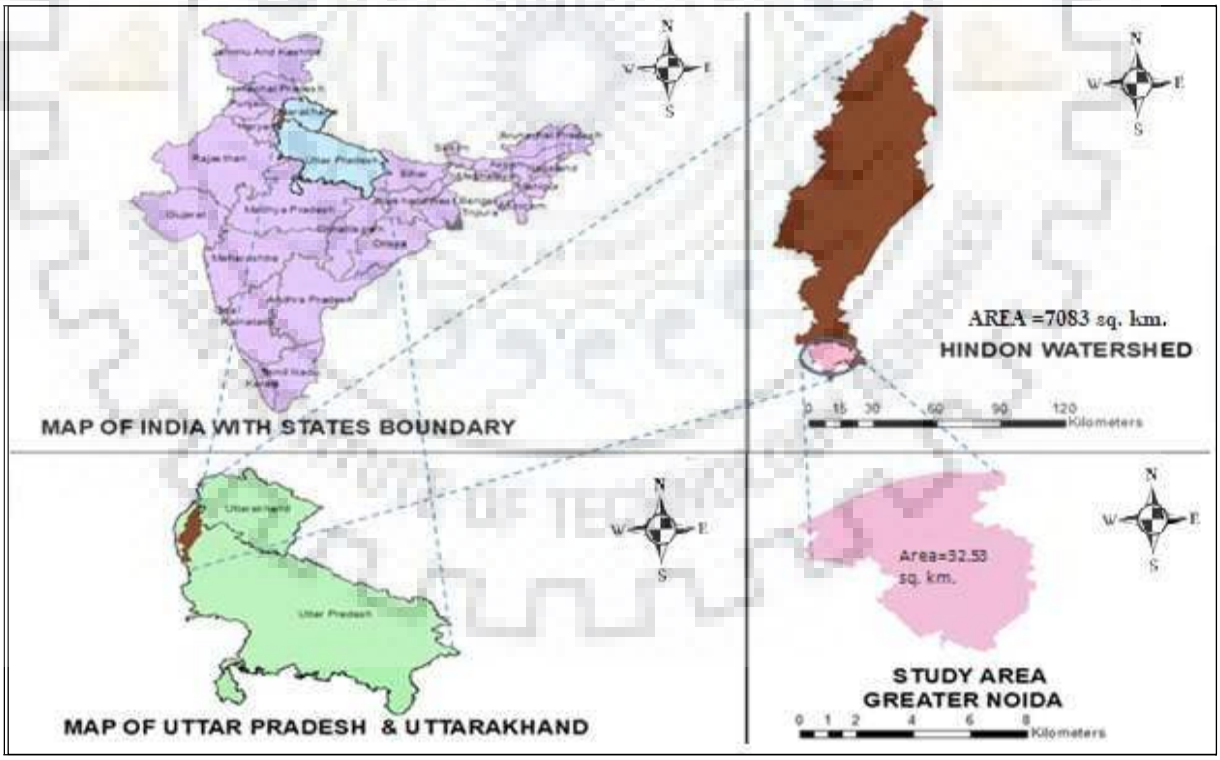

Figure 1 Location map of the study area

3.2. Topography

The study area lies lower part of Hindon watershed in the plain region. The catchment area of Hindon basin is 7083 sq. km and the area of study is 32.53 sq. km. The surface elevation of the study area lies between 188m to 221m.The area is heavily populated and most of the area has been used for settlement purpose. It falls under of the National Capital Region (NCR), India. It is located approximately at 30 km south-east of New Delhi. Due to Noida-Greater Noida Expressway, travel time to New Delhi city is about 30 minutes only. As it is close to the national capital city there are high chances of increase in this area (District Profile, 2009; Wikipedia, updated 2015)

3.3. Rainfall

The annual average rainfall in the study area observed in the nearest rain gauge station, Sikandrabad is about 750 mm. The maximum rainfall occurs from June to September during the monsoon period. The mean value of rainfall recorded in monsoon period is 600 mm which is 80% of annual rainfall. The August month is recorded as a wettest month with an average rainfall of 205.8 mm rainfall. July month is wettest after August month with about 194.4 mm rainfall (District Profile, 2009).

3.4. Climate

The climate of the study area is sub humid. This area experiences very hot summer with normal mean of 32.5 °C. The temperature starts rising from March to till May. June is considered as the hottest month with 32.5 °C followed by May with 31.8°C. January with normal mean temperature of 14.3°C is considered as coldest month followed December normal mean temperature of15.5°C. The average monthly relative humidity of the study area is 83.5%. in the month of August (morning time) and that of May is recorded as 41.2% (District profile, 2009).

3.5. Drainage

The study area is drained by Yamuna River, Hindon river and Bhuriya river (tributaries of Yamuna river). The Hindon River flows from the north towards a south or southeast direction. The Hindon River follows a meandering course and has narrow floodplains. There is a good network of surface drainage in this area to drain out excess rainfall during heavy (District profile, 2009).Hindon river is 6^{th} order river. The stream order of Hindon River was generated from Digital Elevation Model (DEM) and is shown in Figure 2.

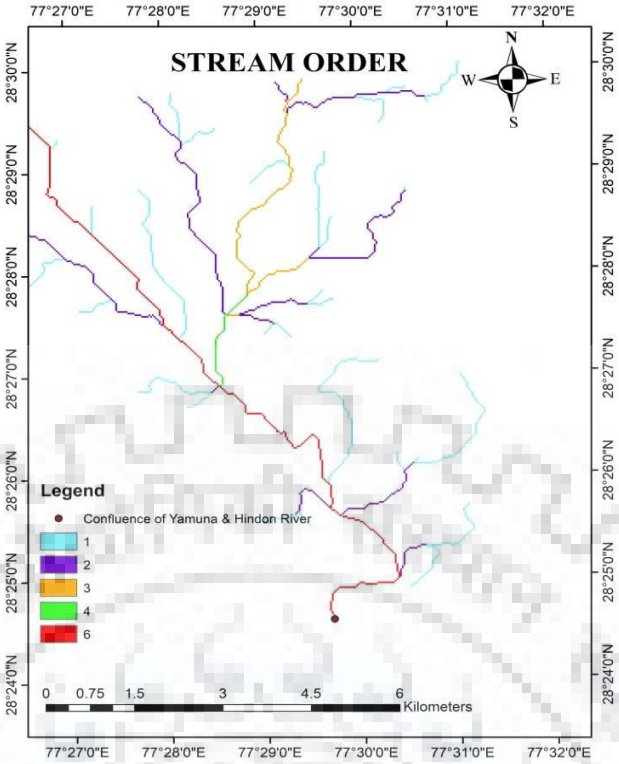

Figure 2 Stream Order

3.6. Land Use

The district statistical data (2005) shows that 67.93% of the land had been used for agriculture, 1.4% for forest, 0.23% for orchids & bushes and negligible 0.3% for pasture. There are four blocks covering the area under forest, Bisrakh block was under urban planning maximum forest (District profile, 2009). The land use of Hindon basin is shown in Table 1

Table 1 Classification of Hindon basin area based on LU/LC

S. No.	Class Name	Land Use/Land Cover	
		Sq. km.	Percentage
Class-1	Dense Forest	26.04	0.43
Class-2	Open Forest/ Scrub Land/ Plantation	89.89	1.50
Class-3	Agriculture/ Orchard Plantation	3930.24	65.73
Class-4	River/ Water body/ Wetland/ Marshy Land	148.38	2.48

Class-5	Settlements/ Infrastructure	889.23	14.87
Class-6	Sand/ Bright Areas	98.05	1.64
Class-7	Barren Land/ Agricultural & Non-Agricultural Fallow	767.53	12.83
Class-8	Industrial Area	29.3	0.49

For the study area, LU/LC Map (in methodology) was prepared by using ERDAS Imagine. The map shows that most of the part of the study area is occupied by the urban settlement. If only floodplain is considered, the urban settlement is 17.5%, agriculture 50% and barren land 2.5%.

3.7. Geomorphology

The study area falls on the upstream of River Yamuna and Hindon. It contains plain with sandy ridges, sand dunes, and depressions. Due to erosion caused by surface runoff, river ravines are noticed in the form of narrow gullies. It forms bad land topography along Hindon River between Bisrakha and Dankaur areas. There are Kansas seen on beds with forms mounds or pinnacles. The study area has a gentle slope of 0.25 m/km from northwest to southeast.

3.8. Soil Type

The soil type in the study area varies from pure sand (Bhur) to stiff clays (Matiar). The study has Dumat often called as loam. Loam is the mixture of clay and same in same proportion which is good for agriculture soil. The quality of loam depends on their proportion. It also consists of Kallor (bad land patches) which is bad for vegetation growth and Kemp (alluvial soils) which is good for crop yield. Kankars associated with clay in ground water movement

4. DATA & ANALYTICAL TOOLS

Basic data requirement of this study is ASTER DEM, Landsat-8 satellite image, hydrograph and Bathymetry of study area. The present work of sensitivity analysis of Manning's n by changing different land use, effect of different cell size and time step, as well as flood inundation mapping, was carried out using Arc GIS, ERDAS Imagine & HEC RAS 5.0.3 software.

4.1. Data

The DEM (Digital Elevation Model) was acquired from USGS Earth Explorer. The DEM thus acquired give error elevation value of underlying water body. So, to correct this error field survey is carried out using Total Station or any other surveying instrument to know the nature of the terrain. The field data is then incorporated with DEM to modify the DEM. However, for initial planning and demonstration work above surface water, DEM could be used. The ASTER DEM and Landsat- 8 Satellite image without processing is shown in Figure 3.

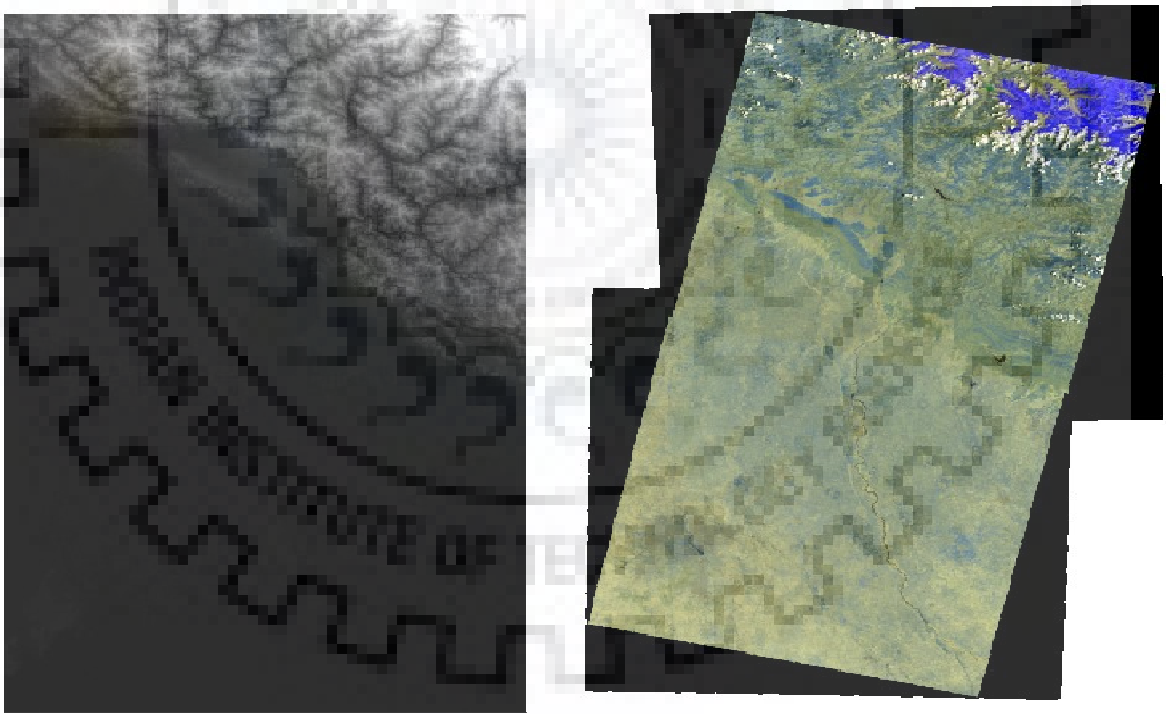

Figure 3 Merged DEM (left) & Landsat-8 image (right) without processing

Landsat-8 satellite image for of study area was acquired from USGS website. Landsat-8 is American Earth observation satellite launched on February 11, 2013. Land use was prepared by using both classification method (i.e. Combined unsupervised/supervised classification).

The bathymetry (cross-section) survey data of study area at 50m interval was acquired. The bathymetry was overlaid on point values obtained from DEM. Hence modified DEM was produced. The cross-sectional data acquired for the study is attached in Appendix 1. The data required for the present study was acquired from various sources. The type and source from which data was acquired are tabulated below in Table 2.

Table 2 Description of Data and Source

S. No.	Data type	Source	Description
1	Digital Elevation Model	www.earthexplorer.usgs.gov	Aster DEM of 30 m resolution
2	Satellite image	www.earthexplorer.usgs.gov	Land-SAT - 8 satellite image of 30 m resolution
3	Hydrograph	Department of Irrigation and Water Resources, Uttar Pradesh	Daily Flood Hydrograph of a different period.
4	Topography of Hindon River	River Bathymetry data	River Bathymetry survey is conducted with a grid size of 50 m X 50 m for entire length of the study area

4.2. Analytical Tools

The following software have been used for the foresaid study.

4.2.1. Arc GIS

Arc GIS is a geographic information system (GIS) is an interface for working with maps, tables geographic information. It incorporates geographical data into series of thematic layers. It is used for creating and using maps, compiling geographic data, analyzing mapped information, sharing and discovering geographic information, using maps and geographic information in a range of applications, and managing geographic information in a database. Arc GIS contains a set of integrated applications with numerous features. Some important features are as follows (Modified 2012).

a. Arc Map.

It is geospatial processing application that allows the user to create maps, analyzing of mapped information, create maps, symbolize features, query attributes as well as analyze spatial data.

b. Arc Catalog

It arranges spatial data contained in a hard disk or any other storage. It helps user to search file and add data to Arc Map. It is useful in managing metadata and set geo-coding.

c. Arc Toolbox

It is the third application used within ArcCatalog and ArcMap. It has tools for geodata conversion, processing, projections system, coordinate systems, etc. This is toolbox used for analysis in Arc Map and Arc Catalog.

4.2.2. ERDAS Imagine

ERDAS (Earth Resource Development Assessment System) Imagine is a software to process remotely sensed image. It was designed by ERDAS for geospatial applications. The latest version was developed in the year 2015. It was mainly aimed to process geospatial raster data. This software is used for extraction of importing and exporting of a satellite image (both raster and vector), digital values of the pixels, combining various bands of satellite imageries. Land Use Map preparation and Land use change detection can be done with its application.

4.2.3. HEC RAS 5.0.3

HEC-RAS 5.0.3, a hydraulic model developed by the USACE, is extensively applied in calculating the hydraulic characteristics of rivers. It is an integrated program and uses the following energy equation for calculating water surface profiles.

$$Y_2 + Z_2 + \alpha\frac{V_2^2}{2g} = Y_1 + Z_1 + \alpha\frac{V_1^2}{2g} + h_e \quad \ldots\ldots\ldots\ldots\ldots\ldots\ldots (1)$$

Where, Y, Z, V, α, h_e, and g represent water depth, channel elevation, average velocity, velocity weighting coefficient, energy head loss, and gravitational acceleration; and subscripts 1 and2, represents cross sections 1 and 2respectively.

HEC-RAS model needs details of river cross sections and upstream flow rate. The thewater depth and mean velocity are calculated for a given cross section using the energy conservation equation. HEC-RAS give WSE (Water Surface Elevation) at each grid, velocity distribution in flow area, depth of flow for each cell of the channel considered for simulation of the model. The water level values are overlaid on a digital elevation model (DEM) of the area to get the extent and flood depth using GIS. Channel roughness though is a sensitive parameter in hydraulic model flood inundation mapping by using HEC RAS and Arc GIS interface.

4.2.4. Stability of model

Stability & accuracy of the model in HEC RAS model is achieved when time step satisfies the following Courant Condition (Cr)given in Equation (1)(Brunner, 2016):

a. Saint Venant Equation

$$C_r = V_w * \frac{\Delta t}{\Delta x} \leq 1 \text{ (Max.} C_r\text{=3)} \quad \ldots\ldots\ldots\ldots\ldots\ldots\ldots\ldots\ldots\ldots \quad (2)$$

Or, $\Delta t \leq \Delta x / Vw$ …… ……..…..…... (3)

b. Wave Diffusion Equation

$$C_r = V_w * \frac{\Delta t}{\Delta x} \leq 1 \text{ (Max.} C_r\text{ =5)} \quad \ldots\ldots\ldots\ldots\ldots\ldots\ldots\ldots\ldots\ldots \quad (4)$$

Where, Cr =Courant Condition

V_w = Velocity of wave, which is approximately equal to 1.5 times average velocity of flow (m/s)

Δt = computational time step (s)

Δx=Average Cell Size (m)

Courant condition plays important role in stability and accuracy of the model,it should be considered while modeling in HEC RAS. Though Courant condition as stated in equation varies with basin, above equation fits well for smaller basin.

Common Stability Problems in HEC RAS may occur if following conditions exist.

- Computational time interval too large.
- Fewer cross sections
- For unsteady flow simulations, if model reaches critical depth model is unstable.
- Downstream boundary condition is normal depth
- Land use with low Manning's n values, etc.
- Cell size too small.
- Bad rating curves.

Computational time interval too large:

When HEC RAS model solves the unsteady flow equations derivatives are calculated with respect to distance and time. If the changes in hydraulic properties at a given cross-section are changing rapidly with respect to time, the program may go unstable. The solution to this problem in general is to decrease the time step. The unsteady flow equation is given below

a. Momentum Equation:

$$\frac{\partial Q}{\partial t} + \frac{\partial\left(\frac{\alpha Q^2}{A}\right)}{\partial x} + g * A * \left(\frac{\partial h}{\partial x} - S_o + S_f\right) = 0 \quad \ldots\ldots\ldots\ldots\ldots\ldots (5)$$

Where, Q= discharge, (m3/s)

g = acceleration due to gravity, m/s2

h= pressure head, m

S_0 is the bed slope,

S_f is the energy slope

b. Continuity Equation

$$\frac{\partial Q}{\partial x} + \frac{\partial A}{\partial t} = 0 \quad \ldots\ldots\ldots\ldots\ldots\ldots\ldots\ldots\ldots\ldots\ldots\ldots\ldots\ldots (6)$$

Where, $\frac{\partial Q}{\partial x}$ = rate of change of channel flow with distance

$\frac{\partial A}{\partial t}$ = rate of change of channel area with time

Computational time interval too small

If a time step is selected that is much smaller than what the Courant condition would dictate for a given flood wave, this can also cause model stability problems. In general, too small of a time step will cause the leading edge of the flood wave to steepen, chances of instability will increase.

Fewer cross sections

Hydraulic properties are greatly influenced when cross sections spacing too apart, as a result, the solution may become unstable. Further, there are chances of numerical diffusion when cross sections spaced too far apart. This is due to the derivatives of flow with respect to long distance. The model also becomes unstable if it does not satisfy courant number condition (i.e. $Cr \leq 1$) due to large the cross-sectional difference.

Cross Sections too close

The derivatives with respect to distance may be overestimated if the cross sections are placed too close. This maybe because the flood wave at a point gets over steepened and results in instability of model.

5. METHODOLOGY

The methodology adopted for performing above stated task is as listed down step by step as follows:

5.1. Acquiring and Processing of DEM

ASTER DEM of different tiles covering watershed was downloaded from USGS website and then merged it to one in Arc GIS. Watershed was delineated using Spatial Analyst Tool in Arc GIS interface. The flowchart of watershed delineation is shown in Figure 4.

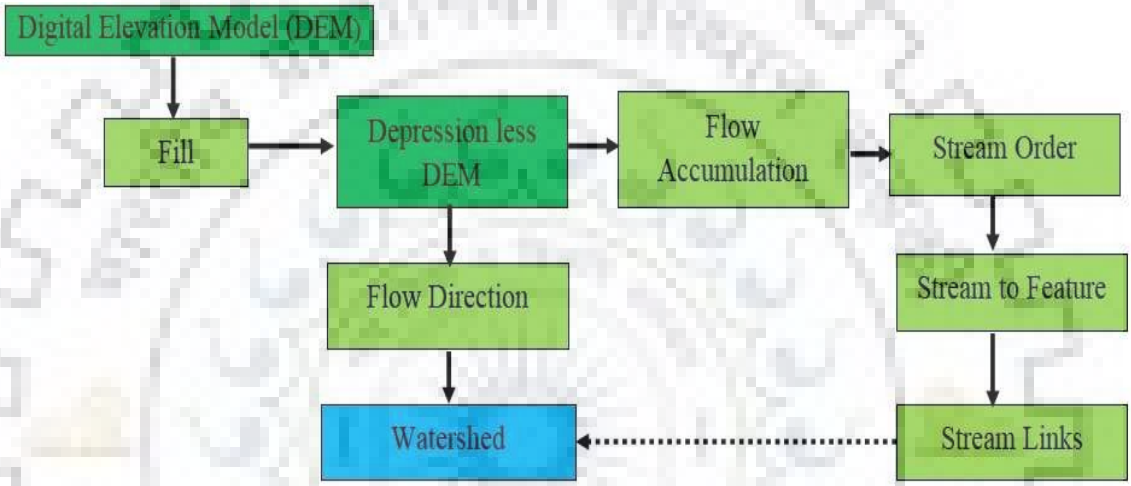

Figure 4 Flowchart of Watershed Delineation

DEM thus acquired is geo-referenced. The watershed delineation flow chat is summarized as follows.

i. Fill is the initial process in the processing of DEM. This process is employed to fill the sink (if any) elevation grid.

ii. To determine the flow direction for each grid in the landscape, it is necessary to find flow direction. Flow direction is a significant factor in hydrologic modeling to identify where landforms drain. In Arc GIS, the flow direction of filled DEM is determined for each pixel (Bhatt & Ahmed 2014).

iii. Flow accumulation is calculated water from a given cell to flow into only one adjoining cell. Drainage network is produced using flow accumulation (Mark 1983; Bhatt & Ahmed 2014). Watershed is delineated using the watershed tool.

The lower portion of the watershed is the study area.

5.2. Modification of DEM

The elevation beneath the surface of water is not accurate in freely acquired DEM. In order to correct this, River bathymetry is incorporated with DEM to modify it. The DEM prior to incorporation River bathymetry is shown in Figure 5.

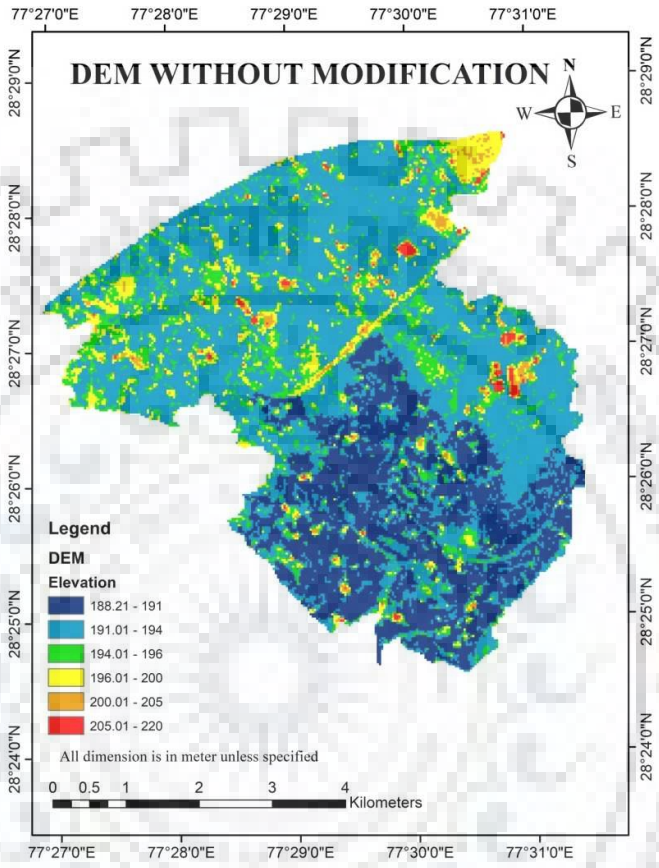

Figure 5 DEM without modification

The DEM of study area was then converted into points so that extra points as per cross-section data can be added, modified or unwanted points can be deleted. While performing modification of DEM, there was a discrepancy (less than measured value) observed in elevation values acquired from DEM and field survey. The elevation value of that points both from DEM and field survey was were noted and compared. It was seen that there was average difference in elevation of 48.21 m. To correct this error the discrepancy, elevations of some permanent structures was noted down and then averaged. This averaged value was added to all respective points. The points were raised in attribute table by 48.21m. The IDW (Inverse distance weighting) interpolation technique was employed to create a smooth surface and hence modified DEM.

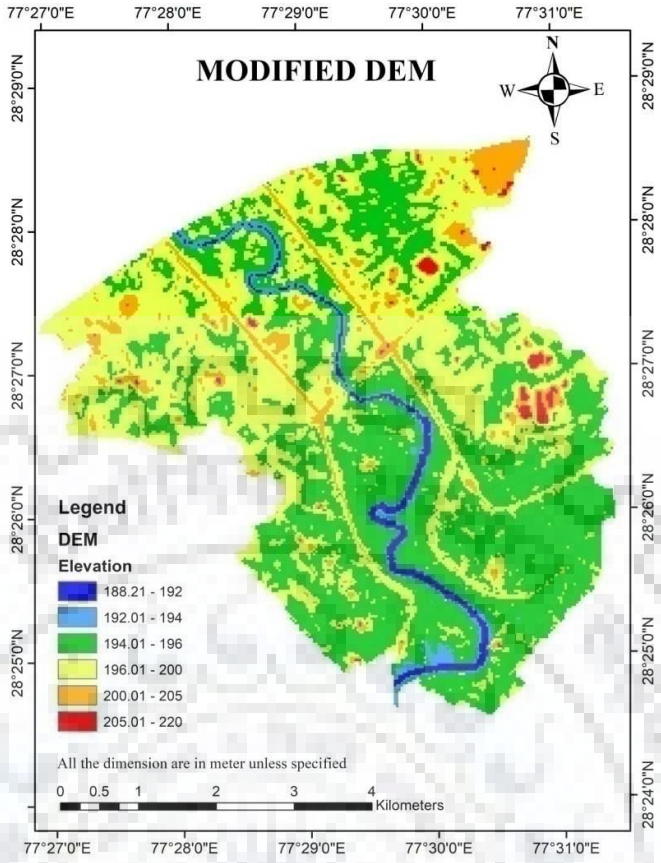

Figure 6 DEM with modification

Figure 6 shows classified DEM after modification of DEM. The modification was done by using Arc GIS software. The raster file thus obtained is the modified DEM. Different color in the map shows a different range of elevation, deep blue showing the deepest area whereas red color highest region. In initially acquired DEM features like river center line, flow path, embankments, roads were not distinct but after modification those features were distinguishable.

5.3. TIN model and Slope map

TIN (Triangular Irregular Network) is a representation of continuous surface having entire triangular facets. The vertices of these triangles are created from field recorded spot elevations through a wide range of methods including surveying through conventional, Level & Theodolite, Global Positioning System Real-Time Kinematic (GPS RTK), Total Station, Photogrammetry, or by any other means. TIN is associated with 3-dimensional data (i.e. x, y, and z coordinates). TINs are also helpful for the description and analysis of horizontal (x and y) distributions and their relationships. TIN model is prepared once DEM is digitized. TIN model is generated by using "create TIN" tool of 3D-analyst tool in Arc GIS interface. The TIN model is required for exporting Arc GIs Map to HEC RAS 5.0.3. The TIN model of the

study area is shown in figure 7.

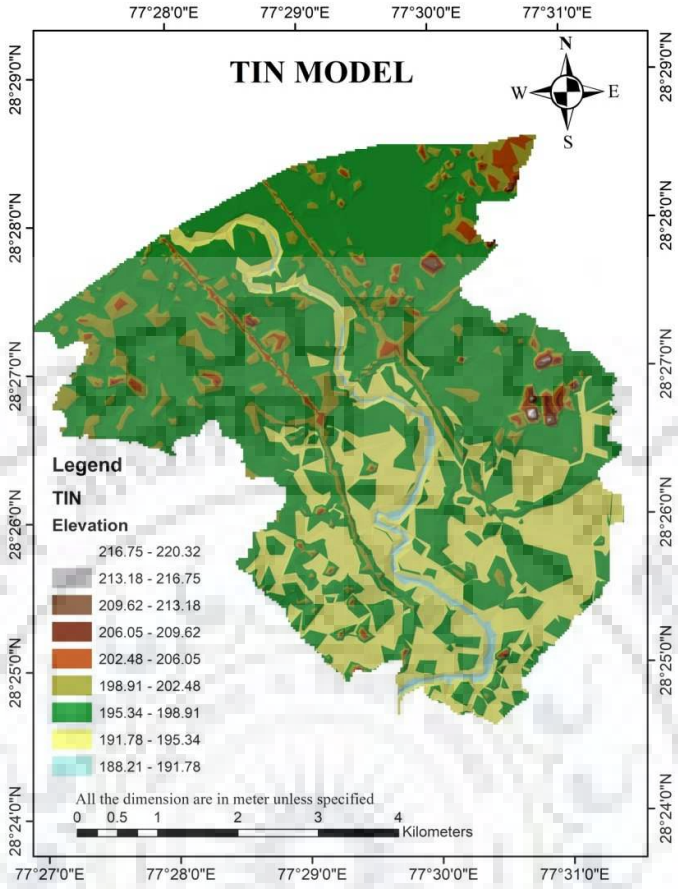

Figure 7 TIN Model

Slope map is a map showing topographical features of an area and gives planner adequate information for the analysis of topographic features which can influence and may influence the process of land development. The slope of the study area can be seen by using the map to which portion of land the slope is steep and which portion is gentle in percentage or in any standard ways as per planner convenience. Slope Map is also prepared in Arc GIS, by using spatial analyst tool by making use of DEM. The slope is the measure of steepness or degree of inclination of a feature with respect to horizontal plane. Gradient, grade, inclination and pitch are interchangeable with slope. Slope is typically expressed as percentage, an angle or a ratio. The average slope of terrain feature can conveniently be calculated from contour lines on a topographic map. To find the slope of a feature, the horizontal distance (run) as well as vertical distance (rise) between two points on a line parallel to the feature needs to be determined. The slope is obtained by dividing rise over run. When this value is multiplied by 100 it is expressed in percentage. The slope angle is generally expressed in degrees.

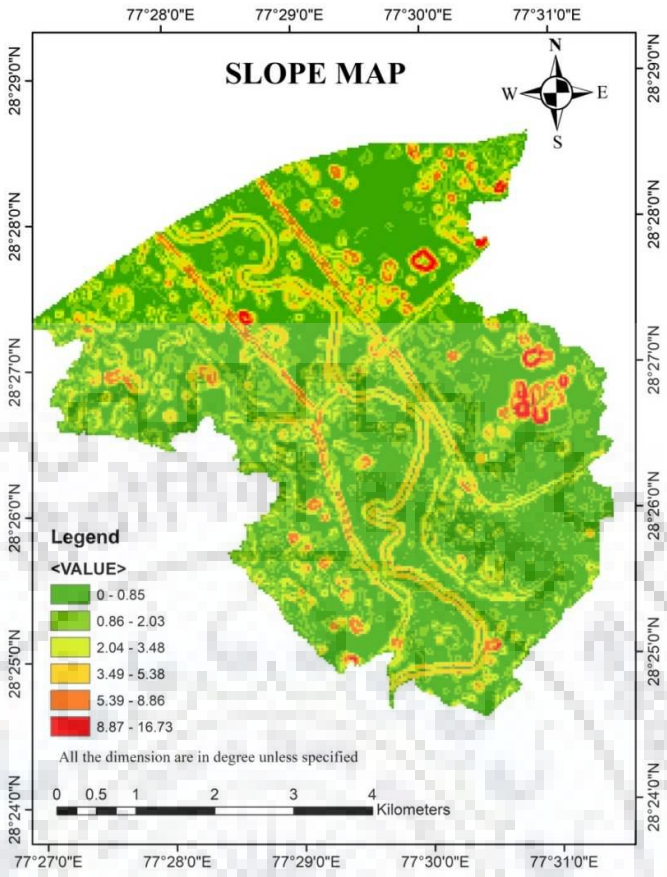

Figure 8 Slope Map

Figure 8 shows a map of study area. The slope of the study area varies from 0 to 16.73 degree. The area with deep green indicates gentle slope followed by light green orange and red. The red color area is the area having a maximum slope. From the figure, it is observed that change in slope near embankments edge, highways and settlement areas is high.

5.4. Land Use Map preparation

Landsat 8 images were used to prepare land use map using Landsat -8 images. Remotely sensed Landsat 8 Operational Land Imager data were acquired from the U.S. Geological website (https://earthexplorer.usgs.gov/). The Landsat 8 satellite consists of two instruments- Landsat 8 OLI and Thermal Infrared sensor (TIRIS). Image used in present study was cloud free and excellent quality. The Landsat 8 OLI data consist of eight spectral bands, band 1 to 7 and band 9, with 30 m resolution and 15m resolution respectively. Land cover classes are typically mapped from digital remotely sensed through the process of supervised, unsupervised and combined classified-unclassified digital image classification. Combined supervised as well as unsupervised classification was done using ground checkpoints and photographs. The area under consideration was classified in five classes: Waterbody, Urban

settlement, Agricultural Land, Barren Land and Urban Plantation. In Figure 9, most of the most are red which indicates urban settlement area, flowed by yellow which indicates agriculture, blue color shows river (water body) etc. In this figure pink color represents barren land and very small pixel of green color represents urban settlement. Urban settlement here is parks, garden, and plantation along edges of the highways etc.

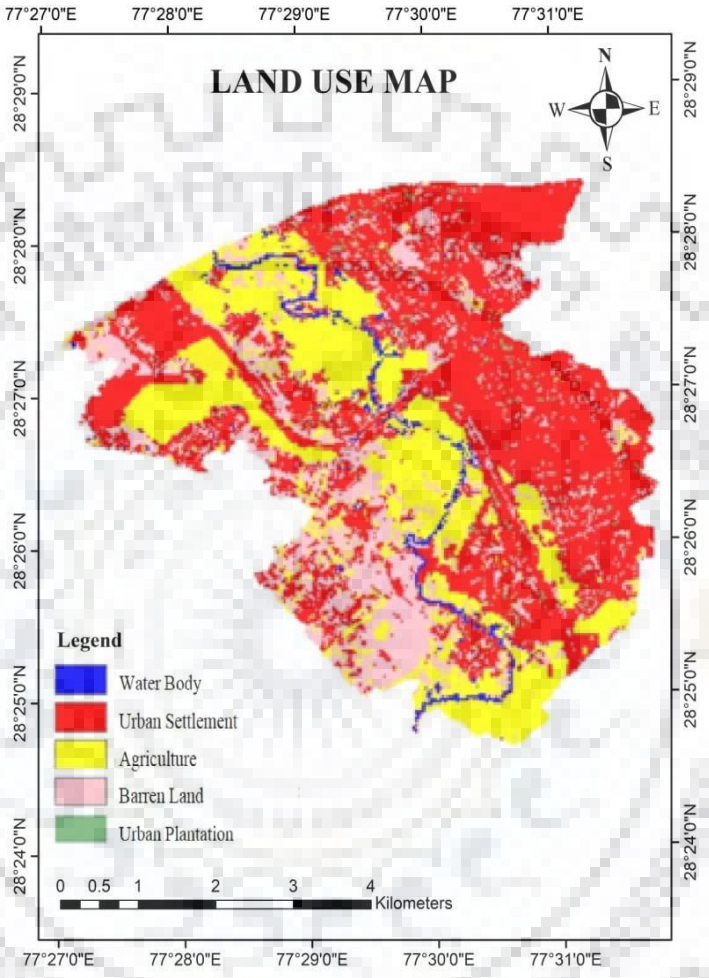

Figure 9 Land use map of the study area

5.5. Estimation of Manning's n

By using land use map, we know the pixel count of each set of land use, and hence the percentage of existing land use is determined. One ideal set of land use with only river bed and barren land was assumed in floodplain and this combination was named as Type 1. The percentage of existing LU/LC determined was named as Type 2. Two more combinations of land used was assumed based on existing LU/LC in the upstream few kilometers above study area and named as Type 3 and type 4. The combination of land used considered for hydraulic modeling shown in figure 10.

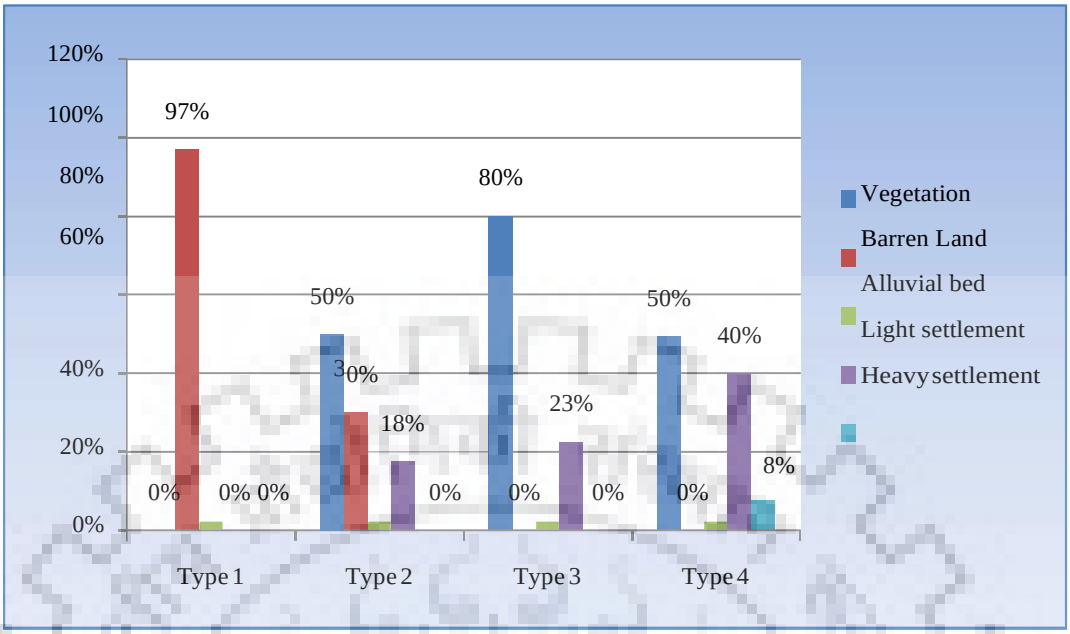

Figure 10 Percentage distribution of land use change for each type

For different land use, Manning's roughness coefficient was estimated. Using Manning's n value and percentage of land cover, weighted mean roughness coefficient were determined. The value of Manning's n was estimated using Chow, 1959 Manning's n table shown Table 3.

Table 3 Manning's n for Channels (Chow, 1959)

S. No	Type of Channel and Description	Minimum	Normal	Maximum
	Natural rivers - minor rivers top width at flood stage = 100 feet or 30.48 m			
1	Main Channels			
a.	straight, clean, full stage	0.025	0.03	0.033
b.	same but more stones and weeds	0.03	0.035	0.04
c.	winding, clean, some pools and shoals	0.033	0.04	0.045
d.	same as above with some weeds and stones	0.035	0.045	0.05
e.	same as above with lower stages, more ineffective slopes and sections	0.04	0.048	0.055
f.	same as "d" with more stones	0.045	0.05	0.06
g.	weedy, sluggish reaches & deep pools	0.05	0.07	0.08
h.	deep pools with very weedy reaches or floodways with a heavy stand of timber and underbrush.	0.075	0.1	0.15

3	Floodplains			
a.	Pasture, no brush			
i	short grass	0.025	0.03	0.035
ii	high grass	0.03	0.035	0.05
b.	Cultivated areas			
i	no crop	0.02	0.03	0.04
ii	mature row crops	0.025	0.035	0.045
iii	mature field crops	0.03	0.04	0.05
c.	Brush			
i	scattered brush, heavy weeds	0.035	0.05	0.07
ii	light brush and trees, in winter	0.035	0.05	0.06
iii	light brush and trees, in summer	0.04	0.06	0.08
iv	medium to dense brush, in winter	0.045	0.07	0.11
v	medium to dense brush, in summer	0.07	0.1	0.16

The different values of Manning are n considered for the present study is shown in Table 4.

Table 4 Manning's n value taken for different LU/LC.

S. N.	Land use/ Land cover	Manning's n value
1	Vegetation	0.050
2	Barren Land	0.035
3	Alluvial bed	0.030
4	Light settlement	0.10
5	Heavy settlement	0.15

By using Manning's n value (Table 4), weighted Manning's n was calculated considering its land use pattern. With the Land use distribution shown below, overall weighted Manning's roughness coefficient was calculated as shown below:

$n = n_1*P_1+n_2*P_2+n_3*P_3+ n_4*P_4$ Where, n= overall Manning's n

n_1, n_2, n_3 & n_4 = Manning's roughness coefficient for land use & land cover Type 1, Type 2, Type 3 and Type 4 respectively.

P_1, P_2, P_3 & P_4 = Percentage of land use & land cover Type 1, Type 2, Type 3 and Type 4 respectively in the flood plain

5.6. Processing in HEC RAS

The supporting file .e. projection file (*.prj) and Amiga Disk File (*.adf) is created for respective UTM Zone. Using that supporting file, TIN model is projected and then imported in HEC-RAS model through RAS mapper menu.

5.7. HEC RAS Geometric Model

The TIN model thus imported is processed in Geometric data editor. Flow area& river centerline is defined in geometric data editor. Land use/ Land cover for Manning 's roughness is also defined here. Flow mesh of desired size was defined. In this study, cell size was taken as 10m X 10m, 30m X 30m and 50m X 50m. Upper, lower and intermediate boundary condition line was also defined here. The Geometric Data editor with flow area and flow mesh is shown in Figure 11.

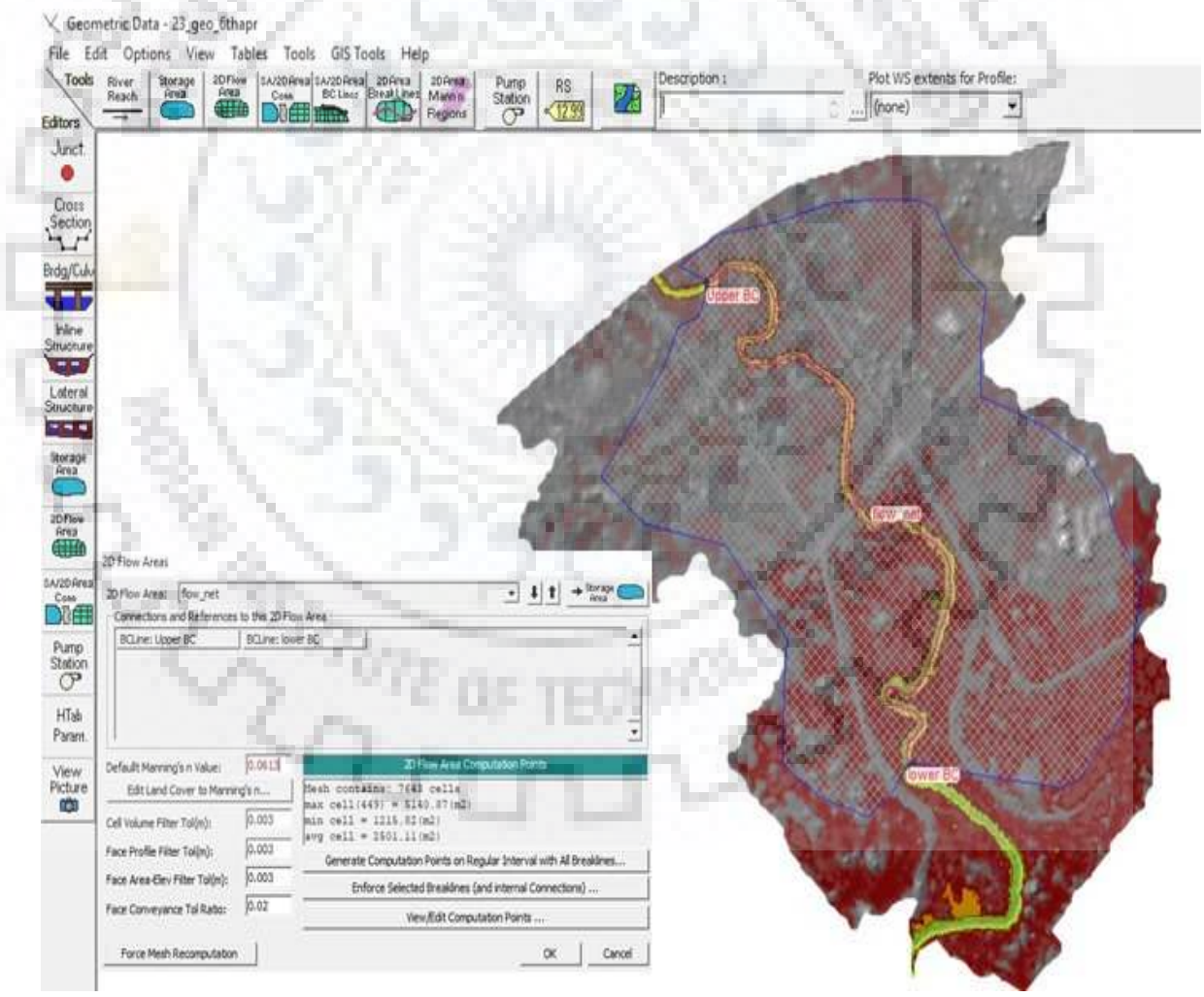

Figure 11 Geometric Editor Window

5.7.1. Boundary conditions

The following boundary conditions that can be applied in HEC RAS 5.0.3 for this type of study are described below:

a. Flow Hydrograph

In HEC RAS 5.0.3, flow hydrograph is used as boundary condition direct flow towards 2D flow area. The data required for using flow hydrograph as boundary condition i) flow hydrograph & ii) Energy Slope. The energy slope is necessary to calculate normal depth. The energy slope is used to calculate normal depth by using cross-section data and flow data. In present flow, hydrograph is used as an upstream boundary condition.

b. Stage Hydrograph

In HEC RAS 5.0.3, stage hydrograph is used bring flow towards or outside of 2D flow area. If WSE in this type of hydrograph is higher than cell WSE, the flow will go into two-dimensional cell and if it is lower than WSE, flow will move away from two-dimensional area. It is also calculated on per cell basis

c. Normal Depth

It can be used as boundary condition to take flow out of two-dimensional flow area. Friction slope value is required while using normal depth as boundary condition. Friction slope is calculated by using land slope in the vicinity of two-dimensional areas. It is also calculated on per cell basis. In present study normal depth condition is used as downstream boundary condition.

d. Rating Curve

Rating curve is water surface elevation v/s flow curve. It is also used to take flow out of two-dimensional flow areas. It is also calculated on per cell basis.

e. Precipitation

Excess rainfall can be used by precipitation boundary condition. Excess rainfall is precipitation minus interception/infiltration. It can be applied as boundary condition through unsteady flow data editor.

In the present study, flow hydrograph was used as upstream boundary condition where as normal depth was used as downstream boundary condition. Due to unavailability of rating curve normal depth was used as downstream boundary condition. Simulation was carried out for various flow conditions to study severe conditions too.

5.7.2. Simulation using HEC RAS 5.0.1

After applying boundary condition and Manning's n values, the model is set for simulation. Simulation plan is created for obtaining the desired output. The plan for simulation content is shown in Figure 12.

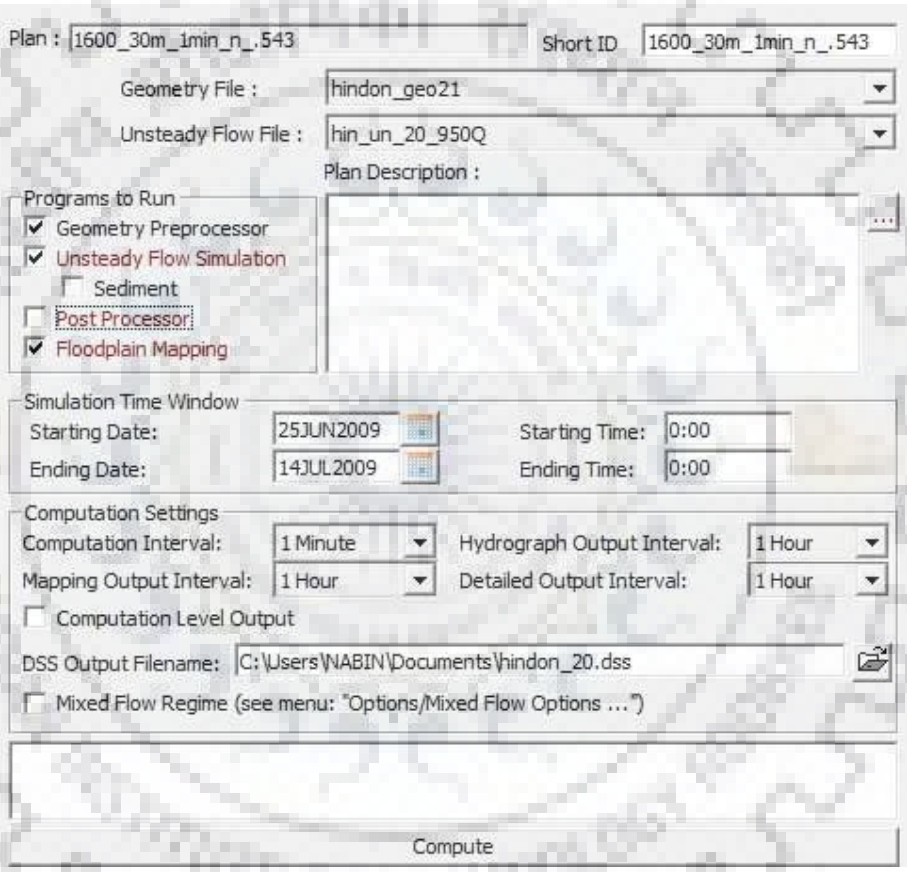

Figure 12 Plan windows of HEC RAS

For model simulation, date and time of simulation were applied in the plan. The computational setting was also modified as per study requirements. It contains hydrograph output interval, mapping output interval, and computational time interval. For present study, computational time interval was set as 10 sec, 1 minute, and 10 minutes. For same set of data if computational time interval is less it requires more time for model simulation. It is more than twice depending on the computational time interval chosen. For running of one model at 30m X 30m cell size and time step 10 sec, the simulation time required may be as big as 30 hrs or so. Though

reducing time step requires lots of simulating time, it is advisable not to do simulation at more than 1min computational time interval for dam break analysis study (Brunner, 2016). After simulation is finished, the following output was observed at every point in the flow area:

a. Water surface elevation
b. Depth of flow
c. Velocity of flow
d. Shear stress distribution

In HEC RAS 5.0.3, one can easily view two-dimensional flow progresses with respect to time will be easily visible. One can easily find out the stage of river with respect to passes of time with velocity distribution in the flow for simulated time. In present study model was simulated for different time step (10 sec, 1 min & 10 min) and different cell size (10 m X 10m, 30m X 30m, 40m X 40m & 50m X 50m). For each flood even model was simulated and result was recorded.

5.8. Sensitivity analysis of Manning's roughness coefficient, n on flood level

For each flood event and different values of Manning's n(0.035, 0.0543, 0.0613 & 0.076) keeping cell size same for each n values, model was simulated. The WSE for each n value v/s time of flow were plotted compared and analyzed. This process was repeated for each flood event. The maximum value WSE's obtained for each flood event and each manning's n value was exported to Arc GIS. In Arc GIS, WSE along the center line of river for each flood event was extracted. The WSEs was plotted against simulated discharges, compared and analyzed.

5.9. Sensitivity analysis of cell size on flood level

For each flood event and different values of cell size, (10 m X 10m, 30m X 30m, 40m X 40m & 50m X 50m) keeping Manning's n & computational time interval same, model was simulated. The WSE for each cell size v/s time of flow were plotted compared and analyzed. This process was repeated for each flood event.

5.10. Sensitivity analysis of time step on flood level

For each flood event and different values of computational time, (10 sec,1 min, &10 min) keeping cell size &Manning's n same, model was simulated. The WSE at each computational time v/s time of flow were plotted compared and analyzed. This process was repeated for each flood event.

5.11. Sensitivity analysis of time step on velocity

For each flood event and different values of computational time, (10 sec, 1 min, &10 min)

keeping cell size & Manning's n same, model was simulated. The velocity at each computational time v/s time of flow was plotted compared and analyzed. This process was repeated for each flood event.

For present study, the velocity distribution for 10 sec time step and 1-minute time step was found to be stable and similar but velocity distribution for 10 minutes time step showed abrupt rise and fall as shown below. The figure shown below is velocity profile for same flow having peak 1100m^3/s and cell size 30m X 30m by varying computational time i.e. 10 sec, 1 min & 10 min. The Figure 13, shows velocities obtained after simulation of model at different time step for flow discharge with peak 1100 m^3/s, cell size 30m X 30m.

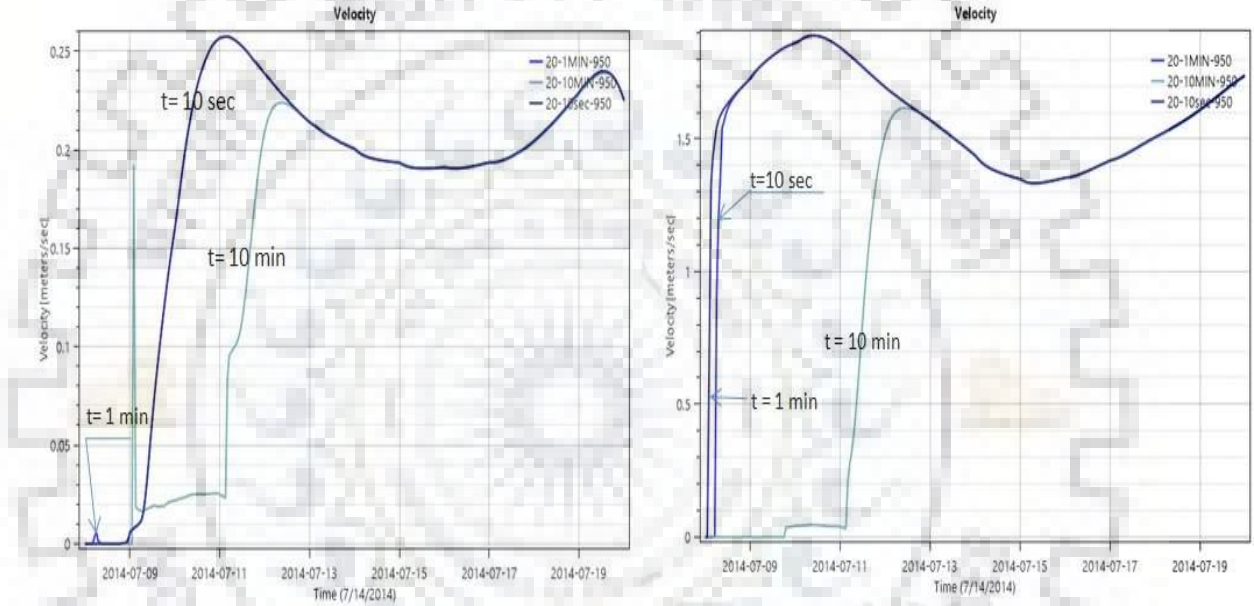

Figure 13 Effect of time step on velocity

5.12. Flood Inundation Mapping

The result from HEC RAS 5.0.3 gives the extent of flooding in two dimensions along with WSEs at each cell. This result was obtained for each manning's n and exported to Arc GIS. The exported raster file is converted to vector and area of inundation for each Manning's n was calculated. The percentage change (increase or decrease) in inundation due to change (increase or decrease) in Manning's n was calculated. This process was conducted for two flood events (with peak 800 m^3/s & 2450 m^3/s). The values so obtained was discussed and analyzed.

5.13. Flowchart of Methodology

This flowchart is a pictorial representation of methodology described in above from 5.1to 5.11. The methodology of can is visualized briefly through the flowchart shown in Figure 14.

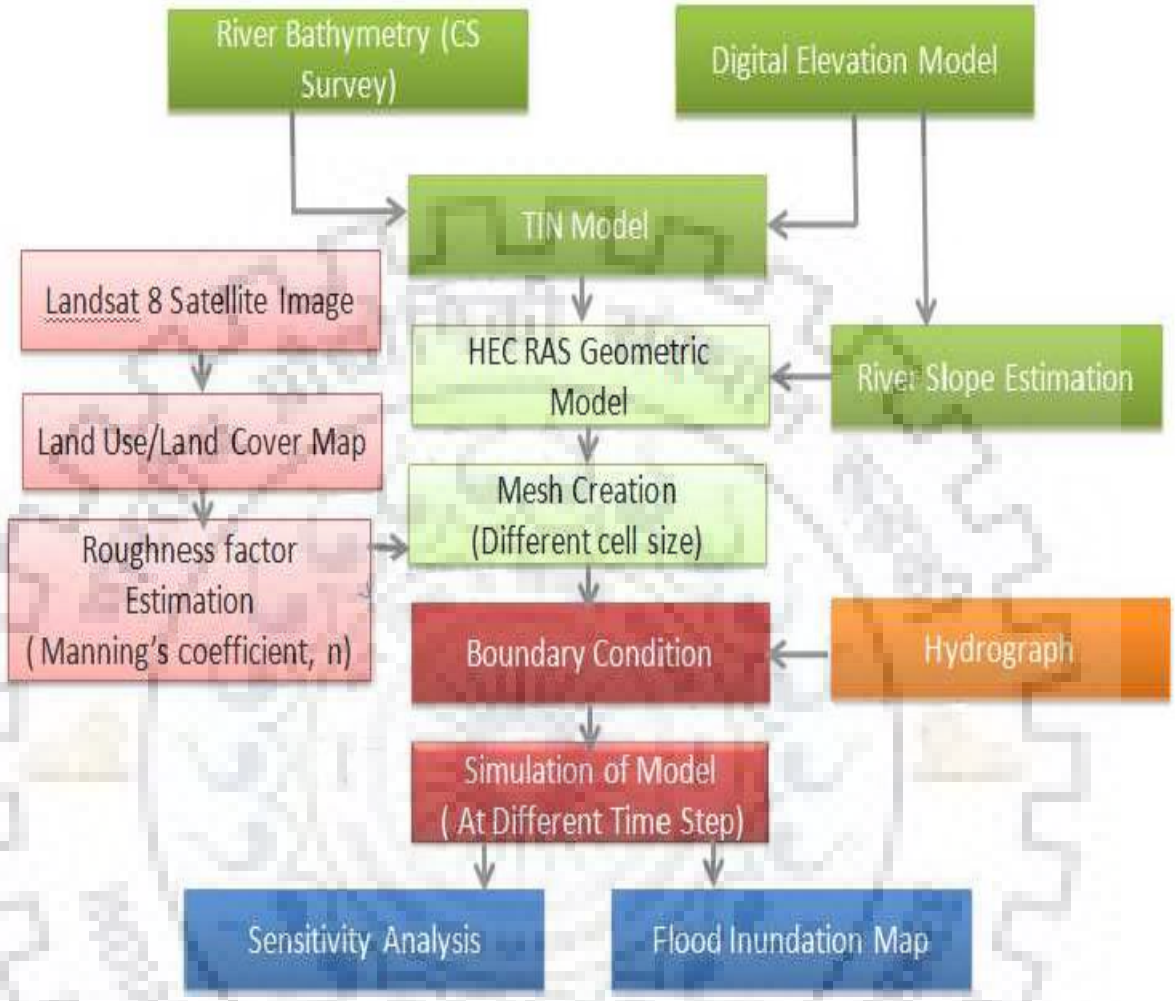

Figure 14 Flow chart of the methodology

6. RESULTS AND DISCUSSION

The sensitivity analysis of land use in terms of Manning's n, the sensitivity of cell size and time step (computational time interval) on HEC RAS model was performed. The sensitivity on inundation or flood level in present study is presented in terms of Water Surface Elevation (WSE). The objective wise result with discussion is presented below.

6.1 Sensitivity of different land uses, i.e. varying Manning's n on WSE

Four combinations of land use were assumed (Type 2 represents present scenario) in flood plain for this study namely Type 1, Type 2, type 3 & Type 4. Type 2 is existing conditions of LU/LC in the study whereas rest of the combination of LU/LC has been taken on the basis of LU/LC practices on few kilometers upstream of study area on Hindon River flood plain. The existing land use is obtained from land use/ land cover map (explained in methodology). Table 5 shows the percentage distribution of LU/LC in each combination assumed.

Table 5 Percent distribution of land uses for each type in the flood plain area

Land use/ Land cover	Type 1	Type 2 (Existing Condition)	Type 3	Type 4
Vegetation	= 0.0	= 50.0	= 75.0	= 49.5
Barren Land	97.5	30.0	0.0	0.0
Alluvial bed	2.5	2.5	2.5	2.5
Light settlement	0.0	17.5	22.5	40.0
Heavy settlement	0.0	0.0	0.0	8.0

The Manning's n value for the present study was estimated by defining n value for each land use/ land cover pixel based on the standard roughness coefficient values (Chow, 1959) shown in Table 3. Manning's n value for heavy and light settlement was taken from LU/LC values used by NRCS for dam breach analysis in State of Kansas, United States. Manning's 'n' values are provided in the model to define the roughness coefficient values for each grid. The roughness coefficient used in HEC RAS model is the weighted mean value of Manning's n and was calculated for each set of land use (Table 5). The method of calculation is explained in methodology. The weighted average value of Manning's n, in each combination is illustrated in

Table 6 below.

Table 6 Calculation of weighted average value of Manning's n

Land use/ Land cover	Manning's n value	Type 1	Type 2	Type 3	Type 4
Vegetation	0.05	0	0.025	0.038	0.0233
Barren Land	0.035	0.0339	0.0105	0	0
Alluvial bed	0.03	0.0007	0.0008	0.0008	0.0007
Low-Intensity settlement	0.1	0	0.018	0.0225	0.04
High-Intensity settlement	0.15	0	0	0	0.012
Weighted average value of Manning's n =		0.035	0.0543	0.0613	0.076

The calculated weighted average manning's n value is then used in Geometric Data Editor of HEC RAS model for sensitivity analysis on WSE for varying Manning's n (i.e. n=0.035,0.0543, 0.0613 & 0.76) value for three different flow conditions. Simulation of model was done with all types of land use considered, WSE of upstream point and downstream point was obtained for all set of land use type (Manning's n) separately. For each set of flood event data, simulation of HEC RAS model was performed four-time (i.e. each time with different manning's value). Three flood events with peak flow 800 m^3/s, 1100 m^3/s& 2450 m^3/s were used for obtaining result regarding the sensitivity of Manning's roughness for varying land uses on flood inundation.

6.1.1. Sensitivity analysis with peak 800 m3/s

This sensitivity analysis was carried out with hydrograph with peak 800 m3/s, cell size 30m X 30m and computational time interval = 10 sec. HEC RAS gave the hydraulic parameters like Water surface elevation, velocity and depth of flow as output of model simulation. For this study, data required for model simulations are flow hydrograph, Manning's n and slope. The flow hydrograph is used as upper boundary condition and normal depth was used upstream and downstream boundary condition. The Manning's n used was taken from Table 6. The flow hydrograph used for simulation of model for this case is shown in Figure 15.

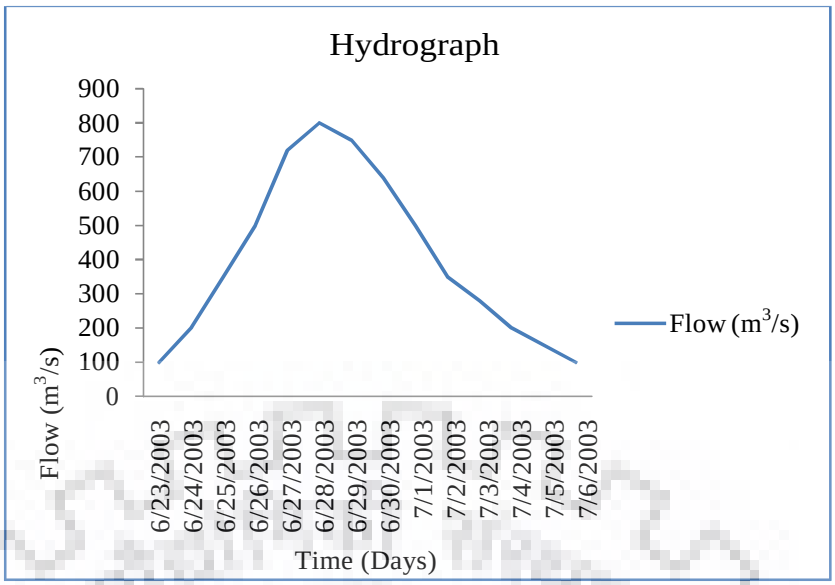

Figure 15 Hydrograph with peak 800 m^3/s

Analysis and discussion

Figure 16 & Figure 17 is represents WSE of 2+400 m u/s & 2+000m d/s point respectively on the river. The result shows WSEs for different Manning's n. The tabular results are shown in Appendix-2.

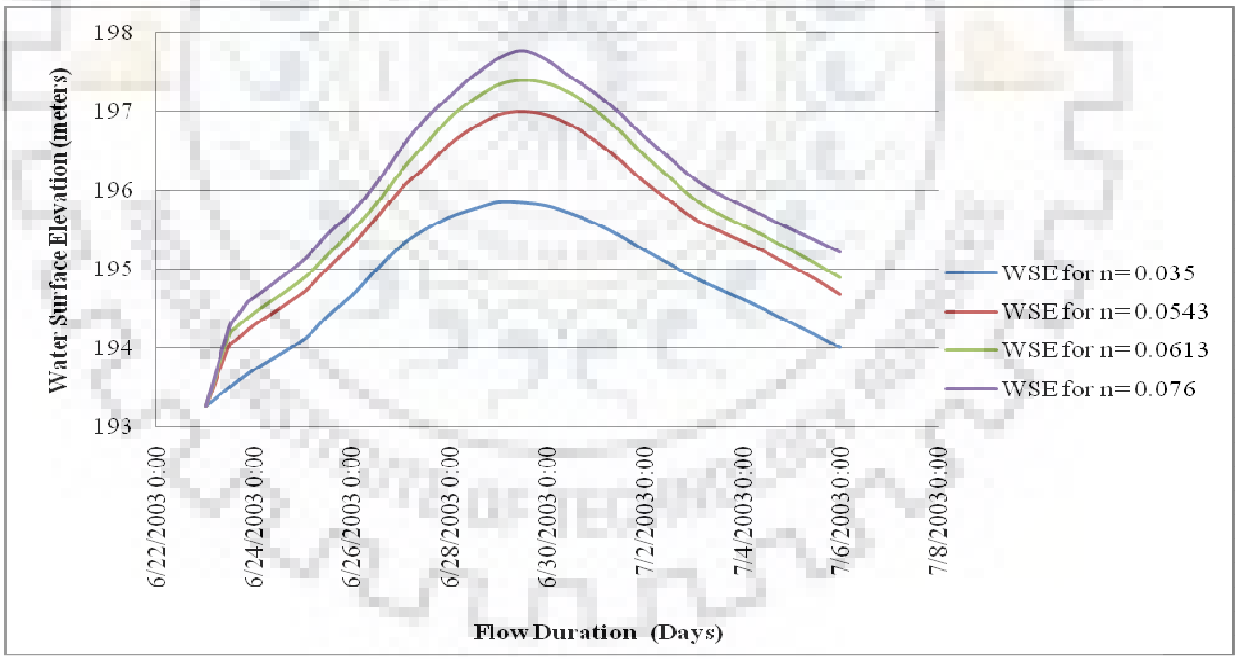

Figure 16 WSE for different Manning's n (with peak 800m^3/s) at u/s point

The above result shows that when Manning's n value is 0.035, 0.0543, 0.0613 and 0.076, the corresponding water surface elevation is 195.93m, 196.65m, 196.83m and 197.73m respectively. The increase in WSE when n changes from 0.35 to 0.76 at the upstream point considered is1.80m.The result shows change in WSE or flow/flood depth is directly proportional to change in roughness coefficient i.e. Manning's n.

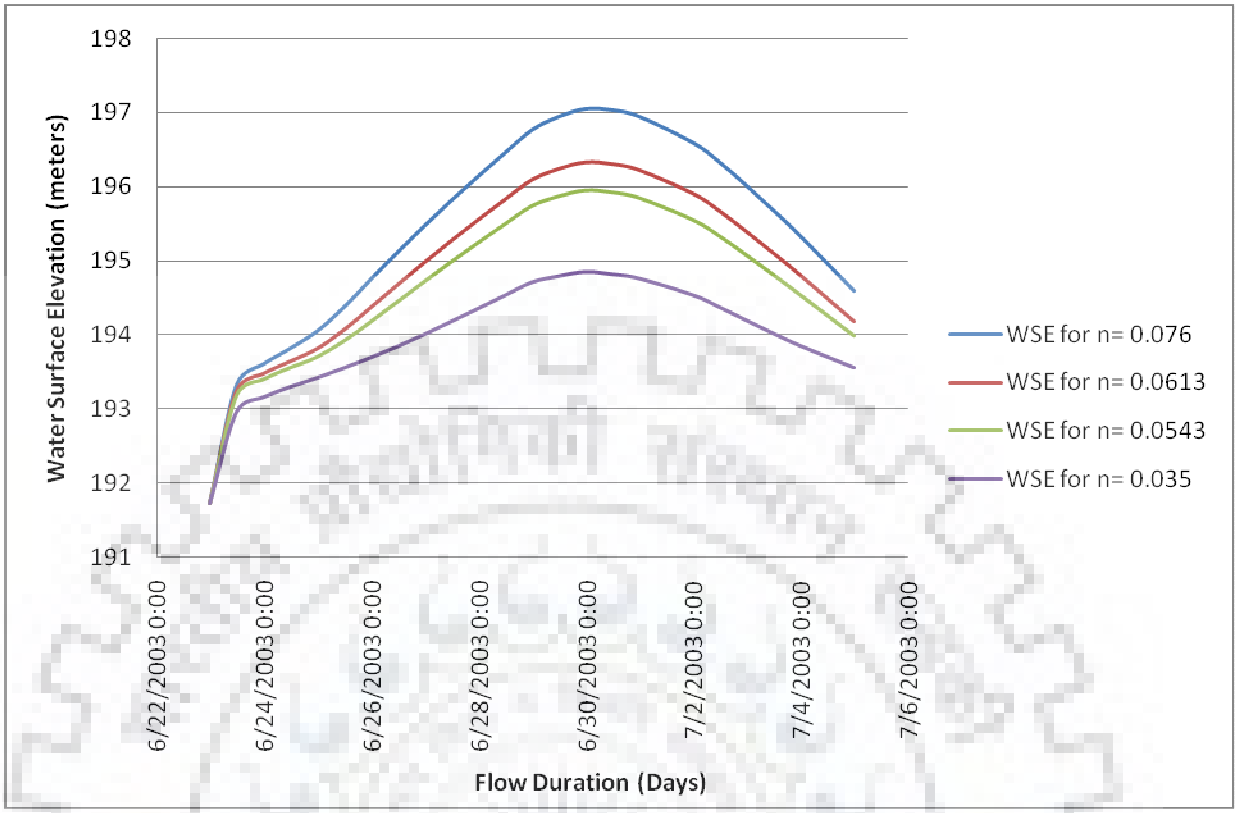

Figure 17 WSE for different Manning's n (with peak 800m^3/s) at d/s point

The result obtained from the downstream point is shown in Figure 17. The result followed a similar trend as an upstream point. When n changes from 0.035 to 0.076, there is a rise in water level by 2.20m. This value is greater than upstream value by 0.40m. It showed that at downstream point increase in WSE's is more for a similar increase in Manning's n value. The WSE's for n= 0.35, 0.543, 0.613 & 0.76 is 194.83, 196.01, 196.37 & 197.03 respectively. The tabular form of this result is shown in Appendix 3.

The Figure 18 is the plot of maximum WSE along the river centerline due to various Manning's n with respect to river bed profile. The different color line shows WSE for particular Manning's n value with respect to river bed level.

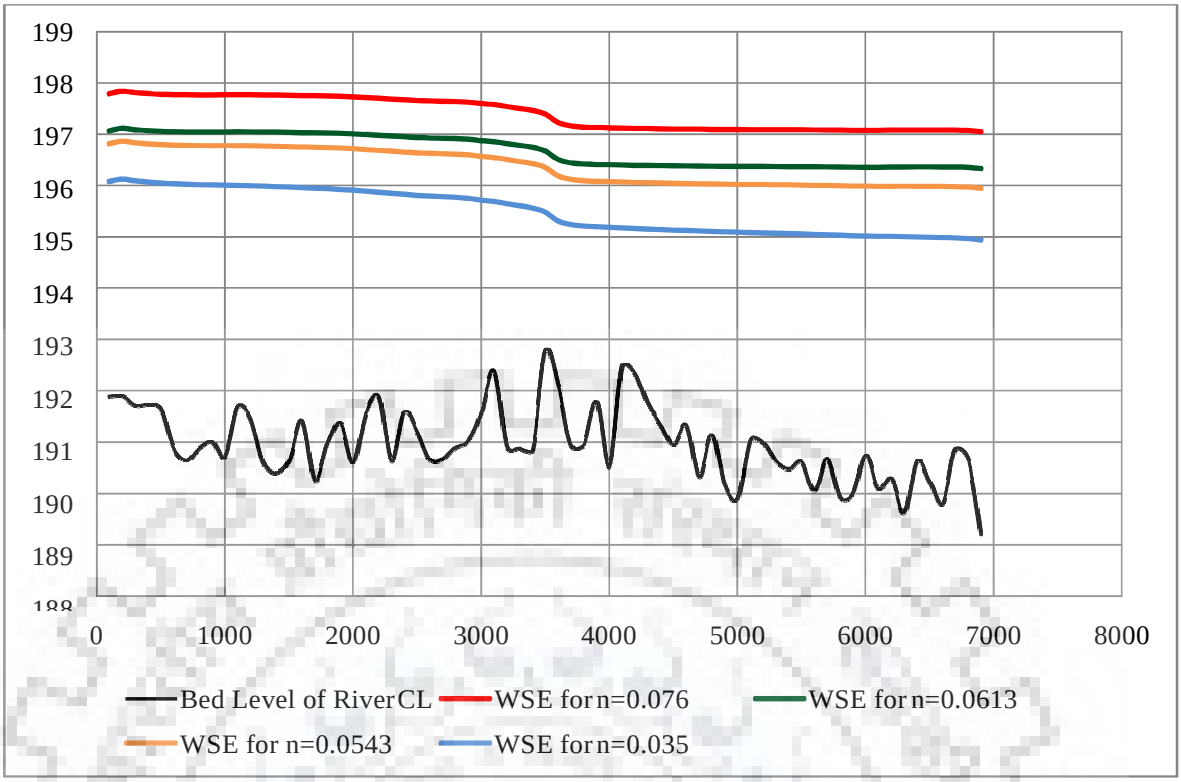

Figure 18 WSE at different Manning's n along the river centerline

The figure shows that there is drop in the WSE level nearly at 3600m from point of start. This drop in WSE may be due sudden to following reasons.

- The decrease in the bed level towards the downstream.
- Encroachment of flow area due to bridge construction.
- The increase in velocity in that portion

There is less drop in the WSE profile for n = 0.076, in comparison to WSE at n=0.035. The reason behind this is an increase in submergence of the nearby ground surface.

6.1.2. Sensitivity analysis with peak 1100 m3/s

This sensitivity analysis was carried out with hydrograph with peak 800 m3/s, cell size 30m X 30m and computational time interval = 10 sec. The hydraulic parameters like Water surface elevation, velocity and depth of flow as the output of the model simulation.

The flow hydrograph used for simulation of the model under above condition is shown in Figure 19.The flow hydrograph and normal depth condition were used as upstream and downstream boundary condition respectively. By using above condition model was simulated and WSE for each value of Manning's n was recorded. The graph of WSE's for particular Land use type (denoted by Manning's n) was plotted. One graph was plotted for the upstream, and one for downstream.

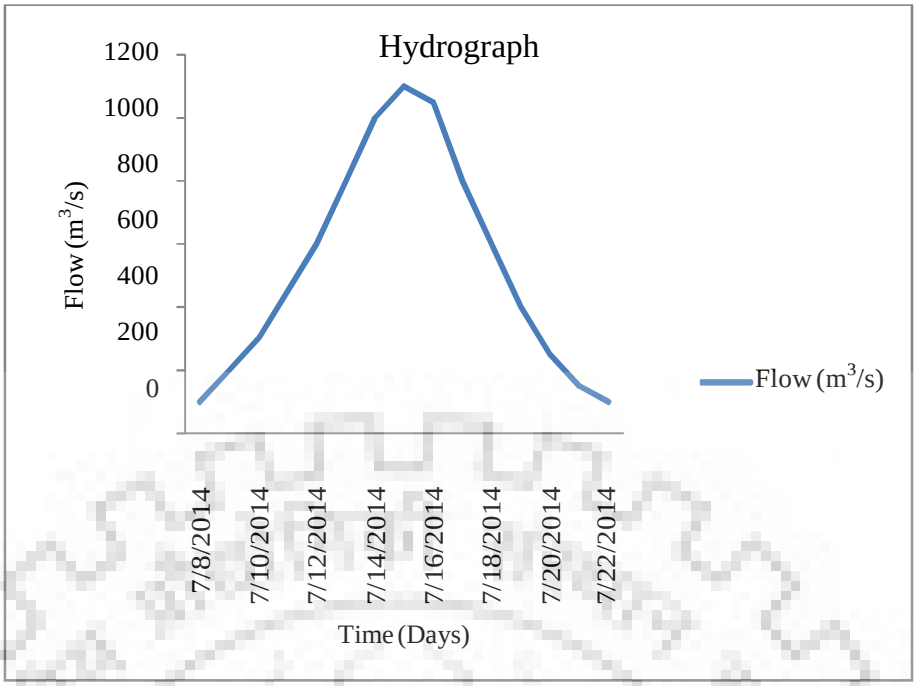

Figure 19 Hydrograph with peak 1100 m^3/s

Figure 19 is the hydrograph of second flood event that was used for this study. This flood event was used for simulation keeping cell size and time step similar to that of flood event one so that further change in WSE can be recorded compared and analyzed.

Analysis and discussion

Figure 20&Figure 21 represents the WSE on 2+400 m u/s & 2+000m d/s point on the river. In this case flood even with peak more than previous was taken to find variation in results. The result shows a variation of WSE with different Manning's n.

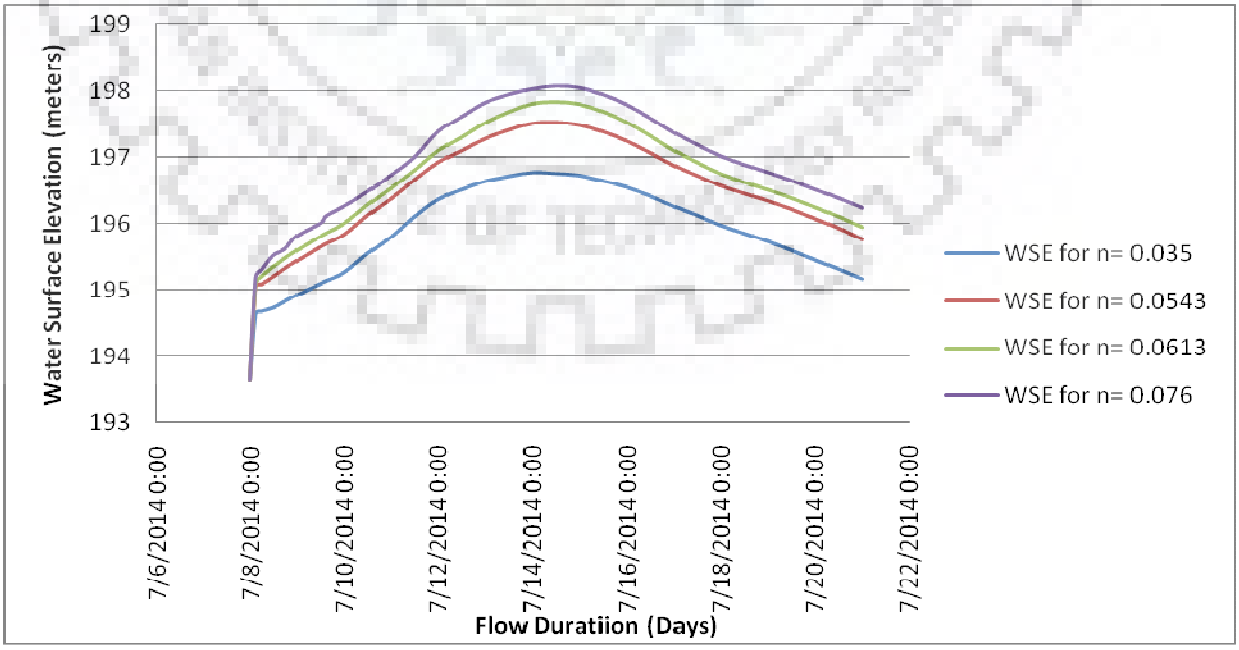

Figure 20 WSE for different Manning's n (with peak 1100m^3/s) at u/s point

The result obtained here shows a similar trend of variation of WSE with different Manning's n value. In this case, the increase in WSE when Manning's n changes from 0.035 to 0.076 is 1.28m. The result shows that when Manning's n value is increased from 55% to 75% and 117% (from 0.0543 to 0.0613 and 0.076), there is an increase in WSE by 0.28 m and0.51m respectively. This means between 20% and 62% further increase in manning value there is 38% and 69% increase in WSE. The tabular form of this result is shown in Appendix 4.

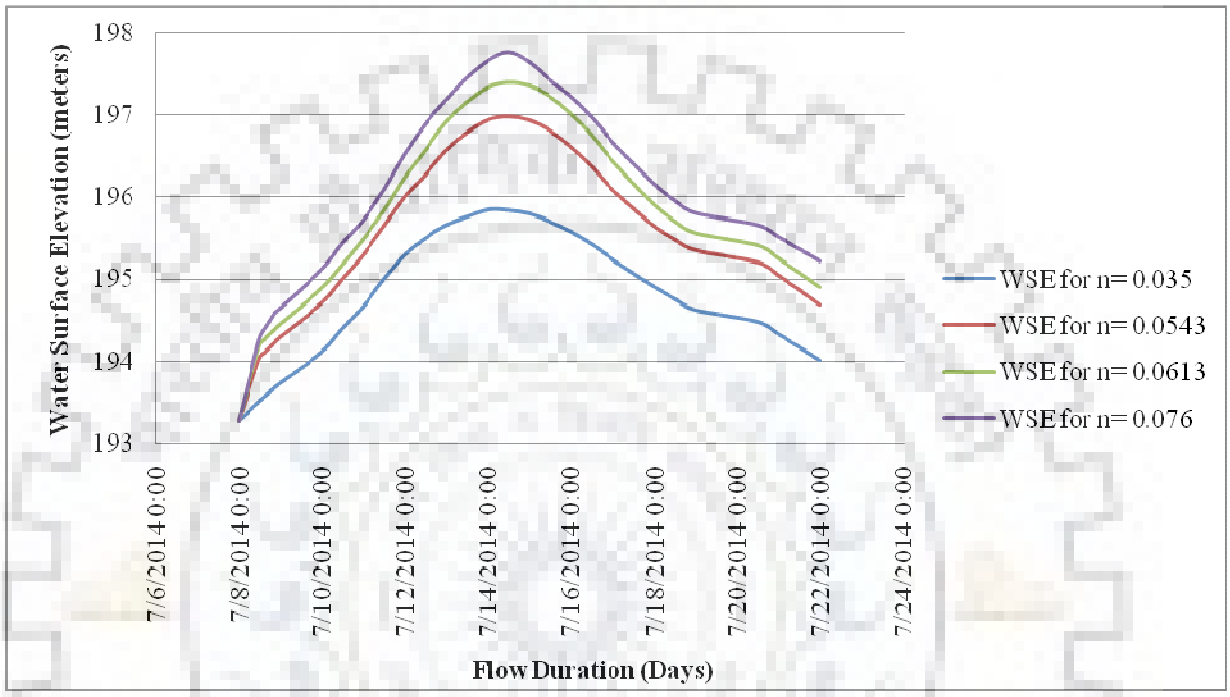

Figure 21 WSE for different Manning's n (with peak 1100m^3/s) at d/s point

The result for d/s point also shows a similar trend as u/s point, In this case, the increase in WSE is 1.82m. The result shows there is an increase in change in WSE by 0.54m. This show change in WSE for each flood event is more in downstream reach of the flood. The change in WSE followed a similar trend as in flood event 1 (with peak 800 m^3/s). The tabular form of this result is shown in Appendix 5.

Figure 22 is the WSE profile along the river centerline due to different Manning's n with respect to river bed profile.

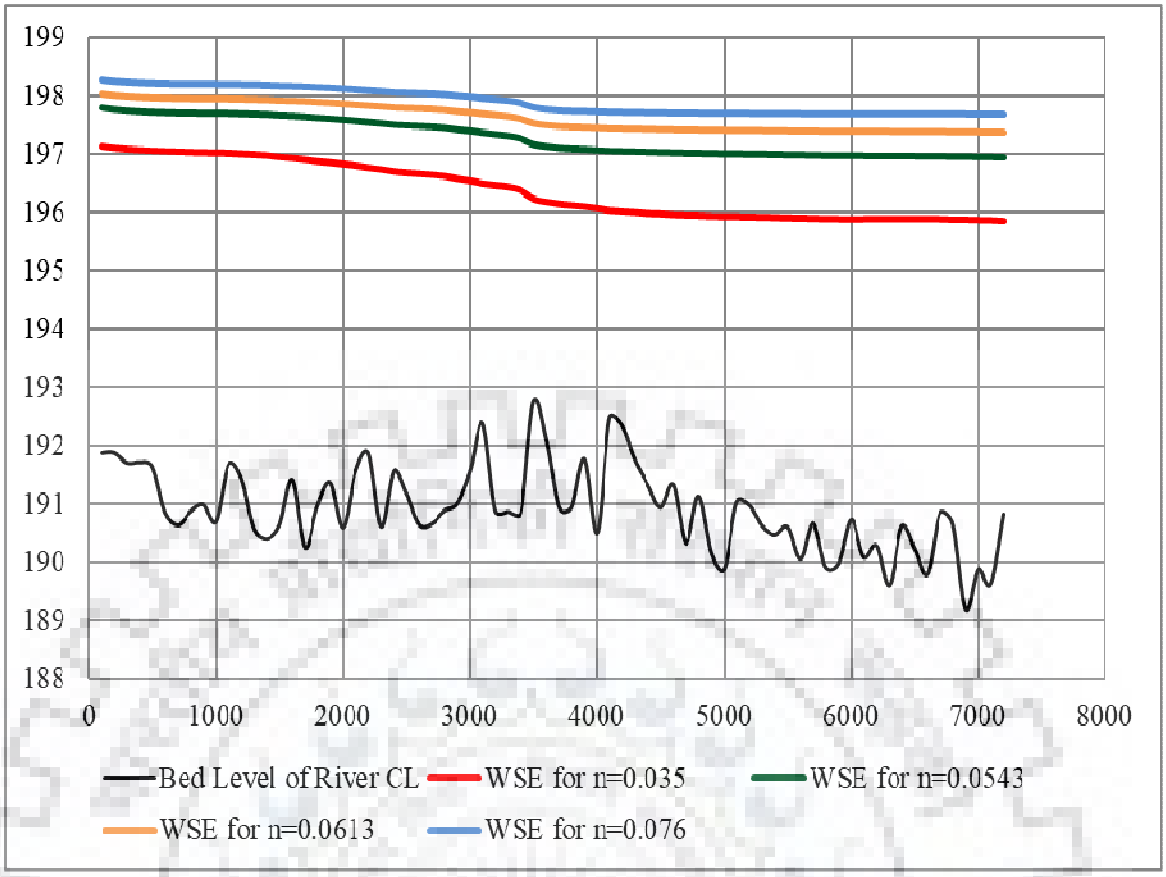

Figure 22 WSE at different Land use along river center line

The graph shown above is a graph showing WSE for different Manning's n obtained by varying land use as discussed in Table 5 & 6 above. It shows a similar trend as in case of flood event with peak 800 m^3/s. It can be clearly seen in the figure below that there is more increase in the difference in WSE's in downstream than in upstream. This fluctuation is due to decrease in velocity observed downstream. The decrease in velocity observed may be due to several reasons but it is mostly due to terrain slope and a decrease in a waterway in the downstream. The different color line shows WSE for different Manning's n value with respect to river bed level.

6.1.3. Sensitivity analysis with peak flow 2450 m3/s

This sensitivity analysis was carried out with hydrograph with peak 2450 m^3/s, cell size 30m X 30m and computational time interval = 10 sec. HEC RAS gave the hydraulic parameters like Water surface elevation, velocity and depth of flow as the output of the model simulation.

The daily hydrograph that is used as boundary condition for simulation of the model for the above case is shown below. This was the extreme condition flood event which showed maximum inundation when the model was simulated. It was the last flood event considered for the analysis of change in flood level for different Manning's n value. The model was simulated and the hydraulic parameters like velocity, depth of water and each cell and water surface elevation were recorded. The graph was plotted to keep WSE as ordinate and Time in days as abscissa shown in Figure 23.

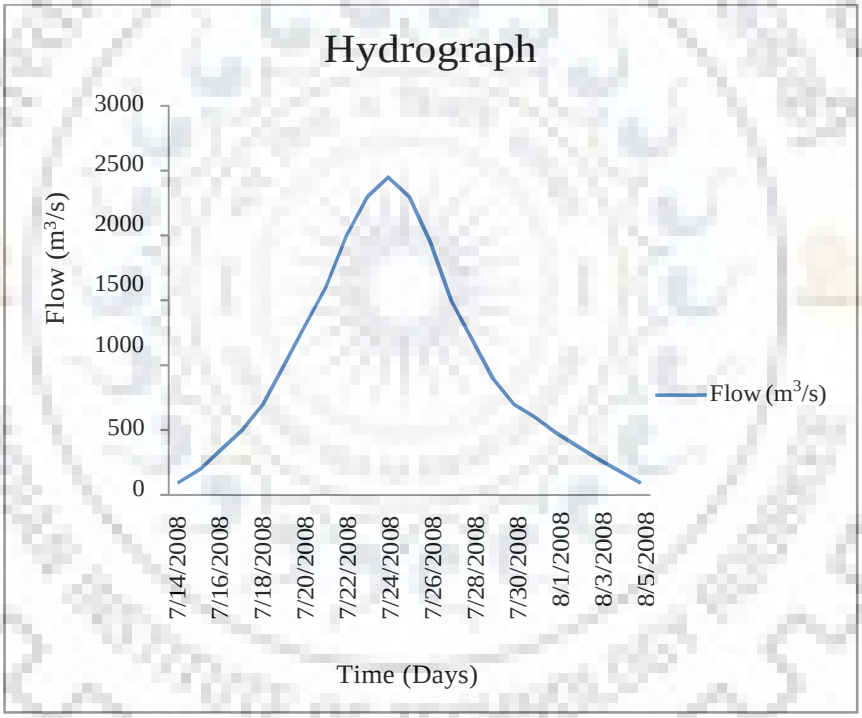

Figure 23 Hydrograph for peak 2450 m^3/s

Analysis and discussion

Figure 24 represents the WSE due to flow with peak of 2450 m^3/s on 2+400 m u/s point on the river. The tabular form of this result is shown in Appendix 6.

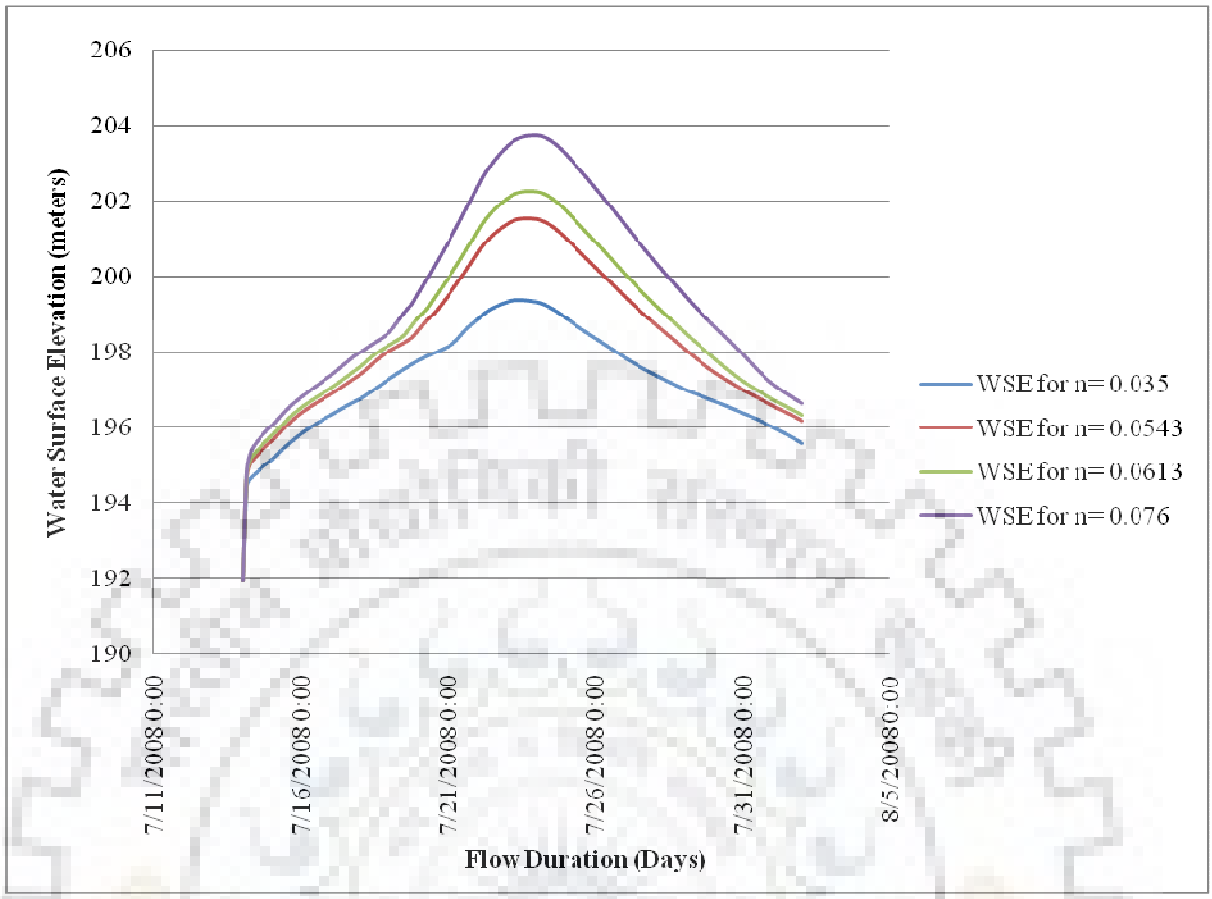

Figure 24 WSE for different Manning's n (with peak 2450m^3/s at u/s point)

The result shows a variation of WSE for different Manning's n. The nature of result obtained in this case is also same as previous results. For upstream point, when n changes from 0.035 to 0.076 there is a rise in water level by 4.35m. The result shows that there is an increase in inundation depth for the same change in Manning's n value. The increase in WSE, in this case, is higher than one storey buildings. It can be observed that when Manning's n value is kept existing scenario (type 2 in this case n =0.0543), the WSE is 2.15m more than type 1 (n=0.035).

Figure 25 represents the WSE due to flow with peak of 2450 m^3/s on the river. The tabular form of this result is shown in Appendix 7. The downstream point considered in this case is at 1+800 d/s of bridge Yamuna Express

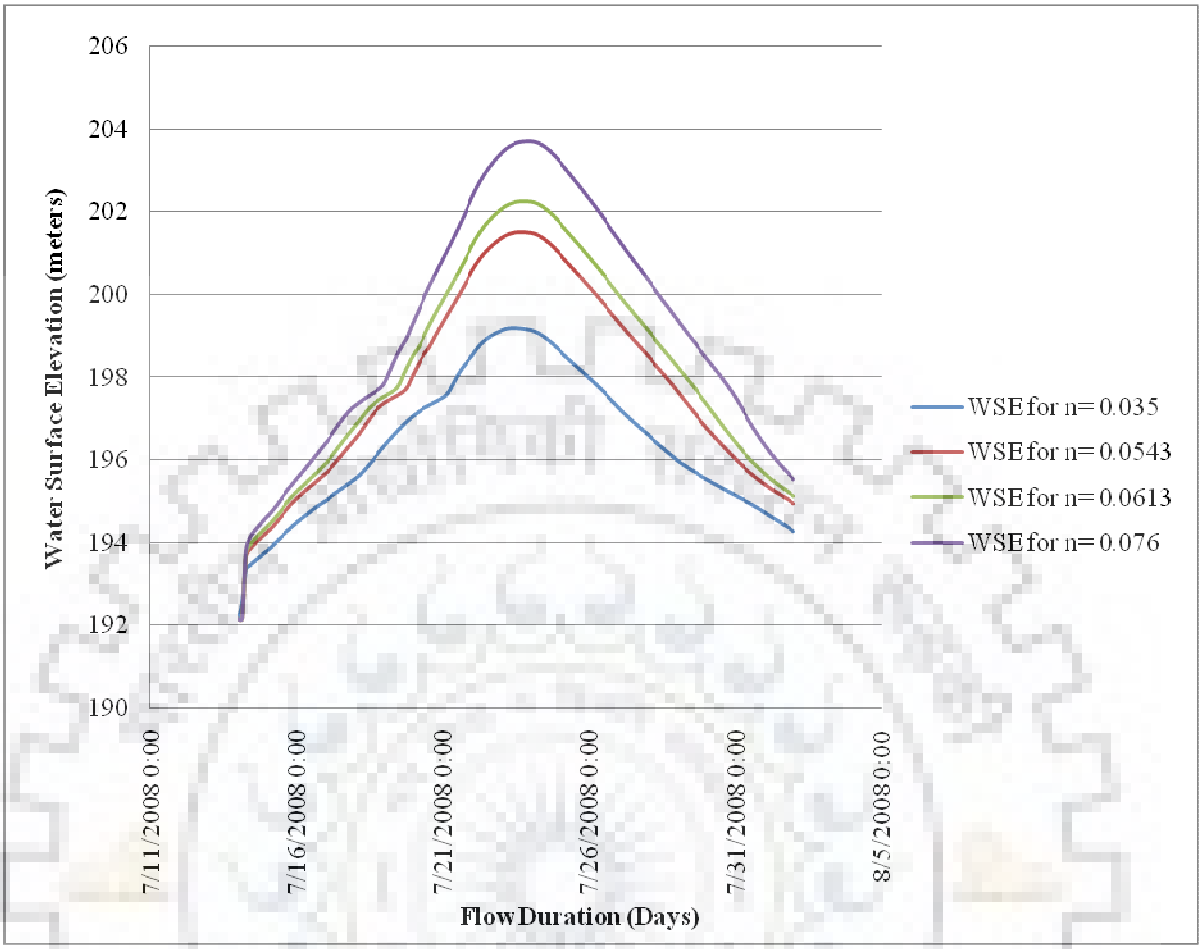

Figure 25 WSE for different Manning's n (with peak 2450m^3/s at d/s point)

The nature of result obtained in this case is also same as previous results. For downstream point considered, when n changes from 0.035 to 0.076 there is a rise in water level by 4. 50m.It can be observed that when Manning's n value is kept existing scenario (type 2 in this case n=0.0543), the WSE is 2.31m more than type 1 (n=0.035). Even in this case, it is observed that there is an increase in WSE in the downstream. The fluctuation in the WSE more in downstream point may be due to several causes but the most prominent cause is the slope of terrain is gentle (less fluctuation) and a decrease in the waterway of flow at the downstream, discussed earlier. The tabular form of this result is shown in Appendix 7.

Figure 18 is the WSE profile along the river centerline due to different Manning's n with respect to river bed profile. It is clearly observed from the figured that there is an increase in WSE with an increase in Manning's roughness coefficient. Manning's n is obtained by varying land use as discussed in Table 5 & Table 6 above.

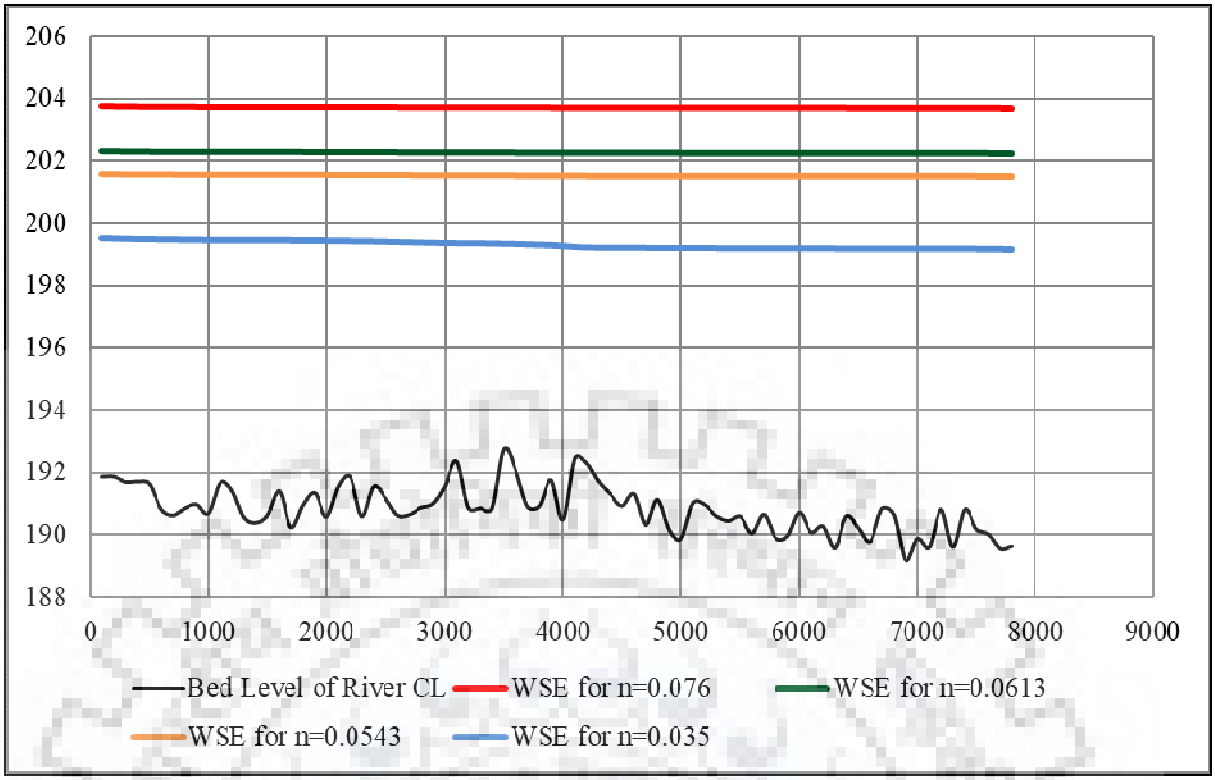

Figure 26 WSE at different Land use along river center line

The graph above shows slight different trend than previous result. It can be clearly seen in the figure that there is slight drop down in the WSE at point near 3900 m from upstream for land use type 1 (n=0.035). WSE for other land use type does not show any drop in the WSE. The WSEs in cases (type 2, 3 & 4) is so high that most of the area is inundated making the water surface elevation in upstream as well as downstream same. In this case it also observes that there is almost uniform fluctuation in WSE in upstream and downstream for same change in Manning's n. The reason behind this may be because the effect of constriction in waterway is no more due to flooding over embankment.

6.2 Sensitivity analysis of different cell size on WSE

When the cell size is larger, and the changes in hydraulic properties are great, the solution can become unstable. In general, larger cell size will cause additional numerical diffusion, due to the derivatives with respect to distance being averaged over to long of a distance. Also, cell size is larger, such that the Courant number would be much greater than 1.0, then the model may also become unstable.

6.2.1 Sensitivity analysis of depth on different cell size (with peak flow 800 m3/s)

The sensitivity analysis of depth was carried out by using HEC RAS model using hydrograph with peak 800m^3/s, computational time interval = 10sec and Manning's n=0. 035.The model

was simulated for cell size 10m X 10m, 30m X 30m & 50mX50m, other data remaining constant. The daily hydrograph that is used as boundary condition for simulation of model for the above case is shown in Figure 27.

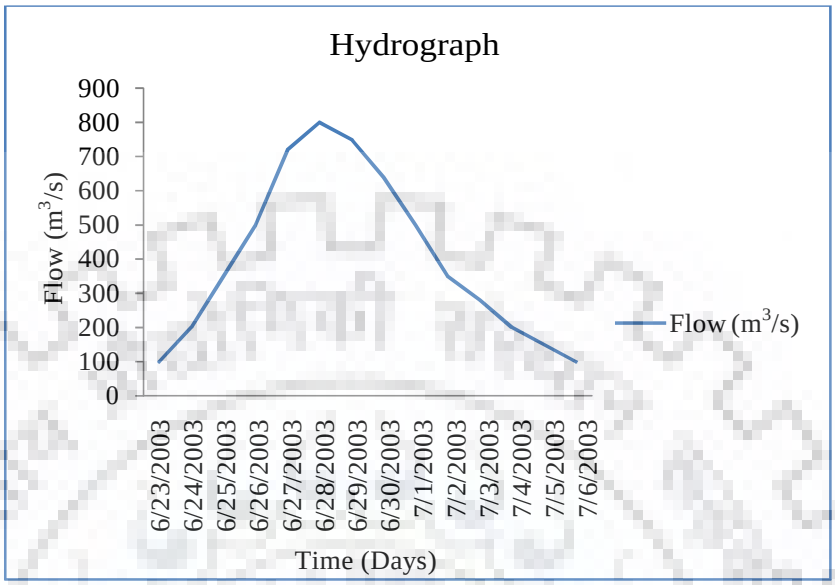

Figure 27 Hydrograph with peak 800 m^3/s

For this case, maximum observed velocity, at centre line of river at any chainage,

V = 1.7 m/s, &

Δt =10sec,

Analysis and discussion

For model to be stable courant condition should be satisfied.

$\Delta t \leq \Delta x / Vw$

Or $\Delta x > \Delta t * Vw$

$\geq 10*1.5*1.7$

$\geq 25.5m$

V_w = Velocity of wave, which is approximately equal to 1.5 times average Velocity of flow

Δt = computational time step (secs)

Δ_x = Average cell size (m)

The Figure 28 is the plot of WSE for particular land use v/s time of flow at different cell size. There is no much distinctive variation in water surface elevation on the result obtained through simulation of varying cell size. The results (Appendix 8 & Appendix 9) can be discussed in brief as below.

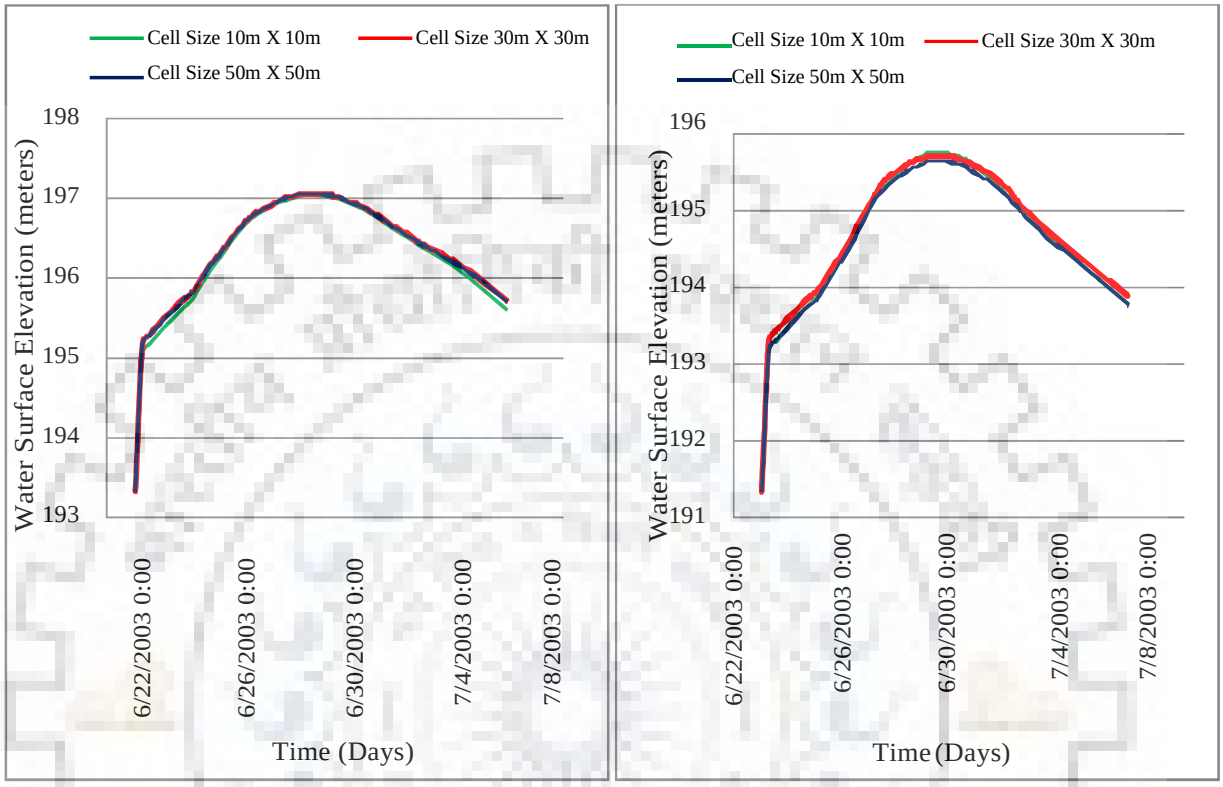

Figure 28 WSE for different cell for u/s and d/s points

From above graph, under flow condition & different cell size in each case, it was observed that WSE at any point in upstream and downstream as a result of 30m X 30 m, 40m X 40 m & 50m X 50 m cell size is similar. However, from the stability point of view result obtained from cell size $\geq$ 25.5m (from courant condition) would give better result. All the cell size in this case is greater than 25.5m thus satisfying Courant condition, results obtained are also similar. The optimal sizeof cell size may or may not be same as cell size obtained by satisfying courant condition. Hence it can be fixed by matching results with real field data.

6.2.2 Sensitivity analysis of WSE on different cell size (with peak flow 1100 m3/s)

The sensitivity analysis of depth was carried out by simulation of model with hydrograph of peak flow 1100m3/s, computational time interval = 10sec and Manning's n=0. 035.The model was simulated at different cell size 30m x 30m, 40m X 40m & 50mX50m. The daily hydrograph that is used as boundary condition for simulation of model for the above case is shown in Figure 29.

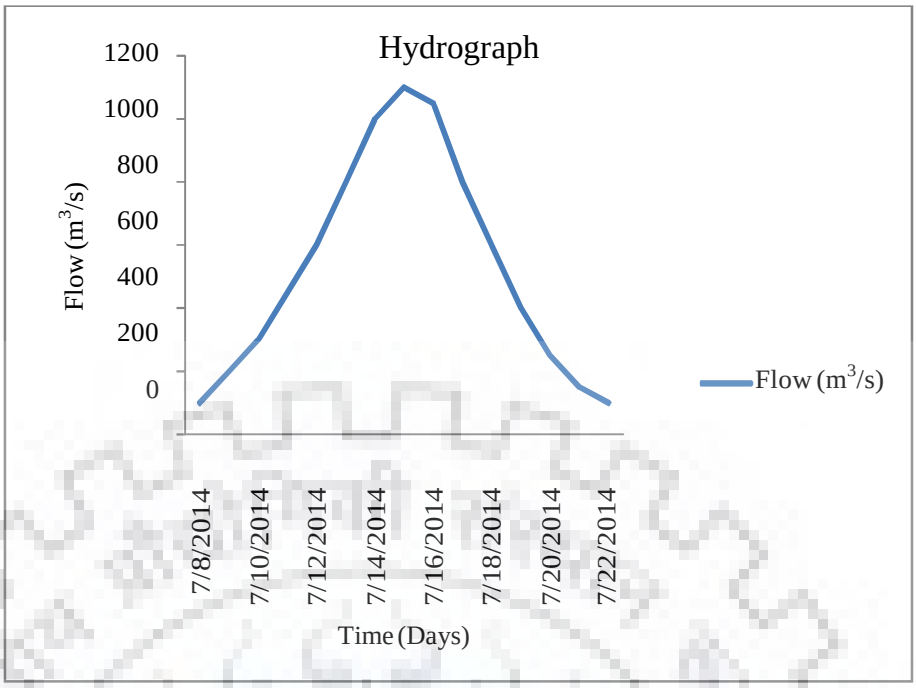

Figure 29 Hydrograph with peak 1100 m^3/s

For this case, maximum observed velocity, it is observed that maximum velocity occurs at centre line of river at chainage 0+000 i.e. 2.2 m/s,

Δt =10sec,

V_{av} = 2.2 m/s

V_w = Wave velocity = 1.5 V_{av}

Analysis and discussion

For model to be stable courant condition should be satisfied.

Or, $\Delta t \leq \Delta x / V_w$

Or $\Delta x \geq \Delta t * V_w$

$\geq 10*1.5*2.2$

$\geq 33m$

V_w = Velocity of wave, which is approximately equal to 1.5 times average velocity of flow, m/s

Δt = computational time step, secondss

Δx= spacing of the grid in the numerical model,m

The plot of variation of WSE at different cell size when model is simulated for same flow event and same time of computation is shown in Figure 30

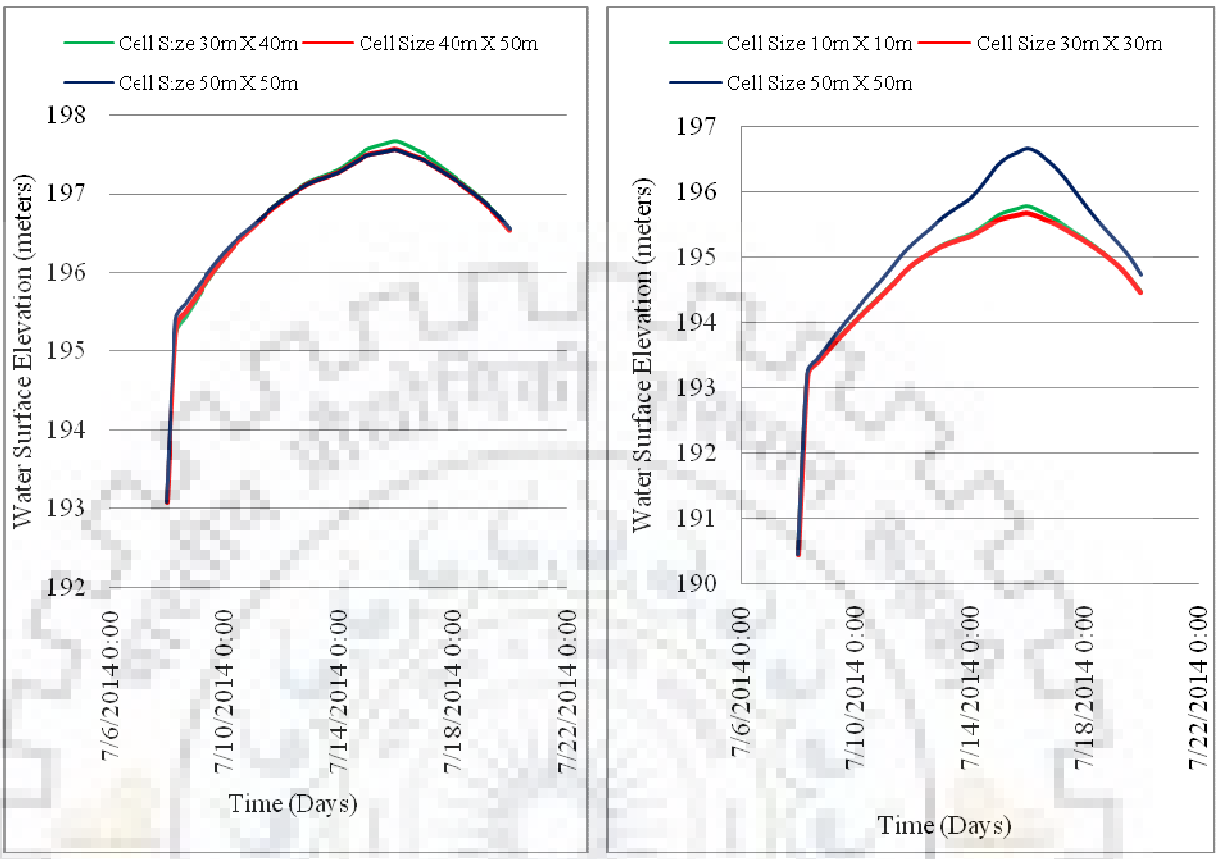

Figure 30 WSE for different cell size for U/S and D/S point

From above two graphs for above flow condition & different cell size in each case, it was observed that depth of flow at any point as a result of 50 m X 50 m cell size in study area is found to be more than 30m X 30 m cell size &10m X 10 m cell size. The deviation of result at upstream point is negligible but it is more at downstream point. This deviation in cell size in the downstream may be reduced /corrected by using optimal cell size. However, from the stability point of view result obtained by 50m X 50m (as >33m from courant condition) should be better. The optimal size of cell size may vary as per study area. Hence it can be fixed by matching results with real field data.

6.3 Sensitivity analysis of different time step on WSE

Time step is the computational time interval at which HEC RAS give one value parameters like depth, WSE, velocity etc. If time step is too large there is attenuation of peak rapidly and model may get unstable. Again, when time step is too small there will be computational problem. High RAM computer may be required to simulate a model or sometime the simulation may end up giving no result or hanging of computers. In this case also courant number condition could be helpful in deciding computational time step.

6.3.1 Sensitivity analysis of different time step (peak flow=800m3/s)

The sensitivity analysis of time step was carried out using HEC RAS 5.0.3 model with hydrograph with peak 800m^3/s, cell size 30m X 30m in each case and Manning's n=0. 035.The model was simulated for computational time 10 sec, 1 min and 10 min. The flow data, cell size and manning's n was kept constant in each case. In this case hydrograph used is same as Figure 27. Sensitivity on WSE was carried out using t = 10 sec, 1 minute and 10 sec. Again, in this study also courant number should be less or equal to one from stability point of view. Maximum observed velocity, it is observed that maximum velocity occurs at centre line of river at chainage 0+000 i.e. 1.7 m/s.

Δx =30 m,

V_{av} = 1.7 m/s

Analysis and discussion

Now from courant condition for stability,

$\Delta t \leq \Delta x / V_w$

$\Delta t \leq 30 / (1.5*1.7)$

$\Delta t \leq 11.76$sec.

Where, V_w = Velocity of wave, which is approximately equal to 1.5 times average velocity of flow

Δt = computational time step

Δx = spacing of the grid in the numerical model

Figure 31 is the plot of WSE at different time step for flow with peak of 800 m^3/s and with cell size 30m X 30m.

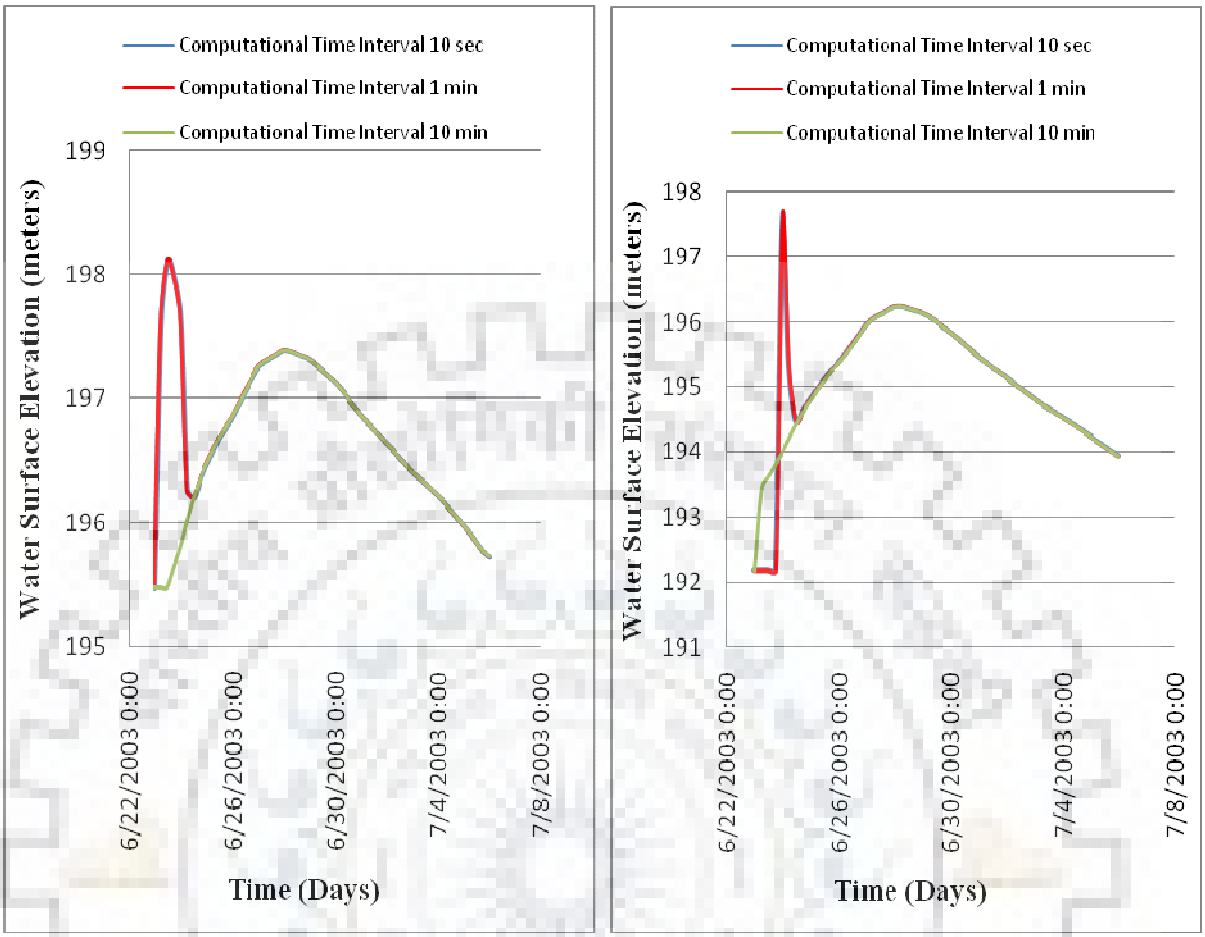

Figure 31 WSE for different time step at U/S and D/S

From courant condition point of view, computational time interval less than or equal to 12 secs may give good stable result. But from the from above two graph it was observed that depth of flow in study area is found to be almost similar when model is simulated at 10 seconds time step & 1 minute time step but depth in 10 minutes time step rose abruptly which is unusual and is more than twice than maximum depth occurred at 10 sec and 1 min time step. Hence it is concluded that for given study area, the model can give better as well as stable result if simulated at for computational t = 3 sec, and simulation of model may give good result if computational time interval is less than 10 secs (or even1 min). The tabular form of this result is shown in Appendix 10 & Appendix 11.

6.3.2 Sensitivity analysis of different time step (peak flow=1100 m^3/s)

In this case hydrograph use is same as Figure 29. The WSEs for same flow with peak 1100 m^3/sand varying computational time were obtained as output from model. The computational time intervals used in model are 10 seconds, 1 min and 10 minutes. From stability point of

view, the computational time interval should satisfy courant condition described below. Maximum observed velocity was 2.2 m/s which in this case was observed in center line of river at Chainage 0+000 i.e.

Δx =10 min,

V_{av} = 2.2 m/s

Now from Courant condition for stability,

$\Delta t \leq \Delta x / Vw$

$\Delta t \leq 10/(1.5*2.2)$

$\Delta t \leq 3.03$ sec.

Figure 32 is the plot of WSE for different time step, for cell size 30m X 30m and flow with peak 1100m^3/s.

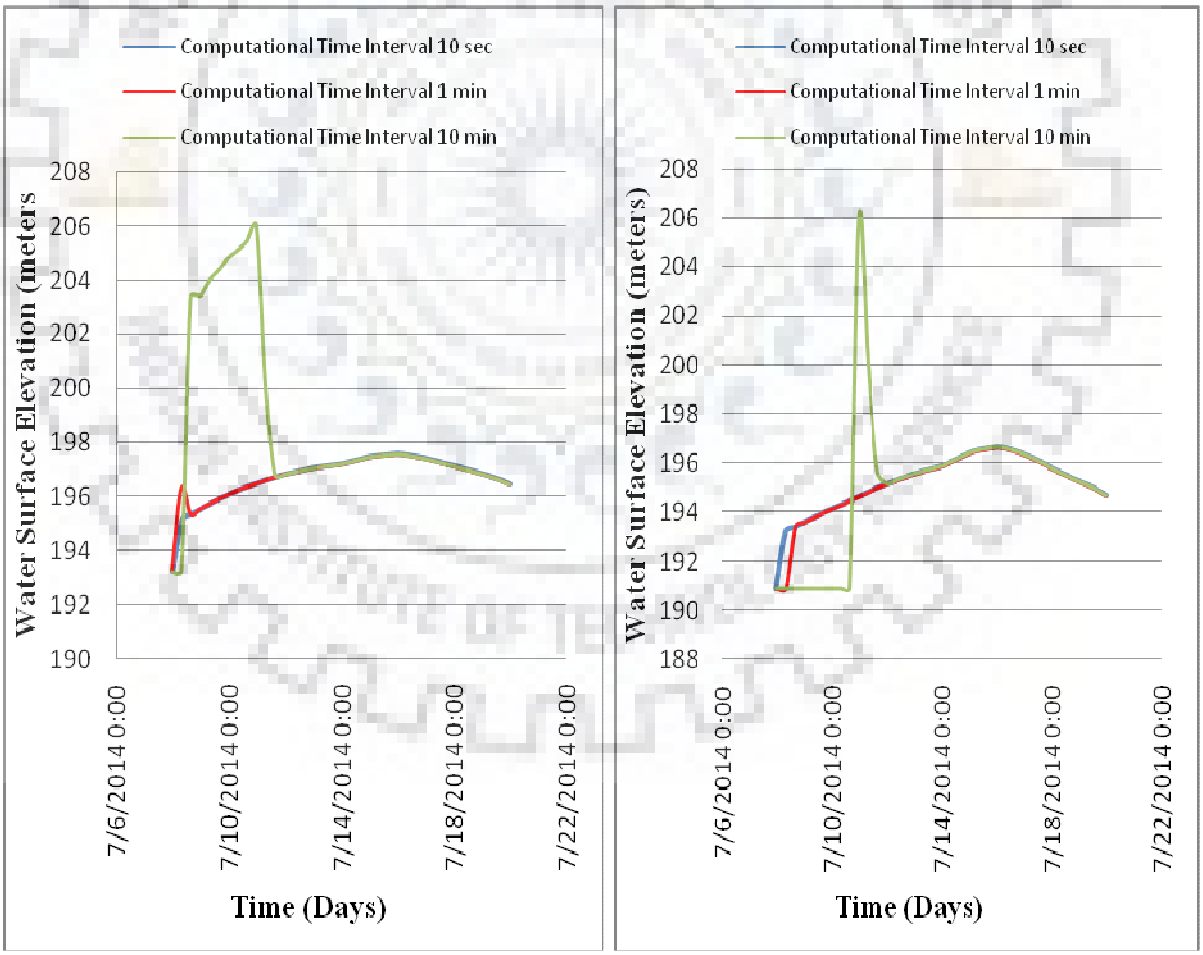

Figure 32 WSE by varying time step at U/S and D/S point

Analysis and discussion

From courant condition point of view, computational time interval less than or equal to 3 secs may give good stable result. But from the from above two graphs for discharge =1100 m^3/s, cell size 10 m in each case, it was observed that depth of flow in study area is found to be almost similar when model is simulated at 10 sec time step & 1 min time step but depth in 10 min timestep rose abruptly which is unusual and is more than twice than maximum depth occurred at 10 sec and 1 min time step. Hence it is concluded that for given study area, the model can give better as well as stable result if simulated at for computational t = 3 sec, and simulation of model may give good result if computational time interval is less than 10 seconds (or even1 min).

6.4 Inundation Map

The objective of preparation of Inundation map was to know the increase in inundation area that would occur due to various land use. The land use in this study is related to manning's n which can be seen in Table 5 and Table 6. The HEC RAS 5.0.3 has feature of 2d modeling. The WSEs at each cell as well as area that might be inundated by flow can be extracted from result. Flood inundation map for two flood events (flood with peak 800 m^3/s & 2450 m^3/s) was prepared by incorporation HEC RAS and Arc GIS. The flood event chosen was one for normal flow condition and other was for extreme flow condition. The inundation map prepared in this study show how much area is being inundated with particular flood event. It will also useful in determining the sensitivity of change in value of Manning's n (i.e. land use change) for flood risk.

6.4.1 Inundation Map for different Manning's n (peak flow = 800 m^3/s)

The inundation map for different manning's n value (i.e. using different land use type shown in table 5) under similar flow condition, cell size and computational time interval was prepared. Inundation map was prepared for separately for manning's n=0.035, 0.0543, 0.0613 & 0.076 as shown in Figure 33 & Figure 34.

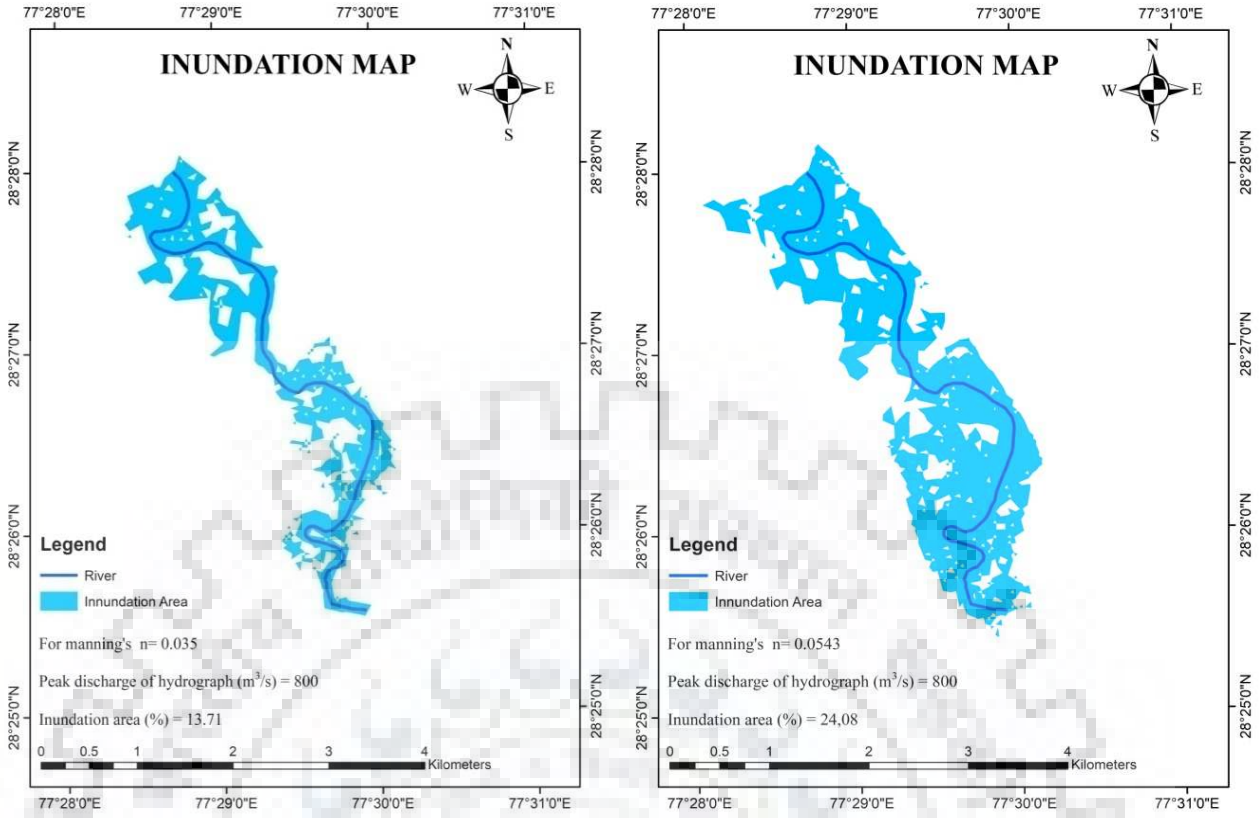

Figure 33 Inundation Map for n= 0.035 & n =0.0543

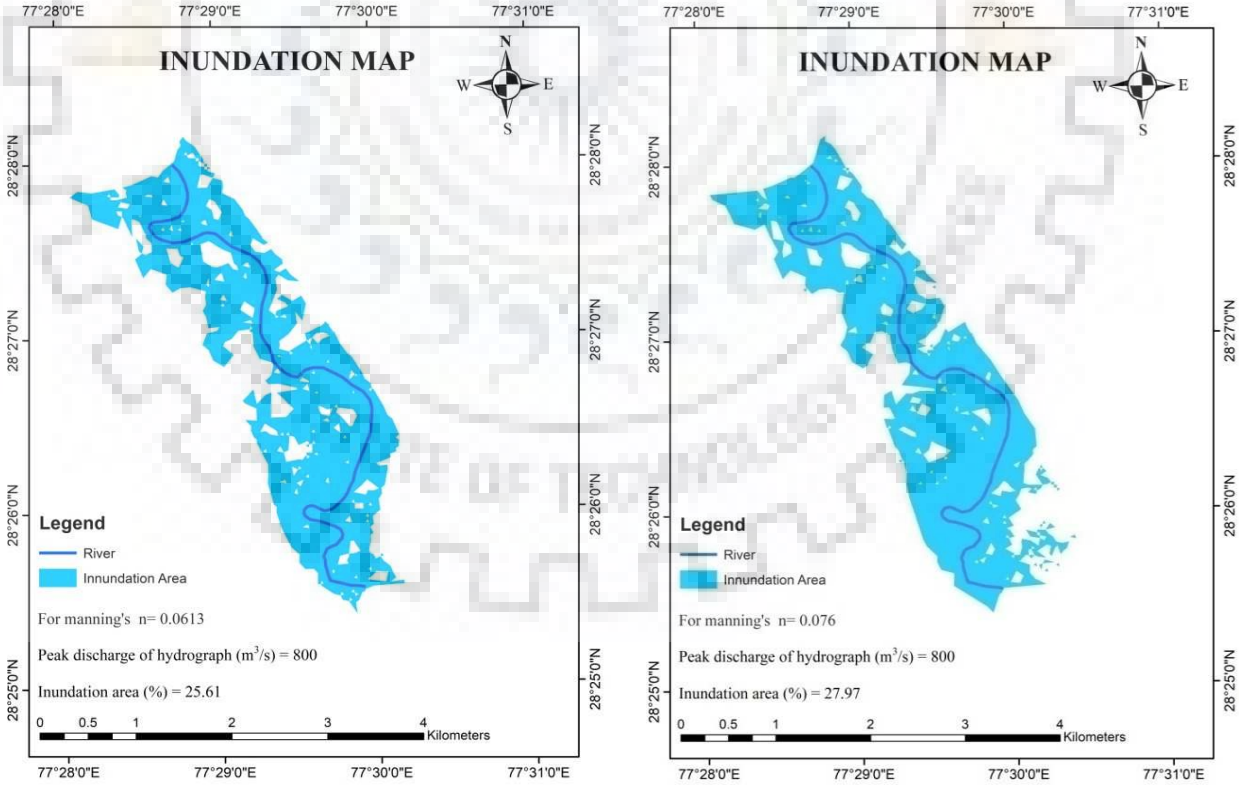

Figure 34 Inundation Map for n =0.0613 & n= 0.076

Analysis and discussion

The Table 7 shows percentage increase in inundation area due to increase in manning's n. The maps shown are prepared to analyze the result obtained in case of Manning's n.

Table 7 Inundation map for different Manning's n with peak 800 m^3/s

S. No	Description	Total Area (km^2)	WSE for n= 0.035	WSE for n= 0.0543	WSE for n= 0.0613	WSE for n= 0.076
1	Inundation Area in km^2	18.23	2.5	4.39	4.67	5.1
2	Percentage increase in inundation with respect to successive land use.		-	75.60	6.38	9.21
3	Percentage inundation with respect to total Area		13.71	24.08	25.61	27.97

The result shows that when n changes from n= 0.035 to n=0.0543, inundation area changes abruptly from 2.5 km^2 to 4.39 km^2. It demonstrates that there is 75.6%, 6.38% and 9.28% increase in inundation area with the change of manning's n values from n=0.035 to 0.053, 0.0543 to 0.0613 and 0.0613 to 0.076 respectively. There is increase in flood inundation greatly when manning's n changes from n=0.035 to n=0.0543. This may be because in initial period large amount of flow is acquired with in river itself and once river section is filled it then starts spreading in flood plain. The map shows that there is increase inundation area with the increase in Manning's roughness coefficient provided flow condition is kept constant in each case. The total change in inundation area when n value changes from 0.035 to 0.076 to total change is 14.26%.

6.4.2 Inundation Map for different Manning's n (peak flow = 2450 m3/s).

The Inundation map is prepared for separately for n=0.035, 0.0543, 0.0613 & 0.076 as shown in Figure 36 & Figure 36.

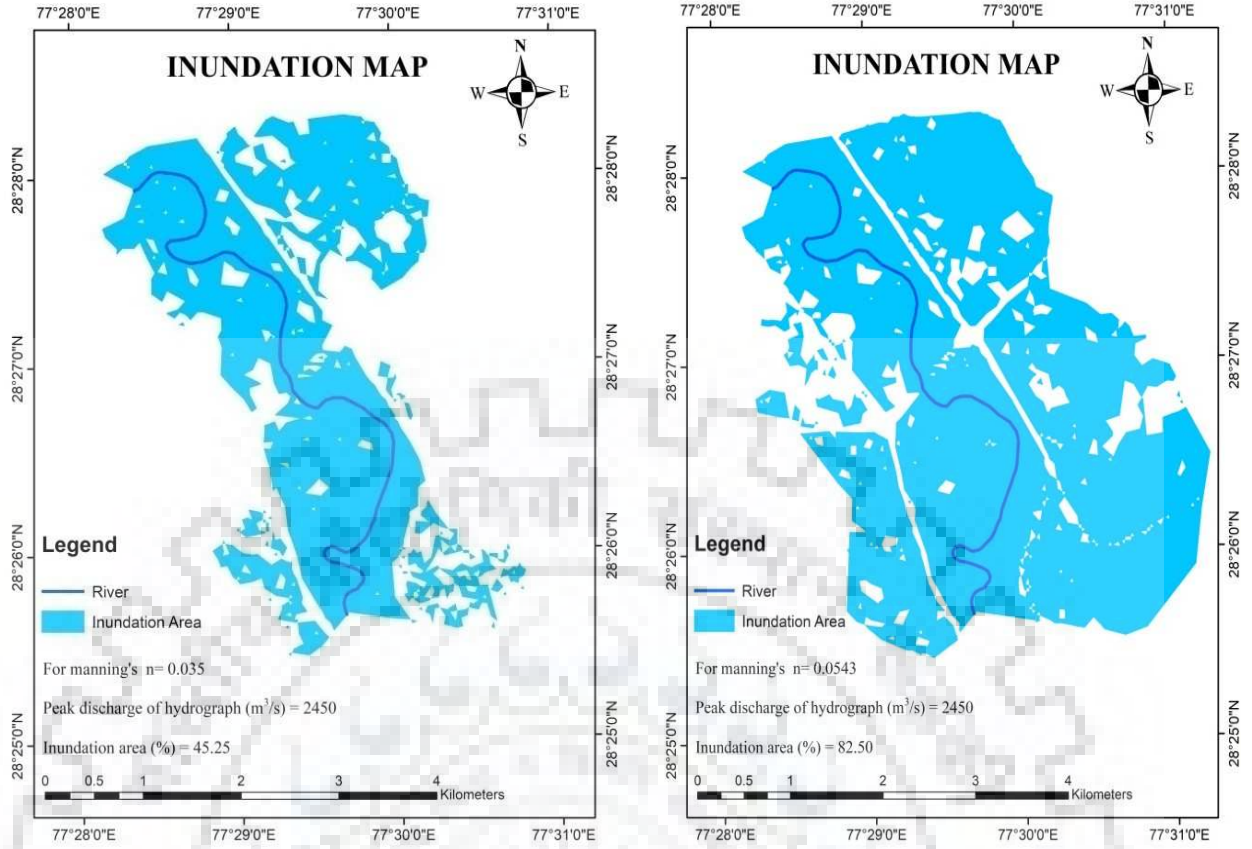

Figure 35 Inundation Map for n= 0.035 & n =0.0543

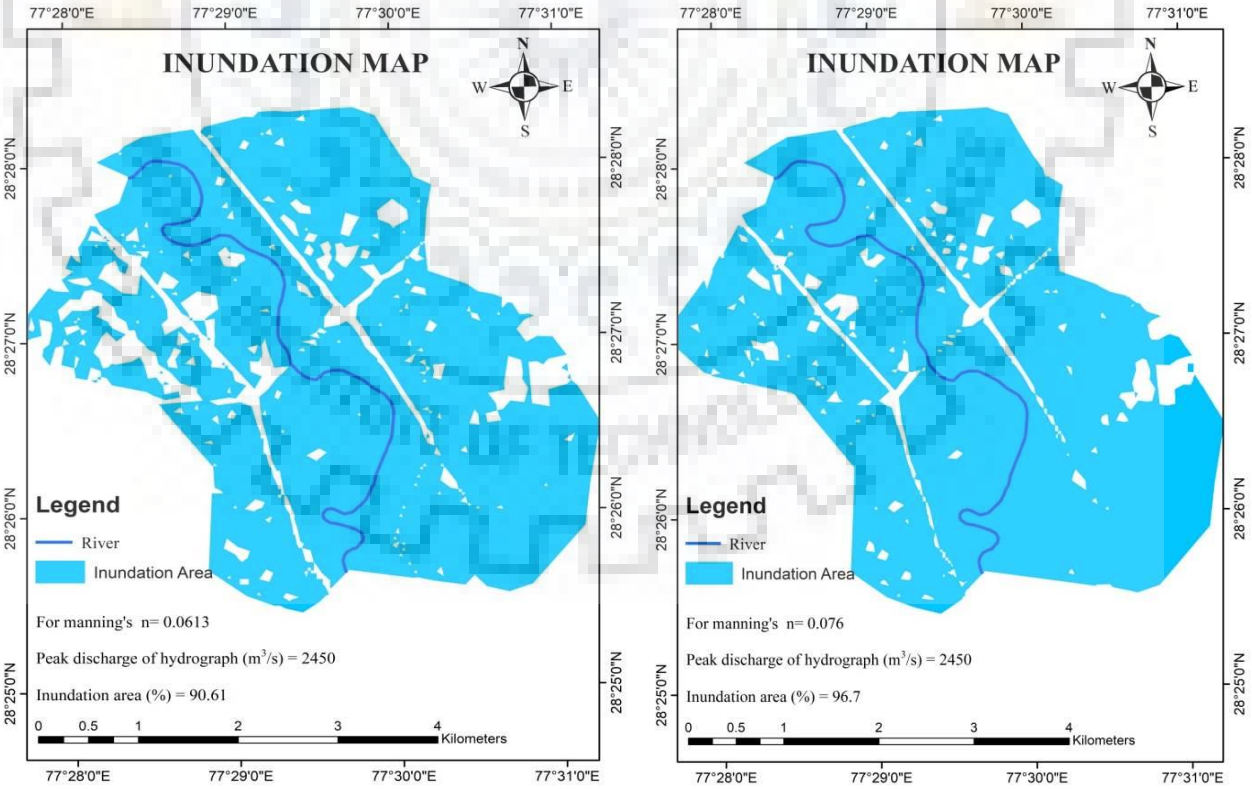

Figure 36 Inundation Map for n= 0.0613 & n =0.076

This map is prepared to shows that 96.97% of flow area gets inundated there is flood event similar to this event and keeping others condition fixed. It also tries to show how inundation area increases with change in land use by varying manning's n. The Table 8 shows percentage increase inundation with respect to total area as well as with respect to consecutive land use change.

Table 8 Inundation map for different Manning's n with peak 2450 m3/s

S. No.	Description	Total Area (km^2)	WSE for n= 0.035	WSE for n= 0.0543	WSE for n= 0.0613	WSE for n= 0.0613
1	Inundation Area in km^2	18.21	8.25	15.04	16.52	17.63
2	Percentage increase in inundation with respect to s u ccessive land use.		-	82.30	9.84	6.72
3	Percentage inundation with respect to total area		45.25	82.50	90.61	96.70

The inundation map shows that when n changes from n= 0.035 to n=0.0543, inundation area change drastically from 8.25 km^2 to 15.04 km^2 which shows 82.3 increase in inundation area which means in initial period large amount of flow is acquired with in river itself and then start inundating. For particular flood (with peak 2450 m^3/s), with the increase in n value from 0.035 to 0.076 inundation area is increased by 51%.

6.5 Velocity Distribution on inundation Area

The velocity distribution map was prepared to identify which zone there will be high velocity and in which zone there will be low velocity. The increase in velocity to the bank of the river calls for the need of protection work or river training work. Through the velocity distribution profile, change in velocity on the study area was observed. Hydrograph used for preparing velocity distribution map is shown in Figure 37.

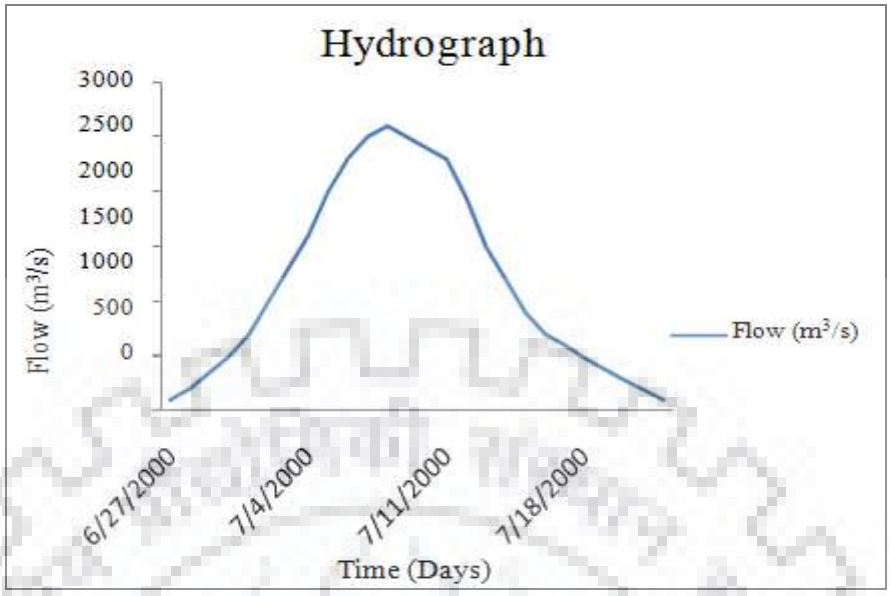

Figure 37 Hydrograph having peak flow 2600 m^3/s

The maximum velocity map was prepared for the most severe condition in the study area with flood event having peak flow 2600 m^3/s. It was prepared by obtaining maximum velocity at each cell for given flow condition using HEC RAS. The velocity profile so obtained is then exported to Arc GIS. Thus, velocity distribution map for each Manning's n (land use type) was prepared the velocity distribution map on inundation area with respect to four set of Manning's n (n = 0.035, 0.0543, 0.0613 & 0.076) is shown in Figure 38 & Figure 39.

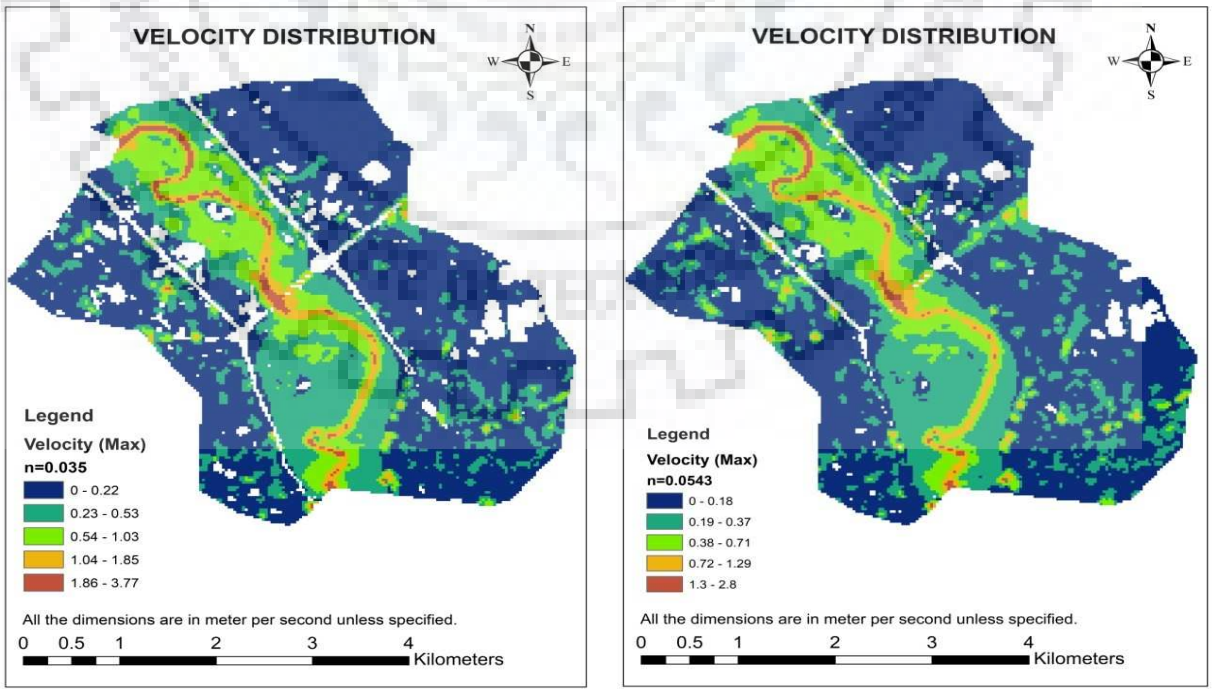

Figure 38 Velocity distribution on inundation area for n=0.035 &n = 0.543

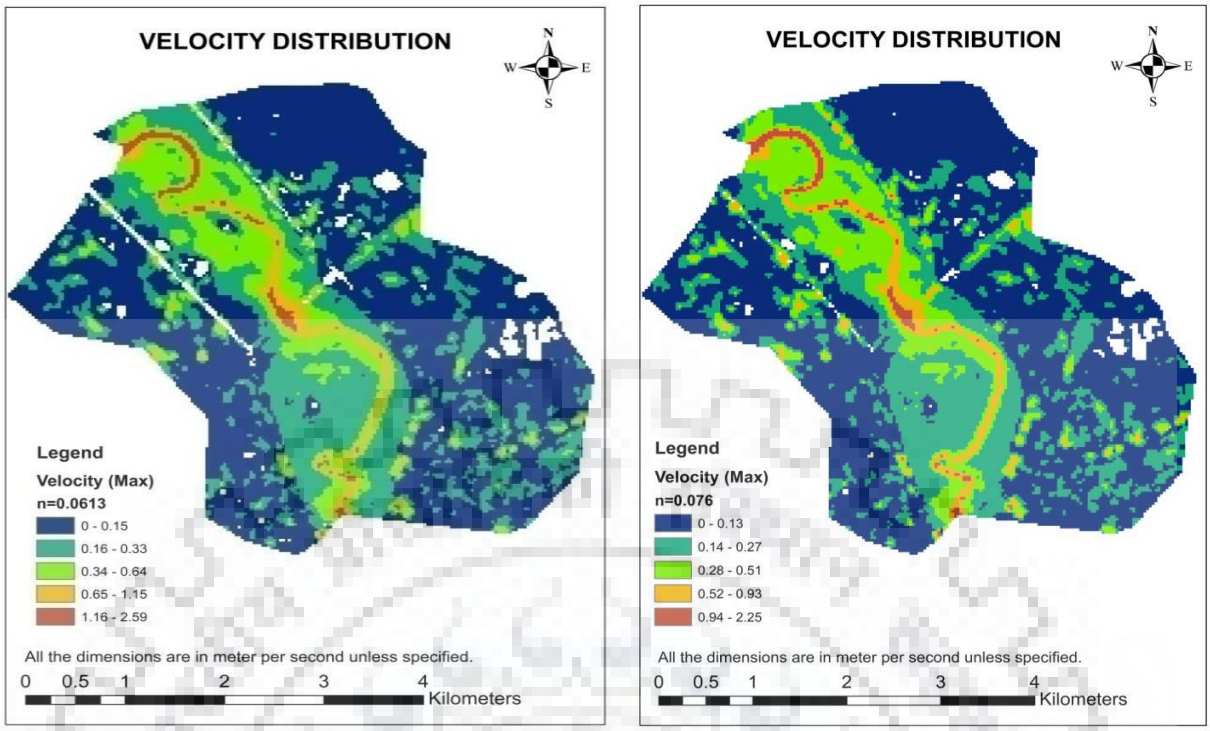

Figure 39 Velocity distribution on inundation area for n=0.0613&n=0.076

Analysis and discussion

The velocity distribution map shows that the velocity distribution of the flow is maximum when flow is simulated with Manning's n value n= 0.035. The range of velocity is lease when model is simulated with n= 0.076. For Manning's n value least, velocity is most and the discharge escapes in relatively short period of time, keeping the flood inundation level least. When there is maximum surface roughness in the flood path, the velocity of flow is minimum resulting in rise in flood level. The result shows that the maximum velocity of flow is concentrated towards center line of the river, moderate velocity in the flood plain whereas lesser velocity in the region beyond embankment (i.e. in country side). The velocity distribution profile shows that there is less probability of cutting bank edges even when there is high flow.

7. SUMMARY & CONCLUSION

Sensitivity analysis for combination of different Land uses/Land covers was carried out by using latest version of HEC RAS 5.0.3. The results obtained show that there is increase in the inundation (or WSE) as Manning's n increase, and vice-versa. To assess the sensitivity of cell size, model was simulated with cell size 10m X 10m, 30m X 30m, 40m X 40m and 50m X 50m. The results obtained for it show that there is decrease in flood level with the increase in cell size in one condition but the flood level obtained in other case showed that there is only slight or no change in flood level with increasing cell size. Thus, the optimum cell size may be obtained by satisfying courant condition as well as comparing the model result for different cell size with observed flood level for similar hydrograph and boundary conditions.

The result for time step was carried out for 10 sec, 1 min and 10 min shows that model shows stable behavior when simulated at computational time interval 10 sec and 1 min but result shows there is abrupt rise in WSE when simulated at time step =10min. The abrupt rise in WSE obtained was even greater than twice than normal WSE obtain by simulation of model with 10 sec & 1 min computational time interval. Hence it may be concluded that for present study area, 10 sec computational time intervals could give stable result. However, time step satisfying courant condition may be considered. The result also shows that velocity distribution for t = 10 sec & 1 min velocity distribution is almost similar with slight deviation whereas the result obtained by 10 min time step showed abrupt rise.

Finally, Inundation map were prepared with varying land use under similar hydrological condition. The results of inundation map show that there is increase in inundation area when Manning's n value changed from n = 0.035 to n = 0.0543 (which is the existing scenario). When Manning's n changes from n = 0.035 to 0.076 there is 14.26% and 51.45% increase in inundation area for flood event with peak flow 800 m^3/s & 2450 m^3/s respectively. This concludes that increase in flow peak increases inundation area. It can be thus concluded that with adverse change in land use, flood risk is raised. Flood risk can be both by increase in water surface elevation (high depth) as well as increase in inundation area. Moreover, while performing simulation in HEC-RAS, stability of model should be taken care to compute optimum results. It is recommended that in the flood prone area, policy of land use should be developed so that one can shift the present land use within the range of influence of river.

REFERENCES

Akar, Î., Kalkan, K., and Maktav, D. (2009). "Determination of land use effects on flood risk by using integration of GIS and remote sensing." *Recent Advances in*, 23–26.

Akbari, A., Mozafari, G., Fanodi, M., and Hemmesy, M. S. (2014). "Impact of landuse change on river floodplain using public domain hydraulic model." *Modern Applied Science*, 8(5), 80–86.

Alexakis, D. D., Hadjimitsis, D. G., and Agapiou, A. (2013). "Integrated use of remote sensing, GIS and precipitation data for the assessment of soil erosion rate in the catchment area of 'Yialias' in Cyprus." *Atmospheric Research*, Elsevier B.V., 131(October 2017), 108–124.

Ashagrie, A. G., de Laat, P. J. M., de Wit, M. J. M., Tu, M., and Uhlenbrook, S. (2006). "Detecting the influence of land use changes on Floods in the Meuse River Basin – the predictive power of a ninety-year rainfall-runoff relation." *Hydrology and Earth System Sciences Discussions*, 3(2), 529–559.

Banasik, K., and Pham, N. (2010). "Modelling of the effects of land use changes on flood hydrograph in a small catchment of the Płaskowicka, southern part of Warsaw, Poland." *Annals of Warsaw University of Life Sciences - SGGW. Land Reclamation*, 42(2), 229–240.

Betsholtz, A., and Nordlöf, B. (2017). "Potentials and limitations of 1D, 2D and coupled 1D-2D flood modelling in HEC-RAS A case study on Höje river." *Lund University*, 128.

Bhandari, M., Nyaupane, N., Mote, S. R., Kalra, A., and Ahmad, S. (2017). "2D Unsteady Flow Routing and Flood Inundation Mapping for Lower Region of Brazos River Watershed." *World Environmental and Water Resources Congress 2017: Hydraulics and Waterways and Water Distribution Systems Analysis - Selected Papers from the World Environmental and Water Resources Congress 2017*.

Bingwa, F. (2013). "A quantitative analysis of the impact of land use changes on floods in the Manafwa River Basin." 1–48.

Blum, M., Weaver, K., Kedia, S., and Laughlin, N. (2015). "Application of New HEC-RAS 2D Tool for 1D/2D Modeling of the Truckee River and Tributaries Key Project Team – HDR Engineering."

Boulomytis, V. T. G., Zuffo, A. C., Dalfré Filho, J. G., and Imteaz, M. A. (2017). "Estimation

and calibration of Manning's roughness coefficients for ungauged watersheds on coastal floodplains." *International Journal of River Basin Management*, Taylor & Francis, 15(2), 199–206.

Brunner, G. W. (2016). "HEC-RAS River Analysis System, 2D Modeling User's Manual Version 5.0." (CPD-68A), 1–171.

Chen, Y., and Yu, B. (1999). "Impacts of climate and land-use changes on floods in an urban catchment in southeast Queensland , Australia." (July 2013), 1–7.

Demir, V., and Kisi, O. (2016). "Flood Hazard Mapping by Using Geographic Information System and Hydraulic Model: Mert River, Samsun, Turkey." *Advances in Meteorology*, 2016.

District, M. (2009). "District Brochure of." 2008–2009.

Dorn, H., Vetter, M., and Höfle, B. (2014). "GIS-based roughness derivation for flood simulations: A comparison of orthophotos, LiDAR and Crowdsourced Geodata." *Remote Sensing*, 6(2), 1739–1759.

Fabio, P., Aronica, G. T., and Apel, H. (2010). "Towards automatic calibration of 2-D flood propagation models." *Hydrology and Earth System Sciences*, 14(6), 911–924.

Gautam, D. K., and Kharbuja, R. a M. G. (2006). "Flood Hazard Mapping of Bagmati River in Kathmandu Valley Using Geo-Informatics Tools." *Journal of Hydrology and Meteorology*, 3(2677 m), 1–9.

Hicks, F. E., and Peacock, T. (2005). "Suitability of HEC-RAS for Flood Forecasting." *Canadian Water Resources Journal*, 30(2), 159–174.

Husain, A. (2017). "Flood Modelling by using HEC-RAS." *International Journal of Engineering Trends and Technology*, 50(1), 1–7.

Janses, C., and SCE. (2016). "Manning ' s n Values for Various Land Covers To Use for Dam Breach Analyses by NRCS in Kansas." (December), 1–2.

Kalyanapu, A. J., Burian, S. J., and McPherson, T. N. (2009). "Effect of land use-based surface roughness on hydrologic model output." *Journal of Spatial Hydrology*, 9(2), 51–71.

Khattak, M. S., Anwar, F., Saeed, T. U., Sharif, M., Sheraz, K., and Ahmed, A. (2016). "Floodplain Mapping Using HEC-RAS and ArcGIS: A Case Study of Kabul River." *Arabian Journal for Science and Engineering*, 41(4), 1375–1390.

Liu, J., Wang, S. yu, and Li, D. mei. (2014). “The Analysis of the Impact of Land-Use Changes on Flood Exposure of Wuhan in Yangtze River Basin, China.” *Water Resources Management*, 28(9), 2507–2522.

Ngo TS, Nguyen DB, S. R. (2015). “Effect of Land Use Change on Runoff and Sediment Yield in Da River Basin of Hoa Binh province , Noorthwest Vietnam.” *Journal of Mountain Science*, 12(4), 1051–1064.

Pfaffle, K. (2011). “Assessing Flood Inundation Mapping with the Use of a DEM and GIS along the Missouri River at Sioux City, Iowa.”

Rahmati, O., Zeinivand, H., and Besharat, M. (2016). “Flood hazard zoning in Yasooj region, Iran, using GIS and multi-criteria decision analysis.” *Geomatics, Natural Hazards and Risk*, Taylor & Francis, 7(3), 1000–1017.

Report, S. I. (2014). “Flood-Inundation Maps and Wetland Restoration Suitability Index for the Blue River and Selected Tributaries , Kansas City , Missouri , and Vicinity , 2012 Scientific Investigations Report 2014 – 5180.” (April).

De Roo, A., Odijk, M., Schmuck, G., Koster, E., and Lucieer, A. (2001). “Assessing the effects of land use changes on floods in the meuse and oder catchment.” *Physics and Chemistry of the Earth, Part B: Hydrology, Oceans and Atmosphere*, 26(7–8), 593–599.

Saghafian, B., Farazjoo, H., Bozorgy, B., and Yazdandoost, F. (2008). “Flood intensification due to changes in land use.” *Water Resources Management*, 22(8), 1051–1067.

Saha, A., and Singh, P. (2017). “Drainage Morphometric Analysis and Water Resource Management of Hindon River Basin, using Earth Observation Data Sets.” *Imperial Journal of Interdisciplinary Research*, 3(4), 2051–2057.

Sahoo, S. N., and Sreeja, P. (2008). “Development of Flood Inundation Maps and Quantification of Flood Risk in an Urban Catchment of Brahmaputra River.” 3(1), 1–11.

Samarasinghe, S., Nandalal, H., Weliwitiya, D., Fowze, J., Harazika, M., and Samarakoon, L. (2010). “Aplication of Remote Sensing and GIS for Flood Risk Analysis:A Case Study at Kalu - Ganga River, Sri Lanka.” *International Archives of the Photogrammetry, Remote Sensing and Spatial Information Science*, XXXVIII(8), 110–115.

Sönmez, O., and Doğan, E. (2016). “Determination of flood inundation area in Cedar River using calibrated and validated 1D and 1D / 2D model Kalibre edilmiş ve doğrulanmış 1D ve 1D / 2D model kullanılarak Cedar Nehri taşkın yayılım alanlarının tespiti.” 337–348.

Sophocleous, C., and Nalbantis, I. (2017). “Effect of land use change on flood extent in the inflow stream of lake Paralimni, Cyprus.” 147–153.

Thorne, C. (n.d.). “Land-use , Sediment and Flood Risk.”

Yang, J., Townsend, R. D., and Daneshfar, B. (2006). “Applying the HEC-RAS model and GIS techniques in river network floodplain delineation.” *Canadian Journal of Civil Engineering*, 33(1), 19–28.

Yerramilli, S. (2012). “A Hybrid Approach of Integrating HEC-RAS and GIS Towards the Identification and Assessment of Flood Risk Vulnerability in the City of Jackson, MS.” *American Journal of Geographic Information System*, 1(1), 7–16.

Zgonina, E. (2016). “Managing Flood Risk with HEC-RAS 5.0 thru Case Studies.”

APPENDICES

Appendix 1: Cross- section of Hindon River in the study area.

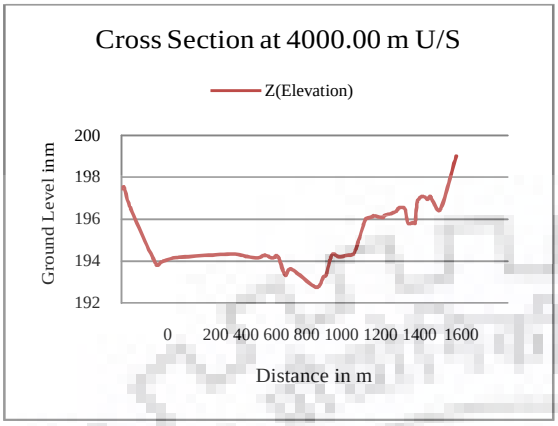

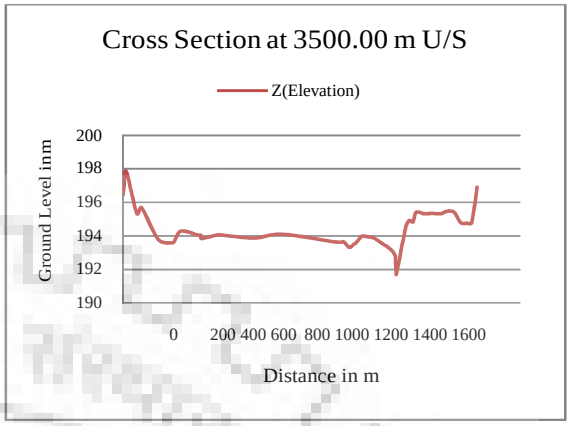

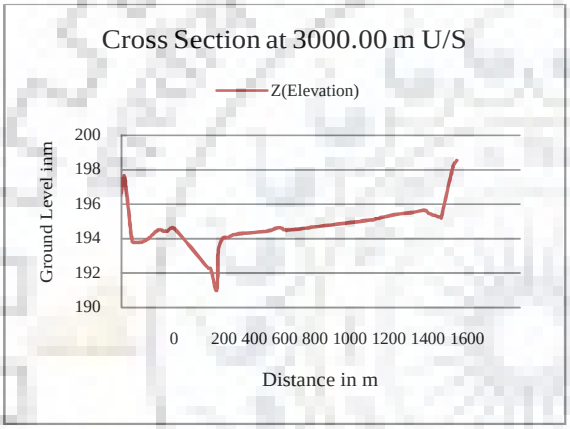

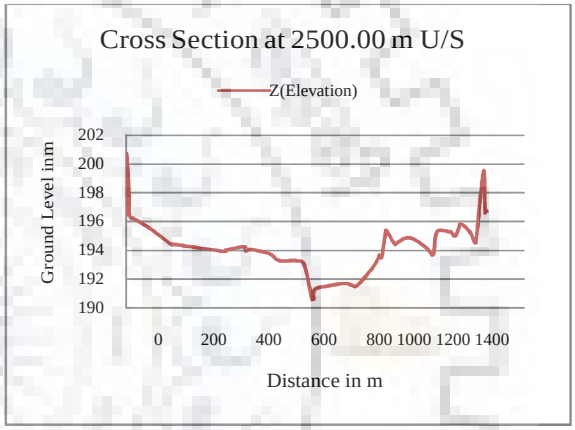

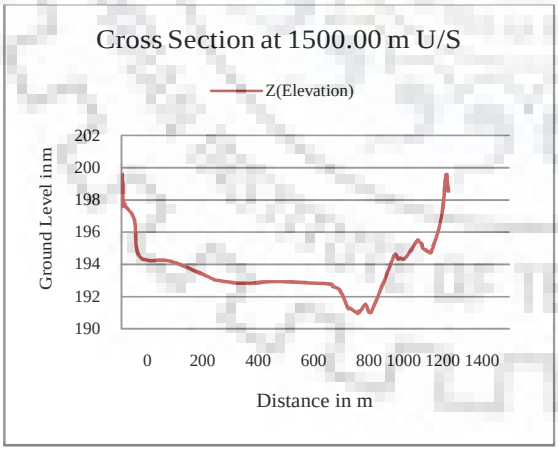

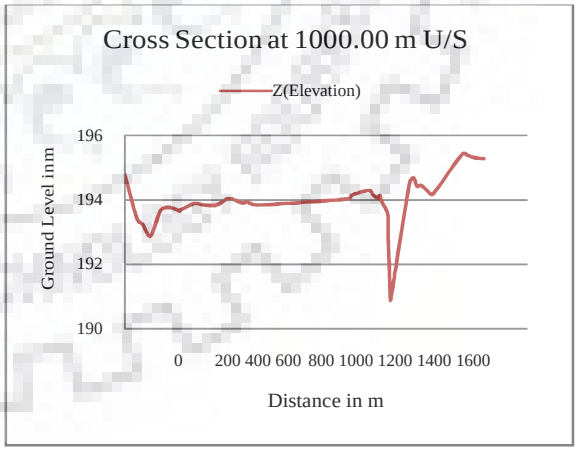

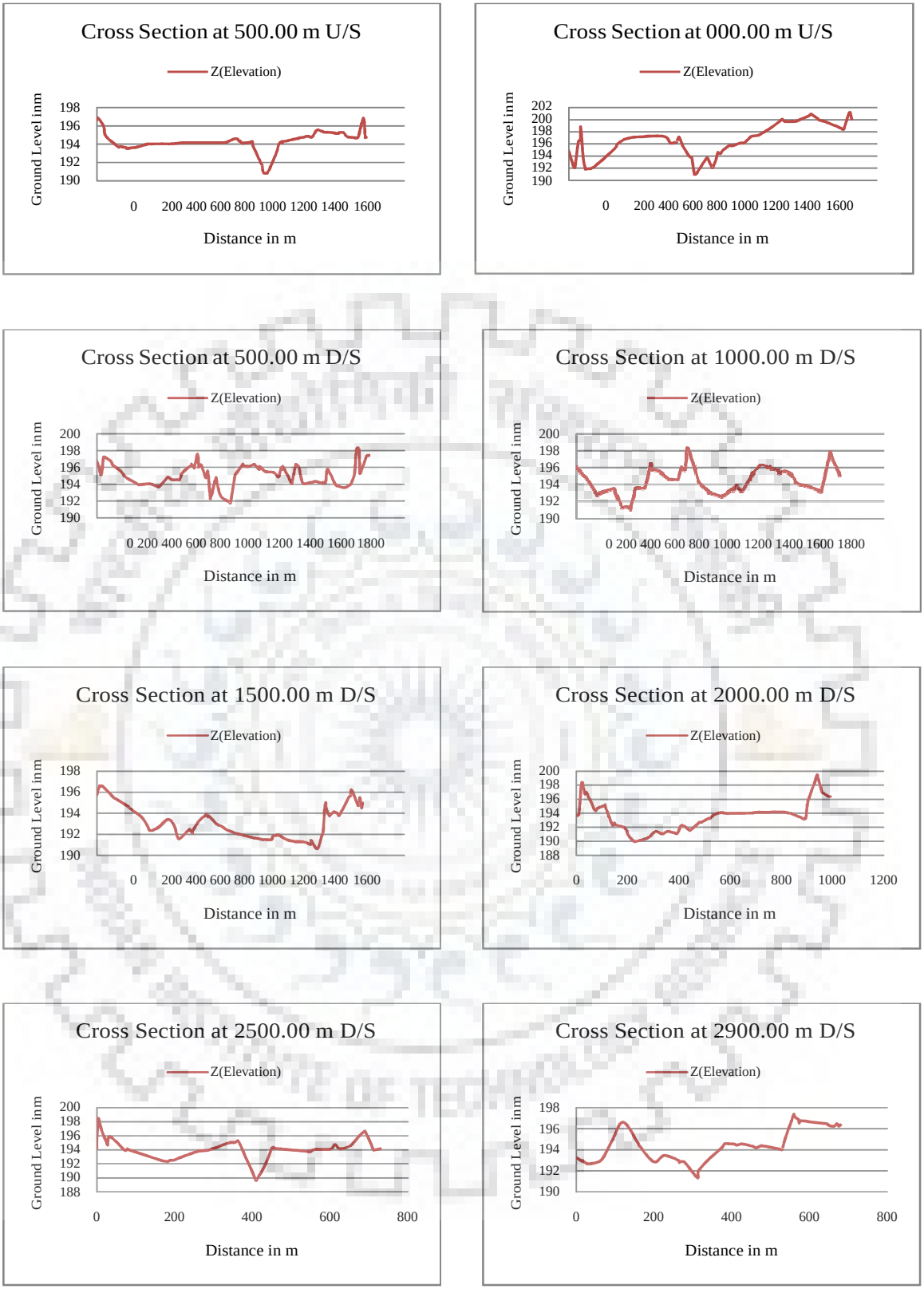

Figure 40 Cross section of Hindon River from Ch 4+000 U/S to 2+900 D/S

Appendix 2: WSE for different Manning's n (peak discharge 800 m^3/s) upstream

S. No.	Simulation Date & time	WSE for n= 0.076	WSE for n= 0.0613	WSE for n= 0.0543	WSE for n= 0.035
1	6/23/2003 0:00	192.2837	192.2837	192.2837	192.2837
2	6/23/2003 8:00	194.6434	194.5336	194.4692	194.2432
3	6/23/2003 16:00	194.8651	194.7166	194.6472	194.3826
4	6/24/2003 0:00	195.0253	194.8693	194.7832	194.5016
5	6/24/2003 8:00	195.1576	194.9907	194.9021	194.601
6	6/24/2003 16:00	195.2794	195.1001	195.0064	194.6961
7	6/25/2003 0:00	195.3941	195.2021	195.1024	194.7796
8	6/25/2003 8:00	195.5426	195.335	195.2278	194.886
9	6/25/2003 16:00	195.6987	195.4698	195.3535	194.9879
10	6/26/2003 0:00	195.8522	195.5995	195.4727	195.0818
11	6/26/2003 8:00	196.0051	195.7264	195.5881	195.1702
12	6/26/2003 17:00	196.1776	195.8675	195.7153	195.2647
13	6/27/2003 0:00	196.3126	195.9766	195.8131	195.3354
14	6/27/2003 8:00	196.4677	196.1017	195.9245	195.4137
15	6/28/2003 0:00	196.783	196.3532	196.1472	195.565
16	6/28/2003 8:00	196.9414	196.4796	196.259	195.6391
17	6/28/2003 18:00	197.1403	196.6396	196.3992	195.7307
18	6/29/2003 0:00	197.2595	196.7362	196.4835	195.7854
19	6/29/2003 8:00	197.3613	196.8121	196.5464	195.8179
20	6/29/2003 16:00	197.4242	196.8599	196.5873	195.8423
21	6/30/2003 0:00	197.4789	196.9038	196.626	195.8666
22	6/30/2003 8:00	197.4766	196.8945	196.6138	195.8508
23	6/30/2003 16:00	197.4344	196.8557	196.5778	195.8264
24	7/1/2003 0:00	197.3837	196.8129	196.5394	195.802
25	7/1/2003 8:00	197.3029	196.7428	196.4752	195.757
26	7/1/2003 16:00	197.2014	196.657	196.3996	195.7077
27	7/2/2003 2:00	197.0647	196.5442	196.3006	195.6425
28	7/2/2003 12:00	196.8792	196.39	196.1633	195.5496
29	7/2/2003 21:00	196.697	196.2437	196.0338	195.4639
30	7/3/2003 7:00	196.4909	196.0802	195.8896	195.3665
31	7/3/2003 23:00	196.1632	195.8184	195.6576	195.2032
32	7/4/2003 8:00	195.9786	195.67	195.525	195.1055
33	7/4/2003 16:00	195.8143	195.5366	195.4046	195.0138
34	7/4/2003 17:00	195.7936	195.5198	195.3894	195.0019
35	7/5/2003 0:00	195.6485	195.4002	195.2802	194.9158

Appendix 3 WSE for different Manning's n (peak discharge 800 m^3/s) downstream

S. No.	Simulation Date & time	WSE for n= 0.076	WSE for n= 0.0613	WSE for n= 0.0543	WSE for n= 0.035
1	6/23/2003 0:00	191.7178	191.7178	191.7178	191.7178
2	6/23/2003 12:00	193.3176	193.2358	193.1809	192.9517
3	6/24/2003 0:00	193.6004	193.4696	193.3957	193.15
4	6/24/2003 12:00	193.8116	193.6359	193.5538	193.2898
5	6/25/2003 0:00	194.0452	193.8068	193.6994	193.4107
6	6/25/2003 12:00	194.3684	194.06	193.915	193.5451
7	6/26/2003 0:00	194.745	194.3634	194.1763	193.6853
8	6/26/2003 12:00	195.1131	194.6709	194.4492	193.836
9	6/27/2003 0:00	195.4694	194.9722	194.721	193.9998
10	6/27/2003 12:00	195.8105	195.2646	194.9876	194.1716
11	6/28/2003 0:00	196.1383	195.548	195.2469	194.3482
12	6/28/2003 12:00	196.4556	195.8215	195.4989	194.5255
13	6/29/2003 0:00	196.7622	196.087	195.7434	194.7011
14	6/29/2003 12:00	196.9444	196.2353	195.8745	194.7837
15	6/30/2003 0:00	197.05	196.3239	195.955	194.8414
16	6/30/2003 12:00	197.0339	196.2998	195.9274	194.8084
17	7/1/2003 0:00	196.9442	196.2175	195.8501	194.7506
18	7/2/2003 0:00	196.5914	195.9013	195.5541	194.5288
19	7/2/2003 12:00	196.3257	195.663	195.3315	194.3633
20	7/3/2003 0:00	196.0099	195.3854	195.0753	194.1849
21	7/3/2003 12:00	195.6771	195.0965	194.8101	194.0105
22	7/4/2003 0:00	195.33	194.7973	194.5376	193.8436
23	7/5/2003 0:00	194.5899	194.1745	193.9863	193.5486

Appendix 4: WSE for different Manning's n (peak discharge 1100 m^3/s) upstream

S. No.	Simulation Date & time	WSE for n= 0.035	WSE for n= 0.0543	WSE for n= 0.0613	WSE for n= 0.076
1	7/8/2014 0:00	193.6398	193.6398	193.6398	193.6398
2	7/8/2014 3:00	194.6374	195.0556	195.0911	195.1911
3	7/8/2014 6:00	194.6709	195.0837	195.2004	195.3004
4	7/8/2014 12:00	194.7233	195.1994	195.3461	195.5161
5	7/8/2014 18:00	194.8206	195.3203	195.4734	195.6134
6	7/9/2014 0:00	194.9157	195.4361	195.5908	195.8108
7	7/9/2014 12:00	195.0894	195.6481	195.8066	196.0066
8	7/9/2014 15:00	195.1308	195.6977	195.8554	196.1154
9	7/10/2014 0:00	195.2537	195.8322	195.9991	196.2591
10	7/10/2014 12:00	195.5367	196.1207	196.2778	196.4778
11	7/11/2014 0:00	195.7911	196.3778	196.5341	196.7341
12	7/11/2014 12:00	196.0969	196.6618	196.804	197.004
13	7/12/2014 0:00	196.3508	196.9222	197.0942	197.3841
14	7/12/2014 12:00	196.5052	197.103	197.3018	197.6171
15	7/13/2014 0:00	196.6282	197.283	197.5204	197.8241
16	7/13/2014 12:00	196.6996	197.4128	197.6792	197.948
17	7/14/2014 0:00	196.7596	197.5156	197.8037	198.0337
18	7/14/2014 12:00	196.744	197.5288	197.8327	198.0788
19	7/15/2014 0:00	196.7144	197.4916	197.7974	198.0529
20	7/15/2014 12:00	196.6326	197.3857	197.6847	197.9442
21	7/16/2014 0:00	196.5381	197.2447	197.5247	197.792
22	7/16/2014 12:00	196.4057	197.0693	197.3231	197.5936
23	7/17/2014 0:00	196.2507	196.8791	197.1022	197.3732
24	7/17/2014 12:00	196.1127	196.7198	196.9167	197.1873
25	7/18/2014 0:00	195.9639	196.5706	196.7485	197.0183
26	7/18/2014 12:00	195.8444	196.4549	196.621	196.8889
27	7/19/2014 0:00	195.7206	196.341	196.5057	196.7709
28	7/19/2014 12:00	195.5864	196.2151	196.382	196.6483
29	7/20/2014 0:00	195.4443	196.0748	196.2445	196.5165
30	7/20/2014 12:00	195.3037	195.9278	196.1012	196.3814
31	7/21/2014 0:00	195.1579	195.7626	195.942	196.2372

Appendix 5: WSE for different Manning's n (peak discharge 1100 m^3/s) downstream

S. No.	Simulation Date & time	WSE for n= 0.035	WSE for n= 0.0543	WSE for n= 0.0613	WSE for n= 0.076
1	7/8/2014 0:00	193.2611	193.2611	193.2611	193.2611
2	7/8/2014 12:00	193.5008	194.0308	194.181	194.2611
3	7/8/2014 15:00	193.5588	194.0967	194.2552	194.3852
4	7/8/2014 18:00	193.6156	194.1609	194.3214	194.4814
5	7/8/2014 21:00	193.6709	194.2267	194.3845	194.5845
6	7/9/2014 0:00	193.7244	194.2874	194.4464	194.6396
7	7/10/2014 0:00	194.1047	194.7061	194.8849	195.1144
8	7/10/2014 12:00	194.3977	195.0044	195.177	195.4384
9	7/11/2014 0:00	194.6653	195.3002	195.4898	195.7195
10	7/11/2014 12:00	194.9963	195.6494	195.8334	196.0866
11	7/12/2014 0:00	195.2941	196.0097	196.242	196.5268
12	7/12/2014 12:00	195.5016	196.2819	196.5806	196.8957
13	7/13/2014 0:00	195.6589	196.5789	196.9197	197.1882
14	7/13/2014 12:00	195.7629	196.797	197.1669	197.4617
15	7/14/2014 0:00	195.8474	196.9492	197.3421	197.6671
16	7/14/2014 12:00	195.8419	196.9944	197.4047	197.774
17	7/15/2014 0:00	195.8017	196.9485	197.3645	197.6511
18	7/15/2014 12:00	195.7022	196.8197	197.2328	197.4286
19	7/16/2014 0:00	195.5809	196.6238	197.0241	197.2327
20	7/16/2014 12:00	195.4258	196.3807	196.7592	196.9769
21	7/17/2014 0:00	195.2425	196.1025	196.4485	196.6776
22	7/18/2014 0:00	194.9048	195.6493	195.9096	196.1607
23	7/18/2014 12:00	194.7604	195.4917	195.7128	195.9634
24	7/19/2014 0:00	194.6212	195.3543	195.5607	195.8062
25	7/20/2014 12:00	194.4755	195.2068	195.4112	195.6571
26	7/21/2014 0:00	194.3211	195.0443	195.2493	195.511
27	7/21/2014 12:00	194.1685	194.8724	195.0797	195.3675
28	7/22/2014 0:00	194.0064	194.6824	194.8966	195.219

Appendix 6: WSE for different Manning's n (peak discharge 2450 m^3/s) upstream

S. No.	Simulation Date & time	WSE for n= 0.035	WSE for n= 0.0543	WSE for n= 0.0613	WSE for n= 0.076
1	7/14/2008 0:00	191.93	191.93	191.93	191.93
2	7/14/2008 12:00	194.83	195.28	195.41	195.64
3	7/15/2008 0:00	195.14	195.65	195.79	196.04
4	7/15/2008 3:00	195.23	195.74	195.89	196.14
5	7/16/2008 0:00	195.84	196.39	196.54	196.81
6	7/16/2008 12:00	196.10	196.65	196.81	197.10
7	7/17/2008 0:00	196.32	196.88	197.05	197.38
8	7/17/2008 12:00	196.55	197.14	197.33	197.70
9	7/18/2008 0:00	196.75	197.41	197.62	197.99
10	7/18/2008 12:00	197.02	197.75	197.96	198.25
11	7/19/2008 0:00	197.29	198.03	198.20	198.53
12	7/19/2008 12:00	197.54	198.25	198.46	199.04
13	7/20/2008 0:00	197.77	198.60	198.94	199.58
14	7/20/2008 12:00	197.96	199.02	199.43	200.25
15	7/21/2008 0:00	198.15	199.51	199.98	200.92
16	7/21/2008 12:00	198.50	200.05	200.58	201.63
17	7/22/2008 0:00	198.86	200.63	201.23	202.39
18	7/22/2008 12:00	199.15	201.10	201.75	203.01
19	7/23/2008 0:00	199.32	201.39	202.09	203.44
20	7/23/2008 12:00	199.36	201.52	202.25	203.67
21	7/24/2008 0:00	199.31	201.51	202.26	203.72
22	7/24/2008 12:00	199.14	201.33	202.08	203.56
23	7/25/2008 0:00	198.87	201.00	201.74	203.21
24	7/25/2008 12:00	198.60	200.61	201.34	202.78
25	7/26/2008 0:00	198.35	200.23	200.92	202.32
26	7/26/2008 12:00	198.09	199.84	200.50	201.84
27	7/27/2008 0:00	197.83	199.46	200.07	201.35
28	7/27/2008 12:00	197.60	199.09	199.66	200.87
29	7/28/2008 0:00	197.39	198.75	199.28	200.40
30	7/28/2008 12:00	197.20	198.42	198.91	199.95
31	7/29/2008 0:00	197.00	198.09	198.54	199.50
32	7/29/2008 12:00	196.85	197.77	198.19	199.09
33	7/30/2008 0:00	196.70	197.48	197.86	198.70
34	7/30/2008 12:00	196.54	197.23	197.53	198.32
35	7/31/2008 0:00	196.37	196.99	197.23	197.93
36	7/31/2008 12:00	196.20	196.79	196.99	197.51
37	8/1/2008 0:00	196.01	196.58	196.76	197.16
38	8/1/2008 12:00	195.81	196.39	196.55	196.89
39	8/2/2008 0:00	195.58	196.18	196.34	196.63

Appendix 7: WSE for different Manning's n (peak discharge 2450 m^3/s) downstream

S. No.	Simulation Date & time	WSE for n= 0.035	WSE for n= 0.0543	WSE for n= 0.0613	WSE for n= 0.076
1	7/14/2008 0:00	192.1488	192.1488	192.1488	192.1488
2	7/14/2008 12:00	193.5142	193.9328	194.0502	194.2475
3	7/15/2008 0:00	193.8154	194.2804	194.4149	194.6641
4	7/15/2008 12:00	194.1635	194.683	194.8356	195.113
5	7/16/2008 0:00	194.485	195.0749	195.2395	195.5541
6	7/16/2008 12:00	194.7753	195.3902	195.5852	195.9953
7	7/17/2008 0:00	195.0278	195.699	195.944	196.4453
8	7/17/2008 12:00	195.2826	196.093	196.3842	196.9338
9	7/18/2008 0:00	195.5447	196.5221	196.8405	197.3229
10	7/18/2008 12:00	195.9252	197.0258	197.2873	197.578
11	7/19/2008 0:00	196.3498	197.3774	197.538	197.8692
12	7/19/2008 12:00	196.7503	197.5878	197.8417	198.6605
13	7/20/2008 0:00	197.0843	198.1125	198.5809	199.3848
14	7/20/2008 12:00	197.3103	198.6942	199.2177	200.1571
15	7/21/2008 0:00	197.5125	199.332	199.8746	200.8722
16	7/21/2008 12:00	198.0627	199.9479	200.5197	201.6008
17	7/22/2008 0:00	198.5314	200.5759	201.1917	202.3676
18	7/22/2008 12:00	198.9336	201.0602	201.7252	202.9992
19	7/23/2008 0:00	199.1369	201.3648	202.0718	203.4312
20	7/23/2008 12:00	199.1915	201.4983	202.2364	203.6612
21	7/24/2008 0:00	199.1378	201.4855	202.2417	203.708
22	7/24/2008 12:00	198.948	201.3042	202.067	203.5522
23	7/25/2008 0:00	198.6358	200.9635	201.7206	203.2008
24	7/25/2008 12:00	198.3035	200.5714	201.3126	202.7677
25	7/26/2008 0:00	197.9762	200.1705	200.8904	202.3079
26	7/26/2008 12:00	197.6352	199.758	200.4542	201.8271
27	7/27/2008 0:00	197.2654	199.3311	200.0027	201.3274
28	7/27/2008 12:00	196.9201	198.9134	199.5588	200.8338
29	7/28/2008 0:00	196.6057	198.5129	199.1314	200.3573
30	7/28/2008 12:00	196.2969	198.1074	198.7048	199.8827
31	7/29/2008 0:00	195.991	197.6732	198.2651	199.3995
32	7/29/2008 12:00	195.746	197.2162	197.8251	198.9274
33	7/30/2008 0:00	195.5319	196.787	197.3685	198.4761
34	7/30/2008 12:00	195.3268	196.3945	196.8838	198.0191
35	7/31/2008 0:00	195.1296	196.0188	196.4221	197.507
36	7/31/2008 12:00	194.9437	195.692	196.0224	196.9139
37	8/1/2008 0:00	194.7225	195.41	195.67	196.3687
38	8/1/2008 12:00	194.494	195.1716	195.3783	195.9119
39	8/2/2008 0:00	194.2581	194.9416	195.1236	195.5299

Appendix 8: WSE for different cell size at u/s point (peak flow 800 m^3/s)

S. No.	Simulation Date & time	WSE for cell size 30m x 30m	WSE for cell size 40m x 40m	WSE for cell size 50m x 50m
1	6/23/2003 0:00	190.9019	190.9019	190.9019
2	6/23/2003 6:00	195.3363	194.6364	194.571
3	6/23/2003 12:00	195.555	194.7419	194.6718
4	6/23/2003 18:00	195.6957	194.8328	194.7643
5	6/24/2003 0:00	195.81	194.9173	194.856
6	6/24/2003 6:00	195.9153	195.0051	194.9444
7	6/25/2003 0:00	196.2053	195.2379	195.19
8	6/25/2003 6:00	196.3296	195.3693	195.3308
9	6/25/2003 12:00	196.4706	195.5015	195.4681
10	6/26/2003 6:00	196.8602	195.8967	195.8723
11	6/26/2003 12:00	197.0154	196.0448	196.0196
12	6/26/2003 18:00	197.1676	196.1763	196.1532
13	6/27/2003 0:00	197.3199	196.293	196.2717
14	6/27/2003 6:00	197.4488	196.3811	196.3569
15	6/27/2003 12:00	197.5631	196.4476	196.4256
16	6/27/2003 18:00	197.6721	196.5067	196.4895
17	6/28/2003 0:00	197.7771	196.56	196.5497
18	6/28/2003 6:00	197.8546	196.6028	196.5847
19	6/28/2003 12:00	197.9083	196.6314	196.6213
20	6/28/2003 18:00	197.9521	196.6591	196.6527
21	6/29/2003 0:00	197.9932	196.6864	196.6828
22	6/29/2003 12:00	198.0421	196.6699	196.6677
23	6/29/2003 18:00	198.0361	196.6562	196.6526
24	6/30/2003 0:00	198.019	196.6423	196.6373
25	6/30/2003 12:00	197.9113	196.5655	196.5546
26	6/30/2003 18:00	197.8366	196.5221	196.5073
27	7/1/2003 0:00	197.7568	196.4771	196.4591
28	7/1/2003 6:00	197.6621	196.4182	196.3971
29	7/1/2003 12:00	197.5549	196.3523	196.3277
30	7/1/2003 18:00	197.4427	196.2827	196.2539
31	7/2/2003 12:00	197.1358	196.0654	196.0387
32	7/2/2003 18:00	197.0482	195.9943	195.9677
33	7/3/2003 12:00	196.8278	195.8002	195.7729
34	7/4/2003 0:00	196.7072	195.6787	195.6484
35	7/4/2003 12:00	196.5828	195.5526	195.5143
36	7/4/2003 18:00	196.5179	195.4909	195.4447
37	7/5/2003 0:00	196.4502	195.4211	195.372
38	7/5/2003 12:00	196.315	195.2897	195.2308

Appendix 9: WSE for different cell size at d/s point (peak flow 800 m^3/s)

S. No.	Simulation Date & time	WSE for cell size 30m x 30m	WSE for cell size 40m x 40m	WSE for cell size 50m x 50m
1	6/23/2003 0:00	191.336	191.336	191.336
2	6/23/2003 6:00	193.1511	193.2833	193.1737
3	6/23/2003 12:00	193.2819	193.4159	193.2945
4	6/23/2003 18:00	193.3937	193.517	193.3965
5	6/24/2003 6:00	193.6002	193.7018	193.5857
6	6/24/2003 12:00	193.6958	193.7931	193.6767
7	6/24/2003 18:00	193.7858	193.8756	193.7666
8	6/25/2003 6:00	194.0134	194.0849	193.9897
9	6/25/2003 12:00	194.1595	194.2292	194.143
10	6/25/2003 18:00	194.3035	194.3709	194.2901
11	6/26/2003 6:00	194.6005	194.6717	194.5906
12	6/26/2003 12:00	194.7856	194.8533	194.7742
13	6/26/2003 18:00	194.9709	195.0292	194.9507
14	6/27/2003 6:00	195.2585	195.3327	195.2291
15	6/27/2003 12:00	195.3548	195.4122	195.31
16	6/27/2003 18:00	195.4451	195.4806	195.3868
17	6/28/2003 0:00	195.5313	195.5441	195.4604
18	6/28/2003 12:00	195.6451	195.6363	195.5582
19	6/28/2003 18:00	195.6944	195.67	195.5961
20	6/29/2003 0:00	195.7404	195.7035	195.6332
21	6/29/2003 12:00	195.7361	195.6946	195.6246
22	6/29/2003 18:00	195.7137	195.6779	195.6062
23	6/30/2003 0:00	195.6907	195.6611	195.5876
24	6/30/2003 6:00	195.6463	195.6262	195.5495
25	6/30/2003 12:00	195.5805	195.5765	195.4945
26	6/30/2003 18:00	195.5128	195.5257	195.438
27	7/1/2003 0:00	195.4454	195.4743	195.3809
28	7/1/2003 6:00	195.366	195.412	195.3125
29	7/1/2003 12:00	195.2735	195.3416	195.2323
30	7/1/2003 18:00	195.1753	195.2681	195.1483
31	7/2/2003 6:00	194.9726	195.0353	194.9529
32	7/2/2003 12:00	194.8821	194.9577	194.8645
33	7/2/2003 18:00	194.7888	194.8613	194.7723
34	7/3/2003 12:00	194.5372	194.608	194.5244
35	7/4/2003 0:00	194.3907	194.4623	194.3806
36	7/4/2003 6:00	194.3155	194.3887	194.3064
37	7/4/2003 12:00	194.2427	194.316	194.2289
38	7/5/2003 6:00	194.0129	194.0891	193.9934
39	7/5/2003 12:00	193.9373	194.0197	193.9174

Appendix 10: WSE for different time step at u/s point (peak discharge 800 m^3/s)

S. No.	Simulation Date & time	WSE for time step=10 sec	WSE for time step = 1 min	WSE for time step = 10 min
1	6/23/2003 0:00	195.5731	195.5731	195.5731
2	6/23/2003 6:00	195.5731	195.5731	195.5731
3	6/23/2003 12:00	195.5731	198.113	195.5731
4	6/24/2003 6:00	195.5731	195.9628	195.5731
5	6/24/2003 12:00	195.5731	195.7234	195.7059
6	6/25/2003 6:00	195.5731	196.1781	196.1717
7	6/25/2003 12:00	195.5829	196.3039	196.2997
8	6/25/2003 18:00	195.718	196.4167	196.4133
9	6/26/2003 0:00	195.8361	196.5163	196.5142
10	6/27/2003 0:00	196.3764	196.9915	196.9877
11	6/27/2003 12:00	196.5215	197.085	197.0835
12	6/27/2003 18:00	196.5832	197.1236	197.1221
13	6/28/2003 0:00	196.6409	197.1618	197.1604
14	6/29/2003 6:00	196.7605	197.0354	197.0371
15	6/29/2003 12:00	196.7473	196.9812	196.9831
16	6/29/2003 18:00	196.7336	196.9257	196.9276
17	6/30/2003 0:00	196.7198	196.869	196.8709
18	6/30/2003 6:00	196.6842	196.7987	196.8009
19	6/30/2003 12:00	196.6412	196.7223	196.7246
20	6/30/2003 18:00	196.5965	196.6423	196.6446
21	7/1/2003 0:00	196.5502	196.5577	196.5601
22	7/1/2003 6:00	196.4894	196.4879	196.4897
23	7/1/2003 12:00	196.4217	196.4197	196.4215
24	7/2/2003 6:00	196.2072	196.205	196.207
25	7/2/2003 12:00	196.1406	196.1385	196.1404
26	7/2/2003 18:00	196.0693	196.067	196.0691
27	7/3/2003 0:00	195.9937	195.9913	195.9935
28	7/3/2003 18:00	195.8342	195.8237	195.8341
29	7/4/2003 0:00	195.7903	195.7628	195.7902
30	7/4/2003 18:00	195.6316	195.6304	195.6315
31	7/5/2003 0:00	195.6049	195.604	195.6049
32	7/5/2003 6:00	195.5799	195.5731	195.5799
33	7/5/2003 12:00	195.5731	195.5731	195.5731
34	7/5/2003 18:00	195.5731	195.5731	195.5731
35	7/21/2008 0:00	197.5125	199.332	199.8746
36	7/21/2008 3:00	197.5867	199.4834	200.0313
37	7/21/2008 6:00	197.7292	199.6369	200.1915
38	7/21/2008 9:00	197.9027	199.7918	200.3546
39	7/21/2008 12:00	198.0627	199.9479	200.5197

S. No.	Simulation Date & time	WSE for time step =10 sec	WSE for time step =1 min	WSE for time step =10 min
40	7/21/2008 21:00	198.4254	200.4188	201.0228
41	7/22/2008 6:00	198.7728	200.8499	201.4905
42	7/23/2008 6:00	199.1865	201.4577	202.1817
43	7/23/2008 9:00	199.193	201.4833	202.2148
44	7/23/2008 21:00	199.156	201.4971	202.2499
45	7/24/2008 15:00	198.8771	201.2297	201.9922
46	7/24/2008 18:00	198.8007	201.1473	201.9087
47	7/24/2008 21:00	198.72	201.0583	201.8178
48	7/25/2008 3:00	198.5509	200.8661	201.62
49	7/25/2008 6:00	198.4675	200.7683	201.5185
50	7/25/2008 9:00	198.3851	200.6701	201.416
51	7/25/2008 18:00	198.1403	200.3723	201.1033
52	7/25/2008 21:00	198.0586	200.2717	200.9973
53	7/26/2008 3:00	197.8929	200.0686	200.7827
54	7/26/2008 9:00	197.7228	199.8624	200.5647
55	7/26/2008 12:00	197.6352	199.758	200.4542
56	7/26/2008 15:00	197.5452	199.6528	200.3428
57	7/27/2008 0:00	197.2654	199.3311	200.0027
58	7/27/2008 3:00	197.1731	199.2236	199.8889
59	7/27/2008 6:00	197.0871	199.1184	199.7773
60	7/27/2008 9:00	197.0029	199.0152	199.6674
61	7/27/2008 12:00	196.9201	198.9134	199.5588
62	7/27/2008 15:00	196.8396	198.8127	199.4512
63	7/28/2008 0:00	196.6057	198.5129	199.1314
64	7/28/2008 6:00	196.451	198.312	198.9189
65	7/28/2008 9:00	196.3739	198.2104	198.8122
66	7/28/2008 12:00	196.2969	198.1074	198.7048
67	7/28/2008 21:00	196.0669	197.7874	198.3771
68	7/29/2008 12:00	195.746	197.2162	197.8251
69	7/29/2008 15:00	195.6907	197.1059	197.7144
70	7/29/2008 18:00	195.6369	196.9973	197.602
71	7/29/2008 21:00	195.584	196.8907	197.4868
72	7/30/2008 15:00	195.2769	196.2998	196.765
73	7/30/2008 18:00	195.2277	196.2054	196.6487
74	7/31/2008 6:00	195.0376	195.8462	196.2123
75	7/31/2008 12:00	194.9437	195.692	196.0224
76	8/1/2008 15:00	194.4366	195.1168	195.3126
77	8/2/2008 0:00	194.2581	194.9416	195.1236

Appendix 11: WSE for different time step at d/s point (peak discharge 800 m^3/s)

S. No.	Date	WSE for time step = 10 sec	WSE for time step = 1 min	WSE for time step = 10 min
1	6/23/2003 0:00	192.1775	192.1775	192.1775
2	6/23/2003 6:00	192.1775	192.1775	193.4299
3	6/23/2003 18:00	192.1775	192.1775	193.8235
4	6/24/2003 0:00	197.6161	197.6161	194.0048
5	6/24/2003 12:00	194.474	194.474	194.435
6	6/25/2003 0:00	194.8122	194.8122	194.797
7	6/25/2003 6:00	194.9725	194.9725	194.9608
8	6/25/2003 12:00	195.1213	195.1213	195.1098
9	6/25/2003 18:00	195.2572	195.2572	195.2509
10	6/26/2003 0:00	195.3666	195.3666	195.362
11	6/26/2003 6:00	195.4991	195.4991	195.4921
12	6/26/2003 18:00	195.8022	195.8022	195.7953
13	6/27/2003 0:00	195.9569	195.9569	195.9516
14	6/27/2003 12:00	196.1205	196.1205	196.1184
15	6/27/2003 18:00	196.1784	196.1784	196.1766
16	6/28/2003 0:00	196.2361	196.2361	196.2343
17	6/28/2003 6:00	196.2441	196.2441	196.244
18	6/28/2003 12:00	196.2119	196.2119	196.2128
19	6/28/2003 18:00	196.176	196.176	196.177
20	6/29/2003 0:00	196.1397	196.1397	196.1408
21	6/29/2003 6:00	196.0802	196.0802	196.0822
22	6/29/2003 12:00	196.0021	196.0021	196.0046
23	6/29/2003 18:00	195.9226	195.9226	195.9252
24	6/30/2003 0:00	195.8435	195.8435	195.8463
25	6/30/2003 18:00	195.5579	195.5579	195.5616
26	7/1/2003 0:00	195.4608	195.4608	195.4646
27	7/1/2003 6:00	195.3783	195.3783	195.3814
28	7/1/2003 12:00	195.305	195.305	195.3079
29	7/1/2003 18:00	195.2303	195.2303	195.2332
30	7/2/2003 0:00	195.1499	195.1499	195.1533
31	7/2/2003 6:00	195.061	195.061	195.0643
32	7/2/2003 18:00	194.9008	194.9008	194.9037
33	7/3/2003 0:00	194.8132	194.8132	194.8162
34	7/3/2003 6:00	194.7376	194.7376	194.7399
35	7/4/2003 0:00	194.5394	194.5394	194.5414
36	7/4/2003 6:00	194.4688	194.4688	194.4708
37	7/4/2003 12:00	194.3946	194.3946	194.3967
38	7/5/2003 18:00	194.009	194.009	194.0111
39	7/6/2003 0:00	193.928	193.928	193.9303